Master's Thesis

Near-Infrared Coherent Raman Spectroscopy and Microscopy

By

Laurynas Lialys

Submitted to the graduate degree program in Electrical Engineering and the Graduate Faculty of the University of Kansas in partial fulfillment of the requirements for the degree of Master of Science.

Committee:

_____

Chair: Dr. Shima Fardad

_____

Member: Dr. Rongqing Hui

_____

Member: Dr. Alessandro Salandrino

Date Defended: November 29, 2021

The thesis committee for Laurynas Lialys certifies that this is the approved version of the following thesis:

Near-Infrared Coherent Raman Spectroscopy and Microscopy

_____

Chair: Dr. Shima Fardad

Date Approved: November 29 , 2021

Abstract

Coherent Raman Scattering (CRS) spectroscopy and microscopy is a widely used technique in biology, chemistry, and physics to determine the chemical structure as well as provide a label-free image of the sample. The system uses two coherent laser beams one of which is constantly tuned in wavelength. Thus, a tunable laser source or optical parametric oscillator (OPO) is commonly used to achieve this requirement. However, the aforementioned devices are extremely expensive and work only for a specific wavelength range. In this study, we replace an OPO system with a photonic crystal fiber (PCF) in order to significantly reduce the cost and increase the flexibility of our microscopy system. Here, by exploiting the nonlinear phenomenon in the fiber called the soliton self-frequency shift (SSFS), we are able to shift the pulse central frequency while preserving its shape. Also, by switching to a near-infrared (NIR) source, the undesired fluorescence is reduced while the penetration depth increases. Moreover, the NIR laser source is more biologically friendly as each photon carries less energy than the visible laser counterpart. This reduces the probability of the photodamage effect. Based on this system, we designed and implemented CRS microscopy and spectroscopy, using Coherent anti-Stokes Raman Scattering (CARS) and Stimulated Raman Scattering (SRS) spectroscopy techniques.

Acknowledgments

First of all, I would like to thank my advisor Dr. Shima Fardad that she gave me the necessary starting theoretical and practical knowledge to start building the system. Moreover, I am grateful that she provided all the necessary components and samples. Also, I would like to thank Dr. Rongqing Hui for proving his lab space, components, and devices. Most importantly, both Dr. Shima Fardad and Dr. Rongqing Hui were always helpful and willing to help and spend their time. Moreover, I would like to thank my family for supporting me through the Master's program.

Table of Contents

Introduction

From the beginning of modern science in chemistry, physics, and biology scientists became interested in the chemical and physical properties of various materials. It was also important to be able to take images of the very small samples. Hence, microscopy and spectroscopy came into existence as they are the main tools to achieve these goals. One of the techniques in getting spectrum and taking images of the sample of interest is Coherent Raman spectroscopy and microscopy. This technique can be split into two main branches. One is known as the Coherent anti-Stokes Raman Scattering (CARS) and another one is known as the Stimulated Raman Scattering (SRS).

Building a typical CARS or SRS spectroscopy system requires theoretical and practical knowledge. Moreover, as most CARS and SRS systems use the laser source in the range of visible light spectrum it can become problematic as they might damage the sample. The reason for damaging the sample is that a smaller wavelength carries more energy than the longer wavelength and it can increase the risk of photodamage. Furthermore, in the typical CARS or SRS spectroscopy system, an expensive optical parametric oscillator (OPO) is used to shift the Stokes beam pulse wavelength. To overcome this an OPO can be replaced with much less expensive photonic crystal fiber (PCF). Due to the nonlinear properties of the PCF, the Stokes beam pulse wavelength can be shifted by controlling the entering power to the fiber. Hence, the system has an advantage compared with typical systems. It is also important to have the optimal spectrum resolution in CARS or SRS spectroscopies. To achieve this the pump and the Stokes beam pulses have to be chirped (stretched in time) equally. Also, spectral widths at the full width at half maximum (FWHM) of both the pump and the Stokes beam pulses have to be equal to have the optimal spectral resolution.

CARS microscopy is a technique that is label-free or fluorescent label-free. This means that no additional chemical components are needed in the sample to achieve imaging. Moreover, the system can be tuned to detect the particular Raman shift or shifts and provide an accurate image of the sample in a heterogeneous environment. This means that the system can provide the image of several particles at the same time that has different Raman shifts. Also, the system in this thesis provides the Stokes wavelength shift without any change in the system besides controlling the entering power into the fiber. Furthermore, as the laser source used in the system is in the near-infrared NIR wavelength range the penetration depth is deeper than in the system with a visible light range laser source. Moreover, the lateral spatial resolution depends on the beam spot size at the sample, which was determined by the pump beam as it had a smaller spot size at the sample compared to the Stokes beam spot size.

Chapter 1 - Theory

1.0 Raman scattering and spectroscopy principles

When the incident photon hits a molecule or a particle two types of photon scattering occur. One of them is elastic light photon scattering. It happens when scattered photon and incident photon has the same energy. This phenomenon is also known as Rayleigh scattering. It was first observed and studied by English physicist Lord Rayleigh in 1871. Another one is inelastic photon scattering which takes place when scattered photon and incident photon do not have the same energy. The first experimental observation of this inelastic scattering of photons was conducted by Indian scientists C.V. Raman and K.S. Krishnan in 1928 [1].

Raman spectroscopy is based on the information that can be obtained from the scattered radiation on the vibration states of the sample molecule. Even though radiation is usually represented by wavelength, in Raman spectroscopy it is convenient to express radiation in terms of energy, frequency, or wavenumber. The expression for the radiation in terms of wavelength can be as follows

$$\lambda = \frac{c}{\nu} \tag{1.1}$$

where λ is radiation wavelength, c is the speed of light, ν is the radiation frequency. Also, the radiation in terms of frequency can be written as

$$\nu = \frac{\Delta E}{h} \tag{1.2}$$

or the energy level difference between two photons can be expressed as

$$\Delta E = \nu \cdot h \tag{1.3}$$

where E is the energy of the photon and h is Plank's constant (6.62607015×10^{-34} J·Hz^{-1}). Moreover, Raman scattering radiation in terms of wavenumber can be described as

$$\tilde{\nu} = \frac{\nu}{c} = \frac{1}{\lambda} \tag{1.4}$$

where $\tilde{\nu}$ is wavenumber.

During scattering the light hits the molecule and distorts the cloud of electrons around the nuclei. This process forms a short-lived state or virtual state in the energy levels. However, this state is very unstable, so photons get quickly reradiated. Moreover, if the electron cloud returns to the starting ground energy level the photons are scattered with the same frequency as the incident photons. This kind of scattering refers to elastic scattering or Rayleigh scattering. It is a dominant process during Raman spectroscopy. On the other hand, if the scattering process provokes nuclear motion, the energy transfer is induced. There are two possibilities of energy transfer. One of them is that the energy can be transferred from the incident photon to the molecule. Another is that the energy can be transferred from the molecule to the scattered photon. In this case, the scattering is called inelastic or Raman scattering because the energy of the scattered photon is different from the energy of the incident photon. This process is very weak and only one in 10^6 photons or even one in 10^8 photons is inelastically scattered [2]. Figure 1.0 depicts the Raman scattering process that shows what happens when light hits the sample molecule.

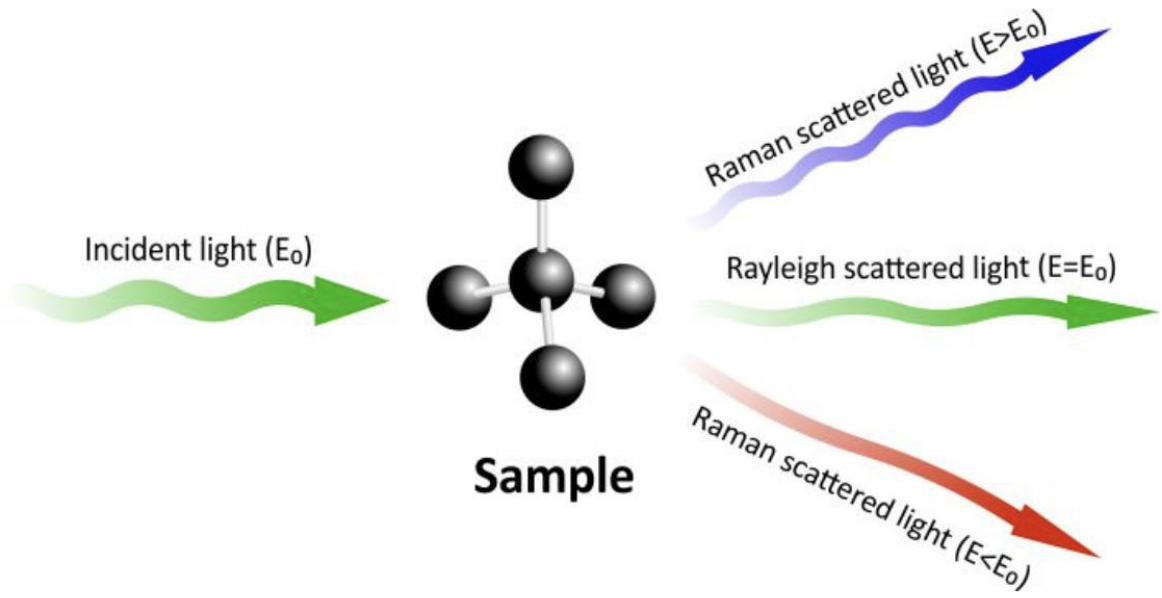

Figure 1.0 Raman Scattering illustration. Incident light with some initial energy and wavelength hits the sample, then the light gets scattered in three ways known as Rayleigh scattering (same energy and same wavelength as initial light), Raman scattering with red shifted wavelength known as Stokes Raman scattering (less energy and longer wavelength than initial light) and Raman scattering with blue shifted wavelength as anti-Stokes Raman scattering (more energy and shorter wavelength than initial light) [3].

If the scattered photon or light has more energy than the incident photon or light that means the photon gets scattered with blue shifted wavelength also known as anti-Stokes shift. On the other hand, if the scattered photon or light has less energy than the incident photon or light that refers that the photon gets scattered with red shifted wavelength also known as Stokes shift [4]. The energy difference between the initial energy level and the final energy level is often referred as Raman shift. It can be expressed as

$$\Delta E = E_{final} - E_{initial} \tag{1.5}$$

where E_{final} is the final energy level after scattering and $E_{initial}$ is the initial energy level before scattering. If the initial energy level is greater than the final energy level the absorption occurs, however, if the initial energy level is less than the final energy level the emission occurs. Also, Raman shift can be expressed as wavenumber

$$\Delta\tilde{\nu} = \left(\frac{1}{\lambda_{inc}} \pm \frac{1}{\lambda_{sc}}\right) \tag{1.6}$$

where λ_{inc} is the incident wavelength or the wavelength of the incident photon and λ_{sc} is the scattered wavelength or the wavelength of the scattered photon. Another more commonly used expression for Raman shift is the same but expressed in terms of centimeters to the power of negative one (cm^{-1}) as it is more commonly used units to view at Raman shift. As nanometers (nm) is commonly used units for wavelength, to convert from nm to cm^{-1} the following formula can be used

$$\Delta\tilde{\nu}(cm^{-1}) = \left(\frac{1}{\lambda_{inc}(nm)} \pm \frac{1}{\lambda_{sc}(nm)}\right) \cdot \left(\frac{10^7(nm)}{(cm)}\right) \tag{1.7}$$

To do the conversion, the key is the multiplication of factor of 10^7. Figure 1.1 shows the energy level diagram for Raman scattering [5,6].

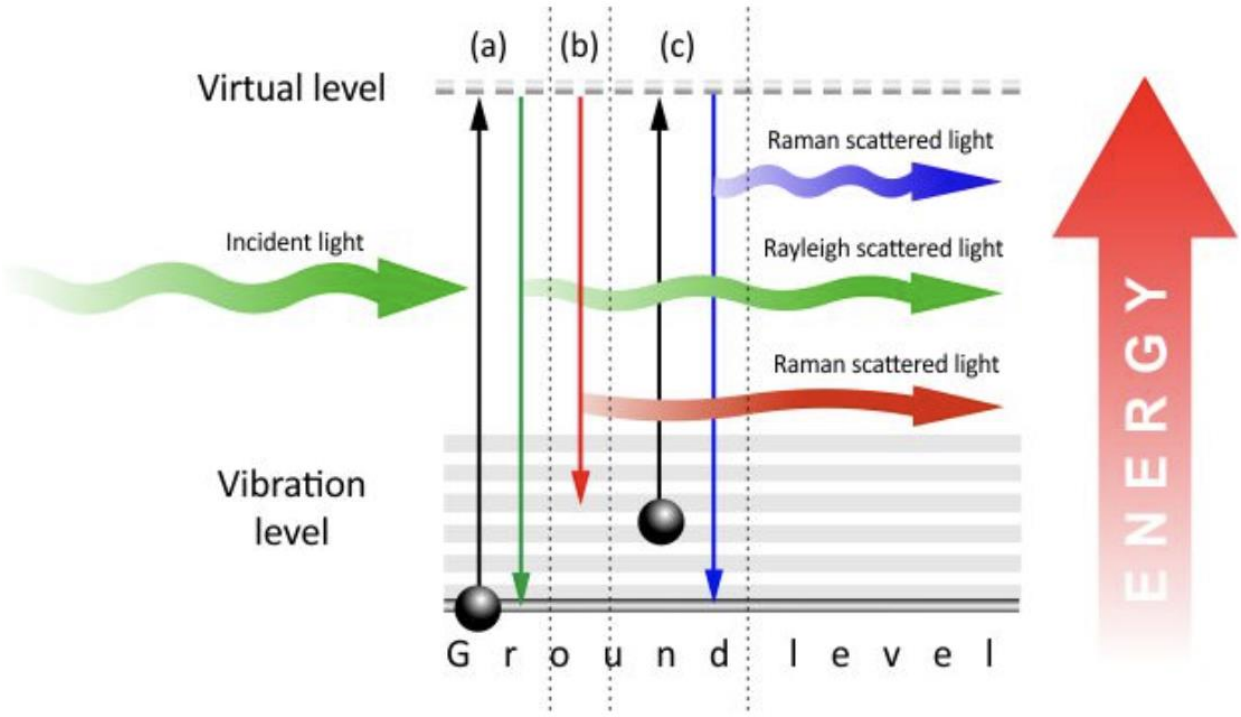

Figure 1.1 Energy level diagram for Raman scattering. Incident green light with some initial energy and wavelength hits the sample, then the light gets scattered in three ways (a) Rayleigh scattering with scattered green light (incident energy of the photon and incident wavelength are the same as scattered energy of the photon and scattered wavelength), (b) Stokes Raman scattering with scattered red light (incident energy of the photon is greater than scattered energy of the photon, also incident wavelength is shorter than the scattered wavelength) and (c) anti-Stokes Raman scattering with scattered blue light (incident energy of a photon is less than the scattered energy of photon and incident wavelength is longer than the scattered wavelength) [3].

Moreover, the spectrum of Raman scattering is another way to look at this phenomenon. It is the most useful and most commonly used representation of Raman scattering. Figure 1.2 represents the Raman spectrum that depicts Raman shift and both Raman pulses (Stokes and anti-Stokes).

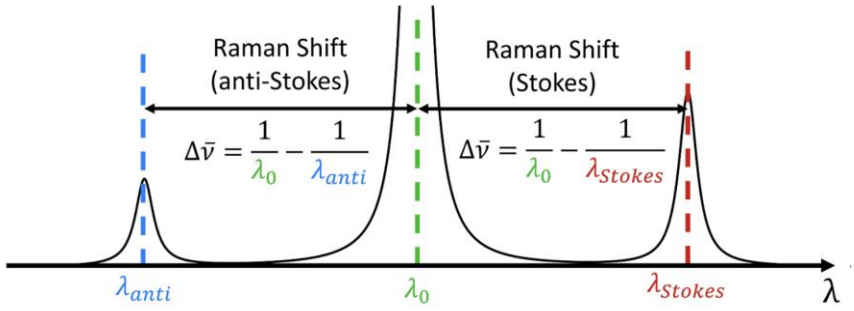

Figure 1.2 Spectrum diagram for Raman scattering. The horizontal axis is in terms of wavelength and the vertical axis is in terms of amplitude, λ_0 illustrates the incident wavelength, λ_{anti} represents anti-Stokes Raman shifted wavelength, and λ_{Stokes} refers to Raman shifted wavelength, also it is important to note that the, λ_{anti} has the smallest amplitude and λ_0 has the biggest amplitude [7].

1.1 Coherent Raman Scattering

Coherent Raman scattering (CRS) can be split into two techniques. One of them is stimulated Raman scattering (SRS) and another one is coherent anti-Stokes Raman scattering (CARS). CARS was first observed by Terhune et al. in 1965 and SRS was first reported by Woodbury and Nag in 1962. These two techniques are improved Raman method that enhances a very weak Raman signal by several orders of magnitude [8,9].

The process of CARS involves three laser beams. One of them is called pump beam which is at frequency ω_p, another one is known as Stokes beam which is at frequency ω_s and the third one is referred to as probe beam which is at frequency ω_{pr}. When the difference between pump and Stokes beam frequencies matches the molecular vibrational frequency Ω_{vib} also known as beat frequency, the anti-Stokes signal is generated [10]. Mathematically beat frequency can be expressed as

$$\Omega_{vib} = \omega_p - \omega_s \tag{1.8}$$

The beat frequency is the same frequency as for Raman shift and it can be expressed by using wavenumber expression in cm^{-1}. Particularly in CARS Raman shift can be represented by two equations that present the same shift. These two equations are as follow

$$\frac{1}{\lambda} = 10^7 \left(\frac{1}{\lambda_{pump}} - \frac{1}{\lambda_{probe}} \right) cm^{-1} \tag{1.9}$$

and

$$\frac{1}{\lambda} = 10^7 \left(\frac{1}{\lambda_{CARS}} - \frac{1}{\lambda_{pump}} \right) cm^{-1} \tag{1.10}$$

where λ_{pump} is the wavelength of the pump beam, λ_{probe} is the wavelength of the probe beam, and λ_{CARS} is the wavelength of the CARS. Moreover, the linear relationship between four frequencies in CARS can be expressed as

$$\omega_{as} = (\omega_p - \omega_s) + \omega_{pr} \tag{1.11}$$

In most CARS processes the pump beam is often used as the probe beam as well. Also, CARS is a nonlinear Raman process, where the pump and Stokes beams are present. Both beams have to be tightly focused on a sample to generate a signal at the anti-Stokes frequency. Also, they have to hit the sample at the same time and the same location. This signal at an anti-Stokes frequency can be expressed as

$$\omega_{as} = 2\omega_p - \omega_s \tag{1.12}$$

Also, CARS can be viewed as nonlinear four-wave mixing (FWM) process which is also coherent when the energy difference between the pump and Stokes beams matches with the energy of the vibration of the specific sample. It is possible to enhance the CARS signal when the beating frequency Ω_{vib} is in resonance with molecular vibration [11,12,13].

Four-wave mixing (FWM) is a parametric nonlinear process with widespread applications. It is also known as a third-order nonlinear optical process. During this process, three incident light waves with frequencies ω_{p1}, ω_{p2} and ω_{probe}, respectively, hit the material to generate a fourth light wave at frequency ω_{idler} known as idler frequency. This idler frequency can be determined as follows

$$\omega_{idler} = \omega_{p1} + \omega_{p2} - \omega_{probe} \tag{1.13}$$

where ω_{p1} is the frequency of the first pump light, ω_{p2} is the frequency of the second pump light, and ω_{probe} is the frequency of the probe light [14,15]. Figure 1.4 depicts the FWM process.

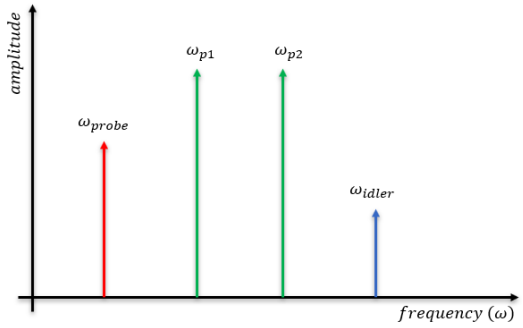

Figure 1.3 FWM process. Two light pumps at frequencies ω_{p1}, ω_{p2}, and the probe light at frequency ω_{probe} hit the sample to generate idler light at frequency ω_{idler} [15].

The process of SRS in principle is an energy transfer process where a high-power pump beam loses the energy and the Stokes beam gains the energy. The loss of energy of a pump is known as

stimulated Raman loss (SRL) and the gain of energy of Stokes beam is known as stimulated Raman gain (SRG). This energy exchange also can be viewed as intensity. When the pump beam experiences the loss in the intensity, the signal intensity I_p drops, at the same time Stokes beam experiences the gain in the intensity, the signal intensity I_s increases. The intensity for SRL and SRG can be described as

$$\Delta \mathrm{I_p} \propto -\mathrm{N} \cdot \sigma_{\mathrm{Raman}} \cdot I_P \cdot I_s \tag{1.14}$$

and

$$\Delta \mathrm{I_s} \propto \mathrm{N} \cdot \sigma_{\mathrm{Raman}} \cdot I_P \cdot I_s \tag{1.15}$$

, respectively, where N is the number of molecules in the probe volume, σ_{Raman} is the molecular Raman scattering cross-section, I_p is the intensity of pump beam, I_s is the intensity of Stokes beam. In particular, this energy exchange or intensity exchange happens when the frequency difference between the pump ω_p and Stokes ω_s beams matches the vibrational frequency of the sample under test. This frequency difference can be expressed as

$$\Delta\omega = \omega_p - \omega_s \tag{1.16}$$

or in terms of wavenumber, it can be represented as

$$\frac{1}{\lambda} = 10^7 \left(\frac{1}{\lambda_{pump}} - \frac{1}{\lambda_{Stokes}} \right) cm^{-1} \tag{1.17}$$

When this difference matches a molecular vibrational frequency Ω in the sample, stimulated emission occurs [16,17,18]. Figure 1.4 illustrates the energy level diagram for CARS and SRS processes.

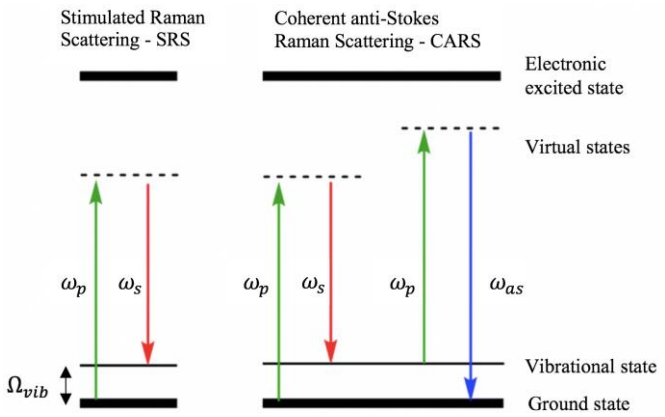

Figure 1.4 SRS and CARS energy diagram. SRS part: the pump beam at frequency ω_p and Stokes beam at frequency ω_s hits the sample to match the vibrational frequency of the molecular at frequency Ω_{vib} and CARS part: the pump beam at frequency ω_p and Stokes beam at frequency ω_s hits the sample and then the pump beam as the probe at frequency ω_p hits the sample at the same time to generate the beam at anti-stokes frequency ω_{as} [17].

1.2 Coherent Raman Spectroscopy and Microscopy

Nonlinear coherent spectroscopy offers the spectral view of the sample of interest within a complex and heterogeneous sample. One of the nonlinear coherent spectroscopies is coherent Raman spectroscopy (CRS), which provides vibrational contrast and characteristic of chemical species. Also, based on the fact that CRS is based on a coherent signal in which the molecular bonds oscillate in phase and the vibrational states are actively pumped, the Raman signal is significantly enhanced. CRS is based on CARS and SRS processes and it is widely used in scientific research. Moreover, this type of spectroscopy is label-free, meaning that the sample does not have to be labeled with external fluorophores or auto-fluorescent proteins. Furthermore, the specific chemical distribution within the sample can be mapped regardless of the other chemical

mixture being present in the sample of interest. This allows multiple chemical detection without the physical separation of the chemicals in the sample [19,20].

It is possible to implement CARS and SRS imaging on the same microscopy with some modifications, by using two synchronized pulse trains. As CARS and SRS usually happen at the same time, they both can use the same light source and microscope system with some modifications, but different signal detection devices. CARS microscopy or imaging usually contains a picosecond pulse laser source, microscope, and a highly sensitive photodetector. A picosecond pulse laser source has been proven experimentally and theoretically as being the optimum choice in terms of the signal-to-noise ratio (SNR) for CARS imaging. Moreover, to improve spectral resolution, the pump and Stokes beams have to be equally chirped. SRS microscopy or imaging can be achieved by adding an optical modulator, a photodiode detector, and a demodulator to the CARS microscopy system. Modulators that are most often used for the high frequency beam pulse to extract the laser beam induced by SRL or SRG in SRS microscopy are acousto-optic or electro-optic modulators. For the demodulation of the SRS signal, the most widely used instrument is the lock-in amplifier [21].

1.3 Light source for CRS

Picosecond pulsed laser sources are preferred for the CRS technique. Moreover, free space picosecond pulsed lasers require very precise mechanical alignment of the system as well as vibrational isolation for a good performance. The selection for the pulse duration for CRS is not trivial. The short pulses have higher peak power and at the same time limited spectral resolution, on the other hand, longer pulses have lower peak power but better spectral resolution. Furthermore, a fairly high power synchronized pulsed laser of two wavelengths with one of the wavelengths

being tunable is required for CRS. Next, the sample of interest can exhibit fluorescence which is a way stronger signal than Raman. As fewer molecules fluoresce in the infrared, IR laser is preferred. It helps to produce high-quality vibrational spectra free from background fluorescence and grants rapid collection of high-resolution vibrational spectra on the picosecond time scale. Moreover, high-resolution vibrational spectra can be produced by using a picosecond pulse laser in coherent Raman spectroscopy [22,23].

1.4 Optical soliton as Stokes pulse

Any soliton in the field of physics can be described as the localized wave entity that propagates in the nonlinear medium and sustains a constant shape. In the field of optics, the pulse that propagates through the medium has a natural tendency to spread. This spreading occurs due to chromatic dispersion and spatial diffraction. When special diffraction is eliminated during the nonlinear process in the medium of propagation, a stable self-localized wave pocket is formed. This trapped wave pocket is referred to as an optical soliton [24].

Moreover, solitary waves or solitons occur in a huge number of fundamental processes in the natural or human created nonlinear systems. One of them is optical fibers. In addition, the development of nonlinear photonic crystal fibers (PCF) gives the possibility of wavelength tunability based on the effect of soliton self-frequency shift (SSFS) which occurs when optical soliton pulses propagate in optical fibers and experience a downshift of their carrier frequencies. This happens when a soliton less than picosecond propagates in Raman active medium. During this propagation, soliton gets continuously red shifted because the low frequency end of the soliton spectrum experiences Raman gain at the expense of the high frequency end. Also, when this occurs group velocity dispersion (GVD) becomes less than zero or chromatic dispersion (D) more than

zero. Hence, SSFS originates from within the pulse stimulated Raman scattering [25,26]. Moreover, PCFs can generate wavelength-shift soliton with a wavelength longer than 1050 nm. Furthermore, the balance between fiber nonlinearity and chromatic dispersion moves towards a longer wavelength with the increase of optical power. To produce soliton wavelength shifting in PCF, the laser pulse power that is launched into the fiber has to be adjusted. The first order soliton produced in the PCF can be mathematically expressed as

$$\frac{2\pi c\gamma P T_o^2}{\lambda^2 |D(\lambda)|} = 1 \tag{1.18}$$

, where P is the peak power, D is the chromatic dispersion of the fiber, T_0 is the pulse width, γ is the nonlinearity coefficient $(W \cdot km)^{-1}$ of the fiber, and λ is the central wavelength [27].

1.5 Frequency chirp for pulse broadening

Pulse broadening occurs when the short duration optical pulse, that has a finite pulse bandwidth, propagates in a dispersive medium. This is referred to as frequency chirp. As the pulse propagates in the dispersive medium different frequency components travel at different group velocities that leading to the fact that these components spread in time. The main contributor to this spreading is group velocity dispersion (GVD). It is the phenomenon that describes the extent of the pulse broadening during propagation. During this process, different frequency components arrive at different times known as the relative time delay. Moreover, this relative time delay between two wavelength components separated by $\delta\lambda$ can be expressed as follows

$$\Delta\tau_g = D \cdot L \cdot \delta\lambda \tag{1.19}$$

where $\Delta\tau_g$ is the relative time delay between two wavelength components, D is group delay dispersion parameter with its units usually $\frac{ps}{nm \cdot km}$, L is nonlinear material length. The group delay dispersion parameter depends on the refractive index of the material that the signal pulse is propagating. This means that by changing the refractive index of the propagation material, group delay dispersion also changes.

Frequency chirping occurs at two different dispersion regimes. One is in the case when instantaneous frequencies of the pulse at the leading edge are lower and trailing edge frequencies are higher than the center frequency of the pulse, it is referred that the pulse is in the normal dispersion regime. This happens when the medium of propagation has a positive GVD group delay dispersion parameter. On the other hand, when instantaneous frequencies of the pulse at the leading edge are higher and trailing edge frequencies are lower than the center frequency of the pulse it is referred that the pulse is in the anomalous dispersion regime. This occurs when the medium of propagation has a negative GVD group delay dispersion parameter. Moreover, it is often said that in the normal dispersion regime the pulse is up-chirped or positively chirped. In the anomalous dispersion regime, the pulse is down-chirped or negatively chirped. Figure 1.5 refers to three pulses. One of the pulses is unchirped pulse as an input to the dispersion medium and two pulses are up-chirped and down-chirped.

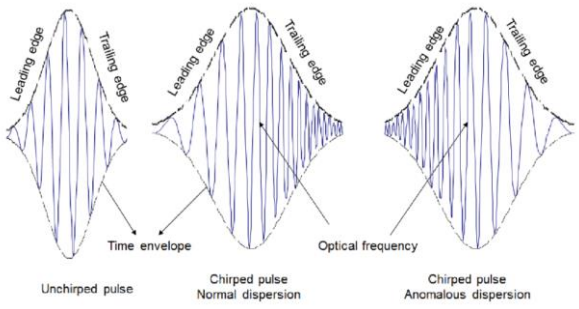

Figure 1.5 Unchirped pulse and two chirped pulses. An unchirped pulse on the left, an up-chirped or positively chirped pulse that occurs in normal dispersion regime in the middle, and a down chirped or negatively chirped pulse that occurs in anomalous dispersion regime on the right [28].

Moreover, it is important to notice that during the propagation of the pulse through dispersion medium in the time domain the amplitude or the intensity of the pulse drops as it gets wider. On the other hand, spectrally the pulse stays unchanged. Figure 1.6 depicts the pulse in the time domain and spectral domain [28,29].

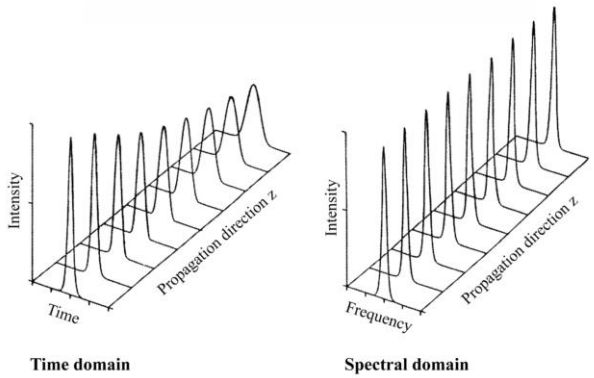

Figure 1.6 The chirped pulse in the time and spectral domain. For the time domain, the pulse width increases, and the amplitude decreases as it propagates through the medium, and for the spectral domain, the pulse width and amplitude do not change as it propagates through the medium [30].

1.6 Pockels cell as linear electro-optical modulator

Pockels cell was first described by Friedrich C.A. Pockels in 1926. The linear Electro-optical effect in the Pockels cell occurs in the crystals that do not have center symmetry. Moreover, this effect can be recognized as a linear change in the reflective index. This can be achieved by applying an electrical field to the crystal which is inside of the Pockels cell. The most commonly used crystals are ammonium dihydrogen phosphate (ADP), potassium dihydrogen phosphate (KDP), potassium dideuterium phosphate (KDP), and lithium niobate (LN). Furthermore, the Pockels cell essentially can be viewed as a waveplate. The effective rotation of the polarization of the light direction can be obtained by retarding one polarization relative to another one. To rotate the polarization of the light by 90° the voltage of several kilovolts has to be applied to the crystal. Furthermore, the electrically controlled optical Pockels cell is typically combined with the polarizer to change the beam direction in the billionths of a second [31]. Figure 1.7 depicts the principles of the Pockels cell.

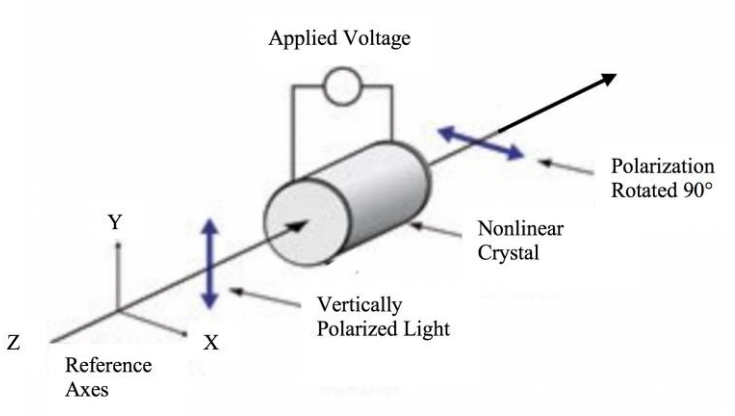

Figure 1.7 The light wave polarization as it propagates through the Pockels cell. The light wave enters the Pockels cell vertically polarized and it leaves the Pockels cell horizontally polarized [31].

The main component of this device is a suitable nonlinear crystal. For the visible to near-infrared region, Potassium Dideuterium Phosphate (KDP) or lithium niobite crystals can be used. For the middle infrared region, cadmium telluride crystal can be used. Another important aspect for Pockels cell is applied DC voltage which generates an electric field that changes the birefringence of the crystal. The birefringence can be expressed as the difference between the refractive indices in two optical directions as follows

$$\Delta n' = n_x - n_y \tag{1.20}$$

where n_x and n_y are indices of the material for x and y directions, respectively. Furthermore, the refractive index of any material can be expressed as

$$n = \frac{c}{v} \tag{1.21}$$

where n is the refractive index and v is the speed of light in the material. As birefringence is due to the change in the refractive index and as the refractive index of an electro-optic medium is the function of the applied electrical field which can be created by applying a voltage to the crystal, the function for the refractive index for the crystal can be expressed as

$$n(E) \approx n - \frac{1}{2} r n^3 E \tag{1.22}$$

where r is Pockels coefficient or the linear electro-optic coefficient (that is why it can be referred to as linear electro-optic modulation) and E is the applied electrical field. Moreover, the beam light that propagates in the Pockels cell of length L with the applied electrical field is experiencing a phase shift. This phase shift can be expressed as

$$\phi = \phi_o - \frac{\pi(rn^3EL)}{\lambda_o} \tag{1.23}$$

where λ_0 is the free-space wavelength and

$$\phi_o = \frac{2\pi nL}{\lambda_0} \tag{1.24}$$

Furthermore, the electrical field that is obtained by applying a voltage V across two faces of the Pockels cell separated by distance d can be expressed as

$$E = \frac{V}{d} \tag{1.25}$$

by applying equations 24 and 25 to expression 23 it can be obtained that

$$\phi = \phi_0 - \pi\left(\frac{V}{V_\pi}\right) \tag{1.26}$$

where

$$V_\pi = \frac{d}{L}\left(\frac{\lambda_0}{rn^3}\right) \tag{1.27}$$

The parameter V_π is known as half-wave voltage. This is the voltage that needs to be applied to change the phase shift by π radian or by 90° [32,33,34].

Moreover, Pockels electro-optical effect specifies the change in phase that is produced in the polarized light which is propagating in a certain uniaxial crystal, and the electrical field is applied to the crystal. The effect is the linear function of voltage. In addition, the applied voltage is parallel to the crystal optical axis in the same direction as the incident light. The Pockels cell can be used in two different modes as an electro-optical modulator (EOM) to control the intensity

of the propagating light [35]. One of the modes is transverse the Pockels effect which occurs when the applied electrical field is perpendicular to the direction of propagating light wave. Another one is the longitudinal Pockels cell. It occurs when the applied electrical field is parallel to the propagating light wave [36].

1.7 Lock-in amplifier

A Lock-in amplifier (LIA) is a device that is used to detect and measure very small AC signals of a few nanovolts which are buried in the noise which might be many thousands of times larger. The technology that LIA is based on to extract the small AC signal is known as a phase-sensitive detector (PSD). The principle of PSD is the extraction of signal components at a specific reference frequency and phase by dismissing noise frequencies. Furthermore, the signal-to-noise ratio (SNR) of the system under the test is the main objective of LIA. To achieve that the main components inside the LIA are an amplifier, a bandpass filter (BPF), a low pass filter (LPF), and a multiplier or phase-sensitive detector. First, the input signal is amplified by an amplifier. After that, the output from an amplifier is fed to BPF to pick up the frequency range for signal detection. Next, the output from the BPF enters the multiplier, and there it gets multiplied with the reference signal. In the last step, the signal passes through the LPF to get rid of the high-frequency components of the signal so that only DC components are present in the output signal [37]. The reference signal might be generated by using the function generator as it can be used as an external source or it can be generated by the internal source that is generated based on phase-locked-loop. In addition, the magnitude of the output signal can be expressed as

$$R = \sqrt{X^2 + Y^2} \tag{1.28}$$

and the phase between the signal and lock-in reference can be written as

$$\theta = \tan^{-1}\left(\frac{Y}{X}\right) \tag{1.29}$$

where R is the magnitude vector of the output signal, X is in phase component, Y is quadrature component [38].

References

[1] H. G. M. Edwards, J. M. Chalmers and N. W. Barnett, Eds., *Raman Spectroscopy in Archaeology and Art History*. Cambridge: The Royal Society of Chemistry, **2005**, p. 18-20.

[2] E. Smith and G. Dent., *Modern Raman Spectroscopy: A Practical Approach*., 2nd ed. Chichester: John Wiley & Sons Ltd, **2019**, p. 3-4.

[3] Lithuanian Laser Association., "Raman Spectroscopy.", Integratedoptics.com., https://integratedoptics.com/Raman-Spectroscopy (accessed Apr. 5, **2020**).

[4] Q. Wang, "Raman spectroscopic characterization and analysis of agricultural and biological systems," Ph.D. dissertation, Dept. Agri. Eng., Iowa State Univ., Ames, IA, USA, **2013**. [Online]. Available: https://lib.dr.iastate.edu/cgi/viewcontent.cgi?article=4026&context=etd.

[5] J. R. Ferraro, K. Nakamoto and C. W. Brown., *Introductory Raman Spectroscopy*., 2nd ed. San Diego, CA: Elsevier Academic Press, **2003**, p. 5,17.

[6] M. Wahadoszamen, A. Rahaman, N. M. R. Hoque, A. I. Talukder, K. M. Abedin and A. F. M. Y. Haider., "Laser Raman Spectroscopy with Different Excitation Sources and Extension to Surface Enhanced Raman Spectroscopy.", *Journal of Spectroscopy*, **2015**, 895317.

[7] Edinburgh Instruments., "Blog What is Raman Spectroscopy.", edinst.com., https://www.edinst.com/blog/what-is-raman-spectroscopy/ (accessed Apr. 5, **2020**).

[8] C. S. Liao and J. X. Cheng., "In Situ and in Vivo Molecular Analysis by Coherent Raman Scattering Microscopy.", *Annual Review of Analytical Chemistry (Palo Alto California)* **2016**, 12;9(1):69-93.

[9] D.Pestov, et al., "Optimizing the Laser-Pulse Configuration for Coherent Raman Spectroscopy.", *Science*, **2007**, 316,265.

[10] C. L. Evans and X. S. Xie., "Coherent Anti-Stokes Raman Scattering Microscopy: Chemical Imaging for Biology and Medicine.", *Annual Review of Analytical Chemistry*, **2008**, 1:883-909.

[11] J. X. Cheng, A. Volkmer, L. D. Book and X. S. Xie., "Multiplex Coherent Anti-Stokes Raman Scattering Microspectroscopy and Study of Lipid Vesicles.", *The Journal of Physical Chemistry*, **2002**, 106, 8493-8498.

[12] T. Ideguchi, S. Holzner, B. Bernhardt, G. Guelachvili, N. Picque and T. W. Hansch., "Coherent Raman spectro-imaging with laser frequency combs.", *Nature*, **2013**, 502, 355-3588.

[13] J. X. Cheng., "Coherent Anti-Stokes Raman Scattering Microscopy.", *Applied Spectroscopy*, 2**007**, 61(9): 197-208.

[14] O. Aso, M. Tadakuma and S. Namiki., “Four-Wave Mixing in Optical Fibers and its Applications.”, *Furukawa Review*, **2000**, no. 19.

[15] B. Jin and C. Argyropoulos., “Enhanced four-wave mixing with nonlinear plasmonic metasurfaces.”, *Scientific Reports*, **2016**, 28746.

[16] M. A. Ferrara and L. Sirleto., “Stimulated Raman Scattering in Micro- and Nanophotonics.”, **2018**, DOI: 10.5772/intechopen.80814.

[17] W. J. Tipping, M. Lee, V. G. Brunton and A. N. Hulme., “Stimulated Raman Scattering microscopy: an emerging tool for drug discovery.”, *Royal Society of Chemistry*, **2016**, 45, 20075-2089.

[18] C. W. Freudiger, et al., “Label-Free Biomedical Imaging with High Sensitivity by Stimulated Raman Scattering Microscopy.”, *Science*, **2008**, 322(5909): 1857-1861.

[19] K. Hashimoto, M. Takahashi, T. Ideguchi and K. Goda., “Broadband coherent Raman spectroscopy running at 24,000 spectra per second.”, *Scientific Reports*, **2016**, 6, 21036.

[20] P. Nandakumar, A. Kovalev and A. Volkmer., “Vibrational imaging based on stimulated Raman scattering microscopy.”, *New Journal of Physics*, **2009**, 11, 033026.

[21] C. Zhang, D. Zhang and J. X. Cheng., “Coherent Raman Scattering Microscopy in Biology and Medicine.”, *Annual Review of Biomedical Engineering*, **2015**, 17:415-445.

[22] S. Y. Lee and D. Zhang., “Theory of femtosecond stimulated Raman spectroscopy.”, *The Journal of Chemical Physics*, **2004**, 121, 3632.

[23] K. Kieu, B. G. Saar, G. R. Holtom, X. S. Xie and F. W. Wise., “High-power picosecond fiber source for coherent Raman microscopy.”, *Optics Letters*, **2009**, 34(13): 2051-2053.

[24] Z. Chen, M. Segev and D. N. Christodoulides., “Optical spatial solitons: historical overview and recent advances.”, *Reports on Progress in Physics*, **2012**, 75(8):086401.

[25] D. V. Skryabin, F. Luan, J. C. Knight and P. S. J. Russell., “Soliton Self-Frequency Shift Cancellation in Photonic Crystal Fibers.”, *Science*, **2003**, 301(5640), 1705-1708.

[26] X. Liu, et al., “Soliton self-frequency shift in a short tapered air-silica microstructure fiber.”, *Optics Letter*, **2001**, 26(6): 358-360.

[27] J. R. Unruh, E. S. Price, R. G. Molla, L. Stehno-Bittel, C. K. Johnson and R. Hui., “Two-Photon microscopy with wavelength switchable fiber laser excitation.”, *optics Express*, **2016**, 14, 9825-9831.

[28] M. Cvijetic and I. B. Djordjevic., *Advanced Optical Communication Systems and Networks*. Norwood, MA: Artech House, **2013**, p. 86,179.

[29] R. Hui and M. O'Sullivan., *Fiber Optic Measurement Techniques*. San Diego, CA: Elsevier Academic Press, **2009**, p. 67-70.

[30] U. Keller and L. Gallmann., "Ultrafast Laser Physics.", [PowerPoint slides], (accessed Mar. 25, **2020**). Available: https://ethz.ch/content/dam/ethz/special-interest/phys/quantum-electronics/ultrafast-laser-physics-dam/education/lectures/ultrafast_laser_physics/lecture_notes/2_Linear%20pulse%20propagation.pdf.

[31] C. Bibeau, M. A. Rhodes and L. J. Atherton., "Inovative Technology Enables a New Architecture for the World's Largest Laser.", *Photonics Spectra*, **2006**.

[32] O. Svelto and D. C. Hanna, Ed., *Principles of Laser*., 5th ed. New York, NY: Springer Science+Business Media, **2010**, p. 322.

[33] The Theory of Birefringence, Cambridge Polymer Group Inc., Boston, MA, USA, **2004.**

[34] A. K. Bain and P. Chand., *Ferroelectrics Principles and Applications*., Weinheim: Wiley-VCH Verlag GmbH & Co. KGaA, **2017**, p. 234.

[35] R. Goldstein., "Pockels cell primer.", *Laser Focus*, **1968**, 21.

[36] F. Pan, X. Xiao, Y. Xu and S. Ren., "An Optical AC Voltage Sensor Based on the Transverse Pockels Effect.", *Sensors*, **2011**, 11, 6593-6602.

[37] S. Bhattacharyya, R. N. Ahmed, B. B. Purkayastha and K. Bhattacharyya., "Implementation of Digital Lock-in Amplifier.", *Journal of Physics*, **2016**, 759, 012096.

[38] Model SR810 DSP Lock-in Amplifier, Stanford Research Systems Inc., Sunnyvale, CA, USA, **2005**.

Chapter 2 - Methodology

2.0 SRS Spectroscopy procedure overview

The setup for SRS spectroscopy is based on the previously conducted experiment with some changes [1]. The whole procedure of building SRS spectroscopy was broken into three parts. Firstly, the Stokes pulse arm was built. This procedure was broken into three steps. The first step was to align the laser beam with the photonic crystal fiber (PCF). The next step was to add Zinc Selenide crystal (ZnSe crystal) to achieve pulse broadening or chirping. The pulse chirp of the Stokes pulse was measured by using the frequency-resolved optical gating (FROG). Next, the central wavelength of the Stokes pulse beam was measured by using the optical spectrum analyzer (OSA). The last step was to align and build the Stokes pulse arm until the dichroic mirror combiner (DMC). The second part in constructing the SRS spectroscopy was to align and build the pump pulse beam arm until the DMC. To achieve this the central wavelength and the pulse broadening or chirping of the pump pulse were measured by using the OSA and the FROG, respectively. The pulse broadening was achieved by adding Sulfur Hexafluoride crystal (SF6 crystal) to the pump pulse path. After that, the alignment proceeded until the DMC. The third part of building the SRS spectroscopy was to build and align the microscope stage as well as connect the rest of the instruments needed for SRS spectroscopy.

The whole SRS spectroscopy system was built on an optical table that works as a vibration control platform. Also, this table provides stability for the system over time as well as it has a rectangular grid of tapped holes to screw and tighten all necessary components and instruments. The name of the table that the system was built on was the RPR-48-8 RPR Reliance™ Industrial and Educational Grade Optical Table. The width, length, and thickness of the table are $4\,ft$,

$8\ ft$ and $8\ in$, respectively. The distance between each of the mounting holes is an inch. Also, the top of the table is made from stainless steel [2]. Moreover, the table legs were connected to the air compressor, so that the table would be floating and would be able to deal with any vibrations from surroundings.

2.1 Laser source for the pump and Stokes pulses

The laser source that was used for the experiment was Coherent Fidelity-2 high power femtosecond fiber laser. This ultrafast fiber-based laser provides high average power over $2\ W$ and extremely short pulses of $55\ fs$ with central wavelength at around $1070\ nm$. Moreover, the laser has two working modes. One of the modes is called alignment mode with an average power of about $120\ mW$ that is used for an alignment. Another mode is called high power mode with an average power of about $2\ W$ that is used for conducting the experiment. The repetition rate of the pulse train of this laser is $70 \pm 2\ MHz$. The beam profile is Gaussian with a beam diameter of $1.2 \pm 0.2\ mm$, a divergence of a beam is less than $1.6\ mrad$, and the typical full width at half maximum (FWHM) is about $50\ fs$. Moreover, it is important to notice that the polarization of the beam is horizontal [3].

2.2 The Stokes pulse arm alignment of the Stokes pulse with the PCF

One of the most important aspects of the Stokes pulse arm was to make sure that the Stokes pulse that comes from the laser source was properly aligned with the PCF. The main reason for that was that the beam had to hit the core of the PCF and not cladding or coating, otherwise the laser beam might damage the PCF. The photonic crystal fiber with serial number SC-3.7-975 was used in the experiments was purchased from NKT Photonics. This fiber is made for single mode usage which means that it is suitable for the light waves that have the same mode but might have

different frequencies. Moreover, it has a high nonlinear coefficient with zero dispersion at around $975 \pm 15\,nm$ to allow efficient nonlinear interactions at $1060\,nm$ wavelength. Also, the nonlinear coefficient at $1060\,nm$ is about $18\,(W \cdot km)^{-1}$ and the numerical aperture (NA) at $1060\,nm$ is 0.25 ± 0.05. Furthermore, the attenuation of the lightwave at $1060\,nm$ is less than $5\,\frac{dB}{km}$ and at $1550\,nm$ is less than $3\,\frac{dB}{km}$. This particular nonlinear optical fiber is suitable for supercontinuum generation applications such as spectroscopies for high power picosecond pulse lasers. Furthermore, the core is made from pure silica and the coating is made from HT Acrylate. The core diameter of the fiber is $3.7 \pm 0.3\,\mu m$, the cladding diameter is $125 \pm 10\,\mu m$ and the coating diameter is $245 \pm 10\,\mu m$ [4]. The length of the fiber is $2\,m$. Figure 2.0 depicts the cross-section view of the fiber.

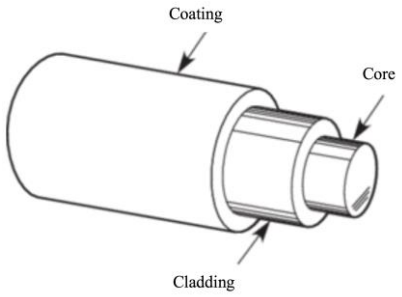

Figure 2.0 Cross section view of the fiber that indicates the core, the cladding and the coating of the fiber [5].

To achieve the desired alignment of the Stokes pulse with the PCF two irises and two mirrors as well as an alignment laser and an optical power meter were used. An alignment laser that was used as a helping tool in making sure that the system was properly aligned was FIS OV-VFL Visible Laser Fault Locator. The maximum output optical power of this laser is less than $1\,mW$ with wavelength from $620\,nm$ to $680\,nm$ [6]. Moreover, an optical power meter that was used as a

helping tool in making sure that the system was properly aligned was TEK TOP200 power meter. This optical power meter can measure dBm or dB for three wavelength settings which are $850\ nm$, $1300\ nm$ and $1550\ nm$. The measurable power range is from $-60\ dBm$ to $+3\ dBm$ [7].

The first step in alighting the Stokes pulse with the PCF was roughly positioning two silver mirrors next to Coherent Fidelity-2 high power femtosecond fiber-based laser so that the beam would go to the PCF. The laser was turned on using the alignment mode option. Next, an iris after the second mirror was placed such that the laser beam would fall on an iris center. After that, some fine adjustments on the silver mirror 1 were performed to center the beam from the laser source on the iris center. Also, it was verified by closing the variable iris diaphragm adjustable aperture until it was just slightly smaller than the laser beam. By the time the laser beam was properly centered, only a halo of light has been seen around the aperture of the iris [8]. After that, the beam splitter for the wavelength range from $700\ nm$ to $1100\ nm$ that transmits 30 % and reflects 70 % of the incoming light beam was placed in front of an iris on the laser beam path. The beam splitter $30/70$ was used to reduce the beam intensity and the optical power as well as to split the laser beam into the pump pulse and the Stokes pulse. The pump pulse beam was the reflected portion of the laser beam and the Stokes pulse beam was the transmitted portion of the laser beam. In addition, to reduce the intensity of an optical power of the Stokes beam even more, a round step neutral density filter was placed after the beam splitter. It was adjusted so that not too much power would enter the PCF. Also, another purpose of this round step neutral density filter was to adjust the power that enters the PCF to create the optical solitons. In this experiment, solitons acted as Stokes pulses. Then the optical collimator (OC) was placed in front of a round step neutral density filter. The usage of the OC was to collimate the Stokes pulse beam from the free space to the PCF. The PCF was connected to the three degrees of freedom-controlled mount (θx, θy and θz) to help

align the Stokes pulse beam with the PCF by adjusting the mount angles. It was important to align this part properly because if the laser beam would hit the coating or cladding of the PCF and not the core the laser beam might damage the PCF. Also, two beam dumpers were used to dump the beams that were coming out from the beam splitter and were not used at this point for the experiment. Then Coherent Fidelity-2 high power femtosecond fiber-based laser was turned off and an alignment laser was connected to the PCF. Then an alignment laser was turned on. It was made sure that its beam was centered on an iris center. Figure 2.1 illustrates the block diagram of this whole procedure. After that, an alignment laser was replaced with an optical power meter and Coherent Fidelity-2 high power femtosecond fiber-based laser was turned on by using the high power mode. The alignment was again adjusted until the maximum reading on an optical power meter screen has been seen. The block diagram of this step can be seen in Figure 2.2. Note that to observe the laser beam that was in the range of invisible light (wavelength more than $1100\ nm$) infrared card (IR card) and infrared camera (IR camera) were used. The IR card was Detector Card VRC2. This card has two absorption bands. One absorption band has a wavelength range from $400\ nm$ to $640\ nm$ and another one has a wavelength range from $800\ nm$ to $1700\ nm$ [9]. The IR camera was Model IRV1-1700 infrared viewing device. The spectral response wavelength of this camera is from $350\ nm$ to $1700nm$. Moreover, the magnification of this device is up to 1.8 times and the focus starts from $0.15\ m$ and goes to infinity [10].

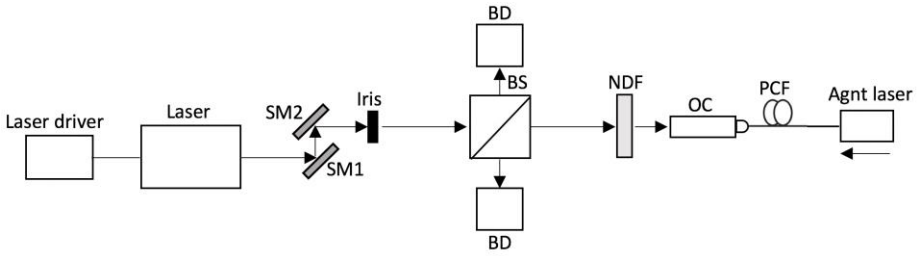

Figure 2.1 The first step for making sure that the laser beam is properly aligned with respect to photonic crystal fiber using two silver mirrors, one iris, and an alignment laser. Laser - Coherent Fidelity-2 high power femtosecond fiber-based laser, SM1 – silver mirror 1, SM2 – silver mirror 2, BS – beam splitter (30 % transmission and 70 % reflection), BD – beam dumper, NDF - round step neutral density filter, OC – optical collimator, PCF – photonic crystal filter and Agnt laser – alignment laser (arrow bellow indicates the laser beam propagation direction).

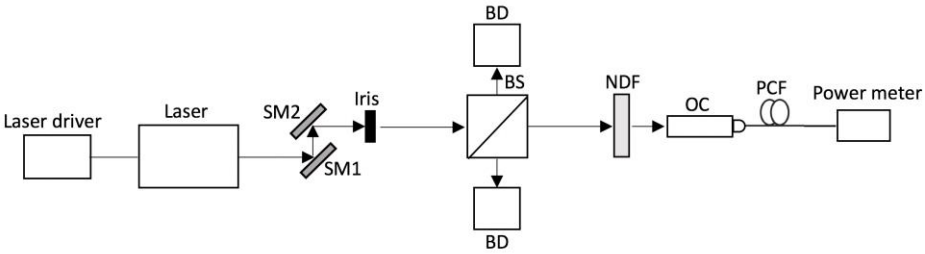

Figure 2.2 Setup for making sure that laser beam is properly align with respect to photonic crystal fiber using one iris and an optical power meter. Laser - Coherent Fidelity-2 high power femtosecond fiber-based laser, SM1 – silver mirror 1, SM2 – silver mirror 2, BS – beam splitter (30 % transmission and 70 % reflection), BD – beam dumper, NDF - round step neutral density filter, OC – optical collimator, PCF – photonic crystal filter and Power meter – optical power meter.

In addition, to making sure that the laser beam was properly aligned and was not tilted or did not propagate with the angle, the second iris was placed in front of the first iris. Next, an optical power meter was replaced with an alignment laser. Moreover, the laser source was switched back to the alignment mode. Then the variable iris diaphragm adjustable aperture of iris 1 was reopened and the beam from Coherent Fidelity-2 high power femtosecond fiber-based laser was centered on the variable iris diaphragm adjustable aperture of iris 2 by adjusting silver mirror 2 so that only a halo of light has seen on the center of iris 2. After that, the variable iris diaphragm adjustable aperture of iris 1 was closed until it is just slightly smaller than the laser beam. The variable iris diaphragm adjustable aperture of iris 2 remained closed to make sure that the laser beam is going through both centers of both irises [8]. Next, Coherent Fidelity-2 high power femtosecond fiber-based laser was turned off and an alignment laser was again connected to the PCF. An alignment laser was turned on to make sure that the beam that went from it was propagating through both centers of both irises. Figure 2.3 depicts the block diagram of this step. After that, an alignment laser was turned off and disconnected from the PCF and an optical power meter was connected to the PCF. The power reading on an optical power meter was read while Coherent Fidelity-2 high power femtosecond fiber-based laser was turned on by using high power mode. Two silver mirrors and the mount of the PCF were adjusted again until the maximum optical power readings have been seen on an optical power meter screen. This was done to make sure that the beam went through both centers of both irises by measuring the maximum optical power. This procedure can be observed in Figure 2.4.

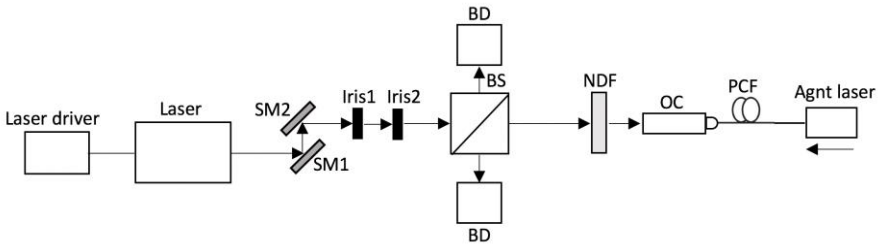

Figure 2.3 Setup for making sure that laser beam is properly aligned with respect to photonic crystal fiber using two irises and an alignment laser. Laser - Coherent Fidelity-2 high power femtosecond fiber-based laser, SM1 – silver mirror1, SM2 – silver mirror 2, BS – beam splitter (30 % transmission and 70 % reflection), BD – beam dumper, NDF - round step neutral density filter, OC – optical collimator, PCF – photonic crystal filter and Agnt laser – alignment laser (arrow bellow indicates the laser beam propagation direction).

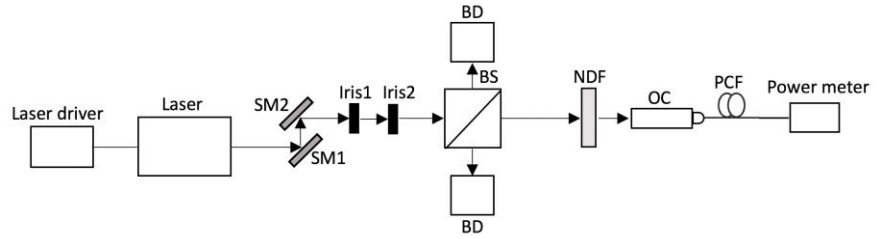

Figure 2.4 Setup for making sure that laser beam is properly aligned with respect to photonic crystal fiber using two irises and an optical power meter. Laser - Coherent Fidelity-2 high power femtosecond fiber-based laser, SM1 – silver mirror 1, SM2 – silver mirror 2, BS – beam splitter (30 % transmission and 70 % reflection), BD – beam dumper, NDF - round step neutral density filter, OC – optical collimator, PCF – photonic crystal filter and Power meter – optical power meter.

2.3 The Stokes pulse arm alignment for the pulse broadening and wavelength measurements

The next step in building and aligning the Stokes pulse arm for SRS spectroscopy was to measure the Stokes pulse broadening or chirping and the wavelength. Firstly, two irises that were used to align the laser source beam with the PCF were opened and an optical power meter was disconnected from the PCF. Then the PCF was connected to another OC. The purpose of this second OC was to collimate the outgoing laser beam from the PCF to the free space to get the collimated Stokes beam. This second optical collimator was placed on the mount with three degrees of freedom (x-direction, y-direction, and z-direction) to help place the collimator in the right position. Next, a long pass filter (LPF) with a cutoff wavelength of $1150\ nm$ was placed in front of the second optical collimator to filter out the lower optical solitons. Furthermore, ZnSe crystal was placed in the Stokes beam's path after the LPF such that the Stokes beam would propagate through it. The crystal was put on the mount with the three degrees of freedom (x-direction, z-direction, and rotation angle of $360°$). The usage of this crystal was to broaden or chirp the Stokes pulse beam. This was necessary to achieve the optimum spectral resolution for the SRS spectroscopy. Figure 2.5 depicts ZnSe crystal and its dimensions. Also, it is important to notice that the whole crystal, except the entering and leaving places of the beam and small window on the top, was covered by gold. The reason for this was that the Stokes pulse beam could be reflected inside the crystal in case if the length of the crystal would be too short for chirping.

There were a couple of reasons for selecting ZnSe crystal for the Stokes pulse broadening. It has optical properties that fit the purpose of this experiment. One of them is that ZnSe crystal has a very wide transmission spectrum, covering the wavelength range from $600\ nm$ up to $22000\ nm$. Moreover, it has a refractive index range from 2.47 to 2.45, and the chromatic

dispersion coefficient range from $895.28\,\frac{ps}{nm\cdot km}$ to $343.39\,\frac{ps}{nm\cdot km}$ in the wavelength range from $1100\,nm$ to $1450\,nm$, respectively. This makes it almost the perfect candidate for using it as an optical element for infrared applications [11,12]. To achieve the optimum spectral resolution for the SRS spectroscopy it was decided to broaden (chirp) the Stokes pulse to around one picosecond. Therefore, to accomplish this picosecond pulse width the Stokes pulse beam has to pass a certain length inside the ZnSe crystal. Hence, the following calculation was performed to figure out the path length of the crystal needed for the Stokes beam pulse at $1150\,nm$ to be broadened up to one picosecond

$$\Delta\tau_g = D_s \cdot L_s \cdot \delta\lambda_s \tag{2.1}$$

$$1.0 = 763.15\,\frac{ps}{nm \cdot km} \cdot L_s \cdot 20nm \tag{2.2}$$

$$L_s = 0.065m = 65mm \tag{2.3}$$

where the pulse width $\delta\lambda_s$ was measured to be $20\,nm$ by using the optical spectrum analyzer while the laser source was turned on using the high power mode, the chromatic dispersion D_s value for wavelength at $1150\,nm$ was obtained to be $763.15\,\frac{ps}{nm\cdot km}$ from the database [12]. Hence, the crystal length L_s needed to achieve one picosecond pulse broadening or chirping was calculated to be $65\,mm$. Therefore, the crystal was positioned in the way that the Stokes pulse beam would enter and leave the crystal with one path inside the crystal as the length of the crystal was measured to be $69\,mm$.

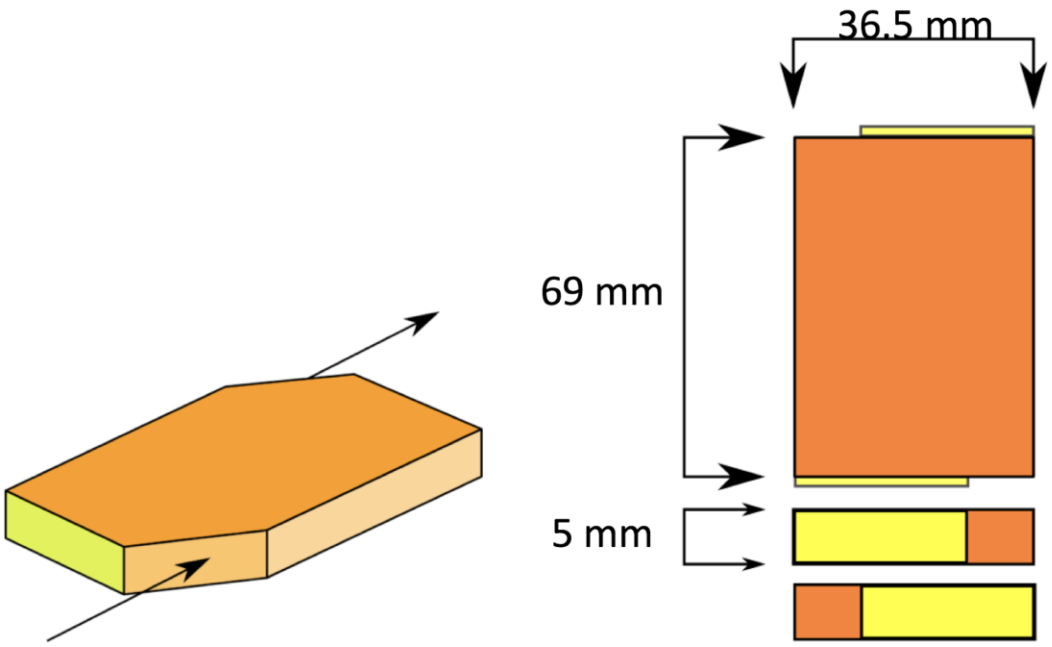

Figure 2.5 ZnSe crystal and indication of entering and leaving positions of the beam, the height, the width, and the length of the crystal are $5\,mm$, $36.5\,mm$ and $69\,mm$, respectively [13].

Next, another round step neutral density filter was placed after the ZnSe crystal to control the power and the intensity of the Stokes pulse beam. After that silver mirrors 3 and 4 were placed to align the laser beam with the FROG. At this time the beam dumper (BD) was placed in front of the silver mirror 4 instead of FROG. The silver mirror 3 was placed on the mount that could flip at a 90° angle. Next, silver mirrors 5 and 6 were placed so that the Stokes pulse beam could be redirected and could be aligned with the optical spectrum analyzer to measure its wavelength. To achieve this the standard single mode fiber (SMF) was placed in front of the silver mirror 6 on the four-dimension mount (x-direction, y-direction, θx and θy). Furthermore, an alignment laser was connected to the SMF. Moreover, the silver mirror 3 was flip a 90° angle so that the Stokes beam

that came from the ZnSe crystal could propagate forward to the silver mirror 5. Moreover, the laser source was turned on using the high power mode. Next, by using the IR card and by adjusting silver mirrors 5 and 6 as well as adjusting the mount of the SMF it was made sure that two beams met at the same spot on the IR card in the path from the silver mirror 6 to the SMF. Also, one half-wave plate was placed between the round step neutral density filter and the OC and another half-wave plate was placed between silver mirrors 5 and 6. The purpose of these two half-waveplates was to make sure that the optical axis of the beam is the same as the optical axis of the PCF and the SMF. Figure 2.6 indicates the block diagram of this step. Next, an alignment laser was replaced with an optical power meter to maximize the power and to achieve the best alignment possible for the Stokes pulse beam with the SMF. Some fine adjustments were made on silver mirrors 5 and 6 as well as on the SMF mount till the maximum reading was seen on an optical power meter screen. Figure 2.7 indicates the block diagram of this procedure. The final step for measuring the wavelength of the Stokes pulse beam was to replace an optical power meter with the optical spectrum analyzer which was HP 70951A OPT 009 Optical Spectrum Analyzer from Hewlett Packard. The spectrum range of this analyzer is from $600\,nm$ to$1700\,nm$ [14]. Figure 2.8 illustrates the block diagram of this final step.

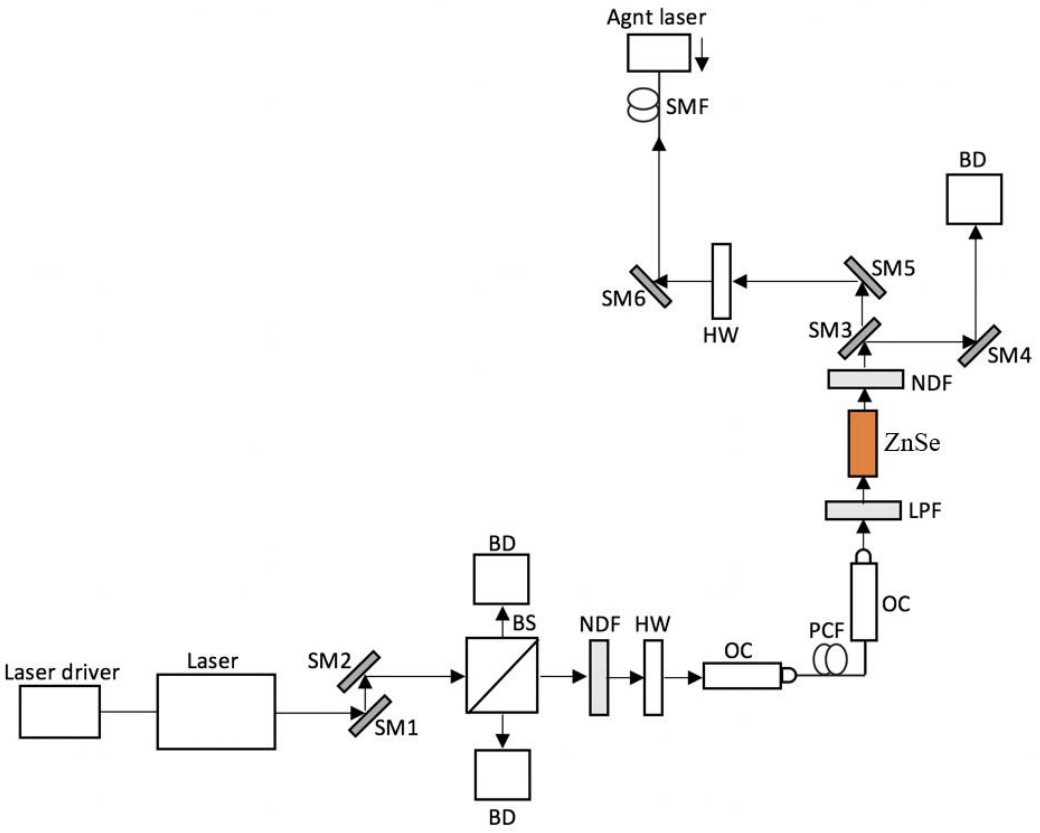

Figure 2.6 The first step for SRS of the Stokes pulse arm is to measure wavelength. Laser - Coherent Fidelity-2 high power femtosecond fiber-based laser, SM1 – silver mirror 1, SM2 – silver mirror 2, SM3 – silver mirror 3 (flipping mirror), SM4 – silver mirror 4, SM5 – silver mirror 5, SM6 – silver mirror 6, BS – beam splitter (30 % transmission and 70 % reflection), BD – beam dumper, HW- half-waveplate, NDF - round step neutral density filter, OC – optical collimator, PCF – photonic crystal filter, LPF – long pass filter ($1150\ nm$), ZnSe – ZnSe crystal, SMF – single mode fiber and Agnt laser – alignment laser (arrow on right indicates the laser beam propagation direction).

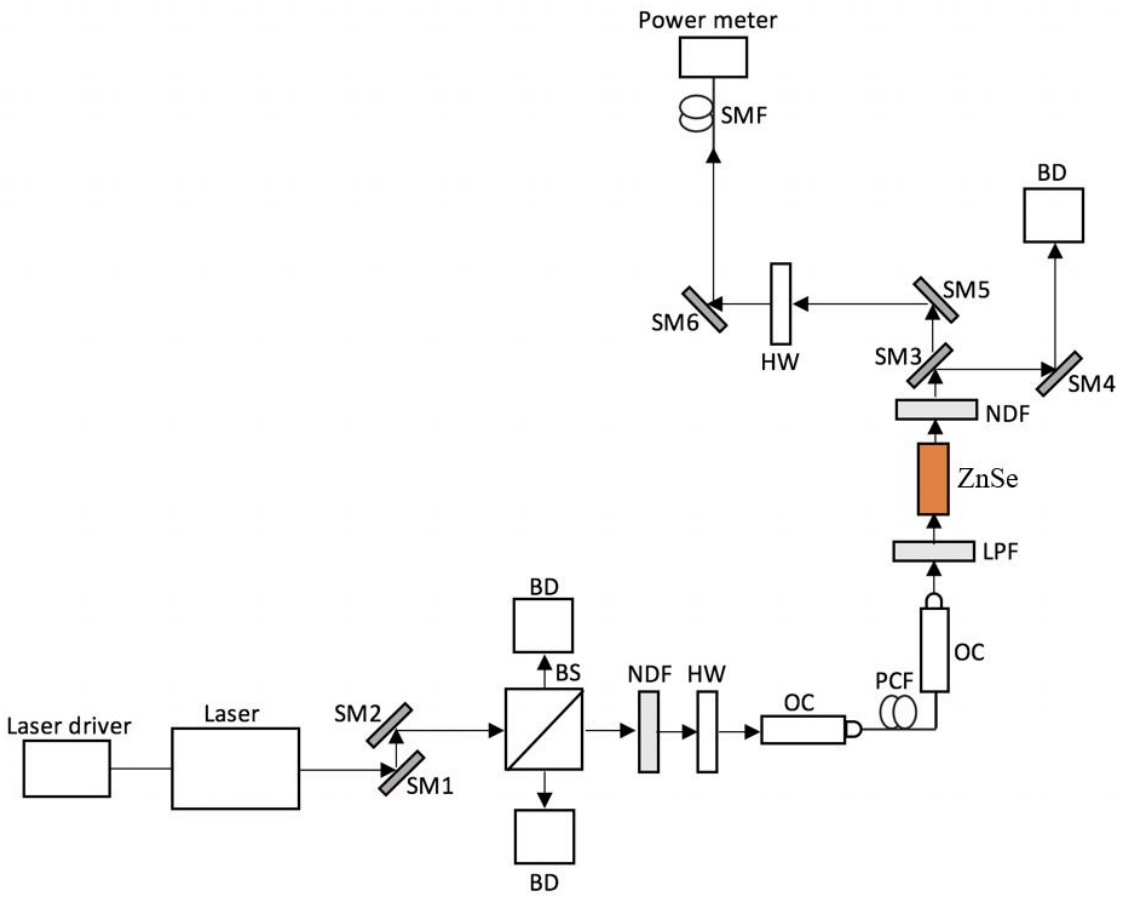

Figure 2.7 The second step for SRS of the Stokes pulse arm is to measure wavelength. Laser - Coherent Fidelity-2 high power femtosecond fiber-based laser, SM1 – silver mirror 1, SM2 – silver mirror 2, SM3 – silver mirror 3 (flipping mirror), SM4 – silver mirror 4, SM5 – silver mirror 5, SM6 – silver mirror 6, BS – beam splitter (30 % transmission and 70 % reflection), BD – beam dumper, HW- half-waveplate, NDF - round step neutral density filter, OC – optical collimator, PCF – photonic crystal filter, LPF – long pass filter ($1150\ nm$), ZnSe – ZnSe crystal, SMF – single mode fiber and Power meter – optical power meter.

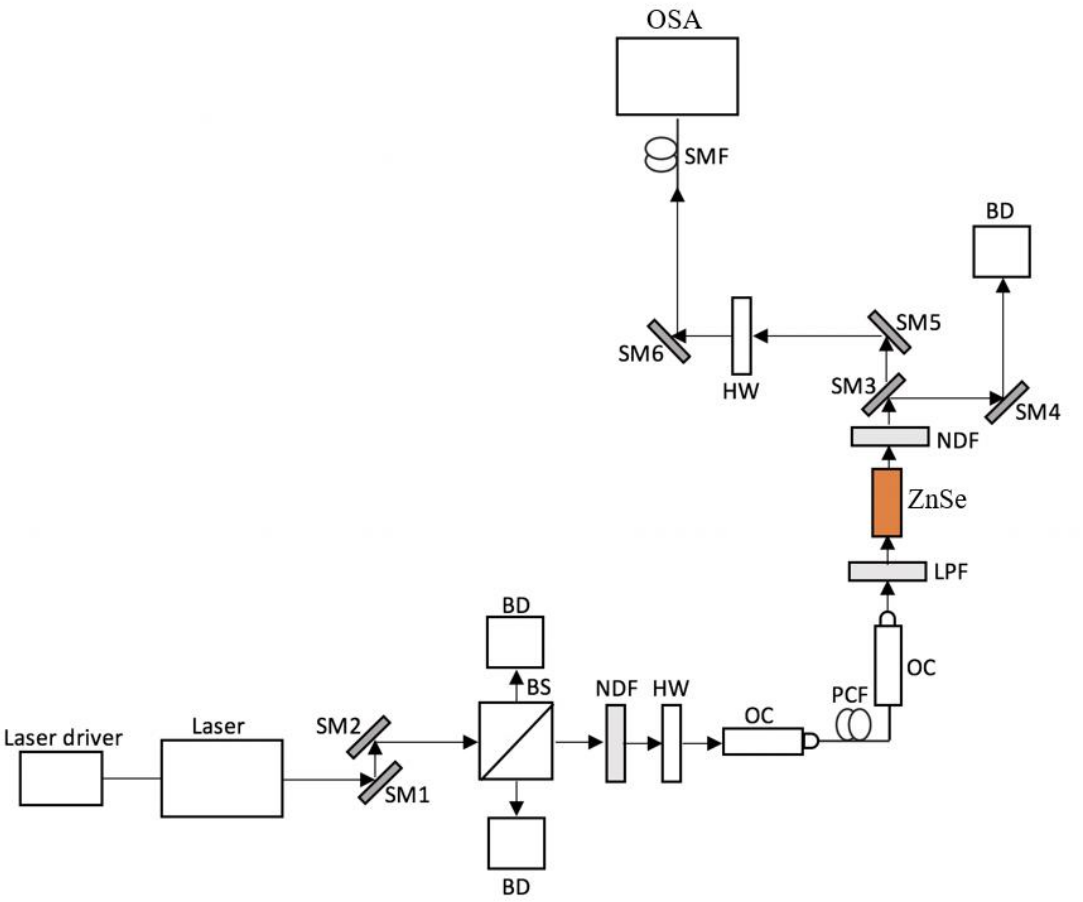

Figure 2.8 The third step for SRS of the Stokes pulse arm is to measure wavelength. Laser - Coherent Fidelity-2 high power femtosecond fiber-based laser, SM1 – silver mirror 1, SM2 – silver mirror 2, SM3 – silver mirror 3 (flipping mirror), SM4 – silver mirror 4, SM5 – silver mirror 5, SM6 – silver mirror 6, BS – beam splitter (30 % transmission and 70 % reflection), BD – beam dumper, HW- half-waveplate, NDF - round step neutral density filter, OC – optical collimator, PCF – photonic crystal filter, LPF – long pass filter (1150 nm), ZnSe – ZnSe crystal, SMF – single mode fiber and OSA - optical spectrum analyzer.

Furthermore, the BD was replaced with FROG in front of the silver mirror 4. Also, the silver mirror 3 was flipped back so that the Stokes pulse beam could be redirected to silver mirror 4 and then to the FROG. The FROG that was used was Grenouille 15-100-USB also referred to as IR Grenouille that can measure the pulse profile in the wavelength range from $1320\ nm$ to $1620\ nm$. Also, it can measure the temporal pulse length from $100\ fs$ to $1000\ fs$. Moreover, it is capable to measure the spectral range of the pulse up to $100\ nm$. Mainly for these reasons it was decided to use this FROG to measure the pulse temporal width for the Stokes pulse arm [15]. Fine adjustments on silver mirrors 3 and 4 were made to make sure that the Stokes pulse beam hit the center of the aperture of the FROG. Next, the FROG was connected to the laptop to view and record the readings of the Stokes pulse broadening. Silver mirror 3 was flipped back and forth to check if the Stokes pulse beam was still on the desired wavelength. Also, it was important to adjust the round step neutral density filter that was placed just after the ZnSe crystal because the FROG is sensitive to optical power. Figure 2.9 depicts the block diagram of this step. After that, the ZnSe crystal was moved away from the Stokes beam pulse path to measure the chirp of the PCF. Figure 2.10 depicts the block diagram of this part.

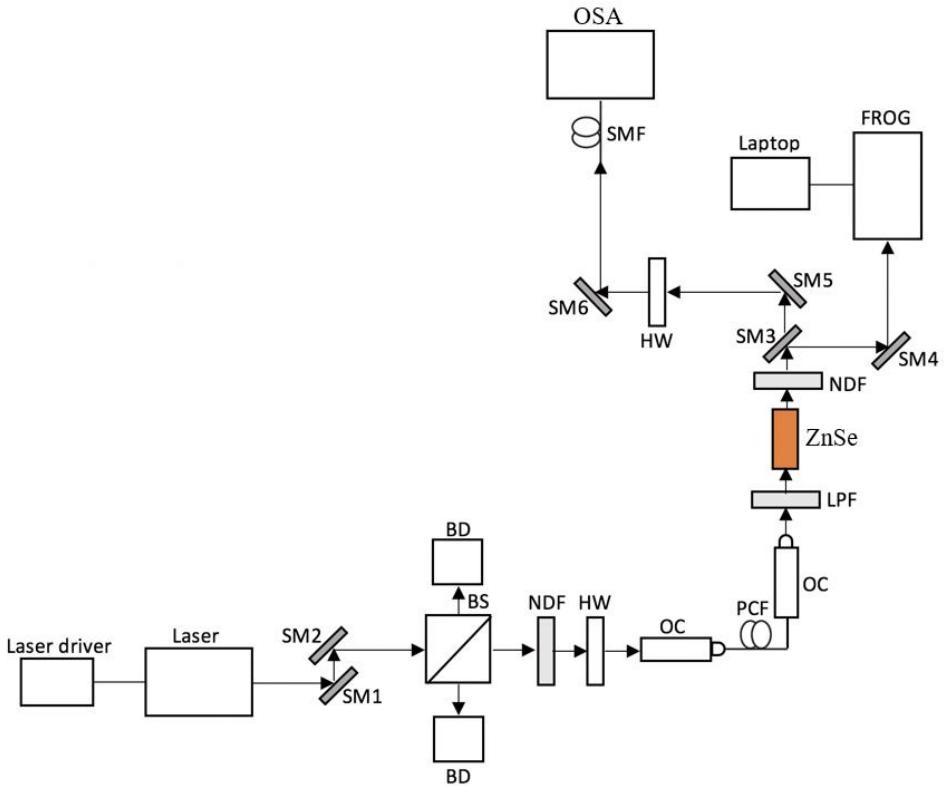

Figure 2.9 The block diagram for the Stokes pulse arm to measure the chirp of the Stokes pulse. Laser - Coherent Fidelity-2 high power femtosecond fiber-based laser, SM1 – silver mirror 1, SM2 – silver mirror 2, SM3 – silver mirror 3 (flipping mirror), SM4 – silver mirror 4, SM5 – silver mirror 5, SM6 – silver mirror 6, BS – beam splitter (30 % transmission and 70 % reflection), BD – beam dumper, HW- half-waveplate, NDF - round step neutral density filter, OC – optical collimator, PCF – photonic crystal filter, LPF – long pass filter ($1150\ nm$), ZnSe – ZnSe crystal, SMF – single mode fiber, OSA – optical spectrum analyzer and FROG – frequency-resolved optical gating.

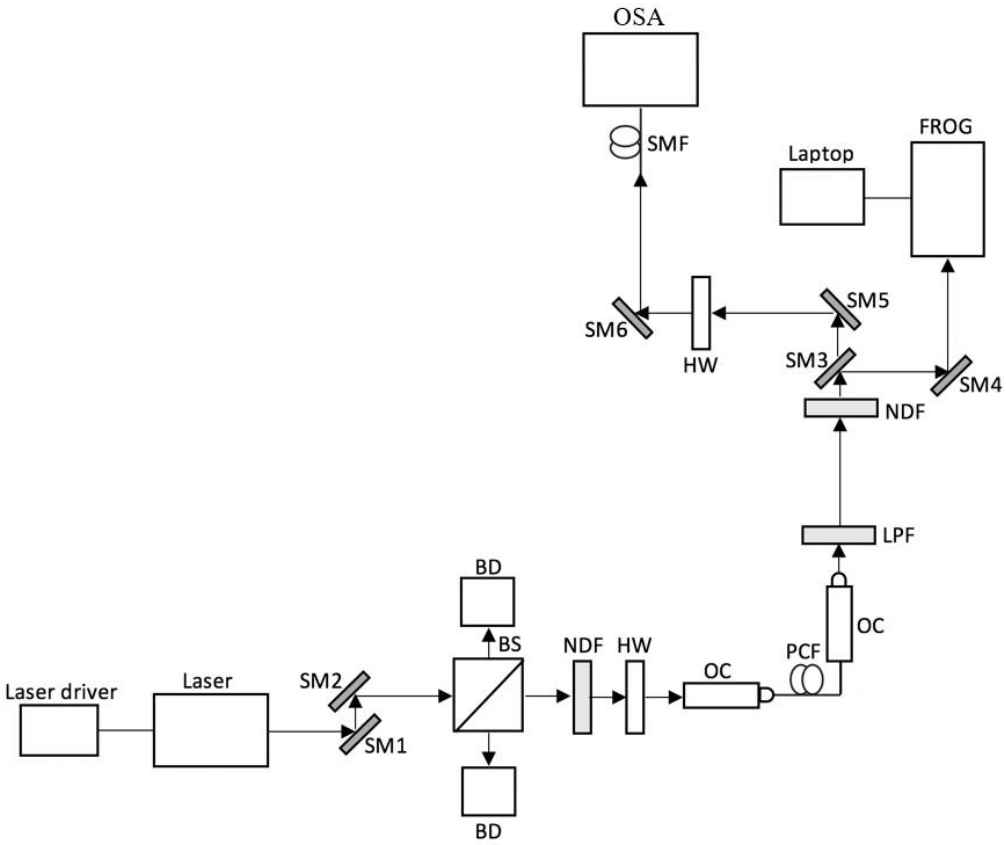

Figure 2.10 The block diagram for the Stokes pulse arm to measure the chirp of the Stokes pulse. Laser - Coherent Fidelity-2 high power femtosecond fiber-based laser, SM1 – silver mirror 1, SM2 – silver mirror 2, SM3 – silver mirror 3 (flipping mirror), SM4 – silver mirror 4, SM5 – silver mirror 5, SM6 – silver mirror 6, BS – beam splitter (30 % transmission and 70 % reflection), BD – beam dumper, HW- half-waveplate, NDF - round step neutral density filter, OC – optical collimator, PCF – photonic crystal filter, LPF – long pass filter ($1150\ nm$), SMF – single mode fiber, OSA – optical spectrum analyzer and FROG – frequency-resolved optical gating.

2.4 The Stokes pulse arm alignment until the dichroic mirror combiner (DMC)

The last step in aligning the Stokes pulse arm was to align this arm till the DMC. To achieve this step the optical spectrum analyzer with the SMF and its mound were removed. Next, FROG as well as silver mirrors 5 and 6 and the round step neutral density filter that were placed in front of the ZnSe crystal have been taken out. Moreover, positions of silver mirrors 3 and 4 were changed to redirect the Stokes pulse beam. After that, the DMC was placed in front of the silver mirror 4. The LPF was placed before the DMC. The DMC had the cutoff wavelength of 1180 nm, so it served as the filer and combiner. Also, to redirect the Stokes pulse beam to the desired position on the DMC fine adjustments were made on silver mirrors 3 and 4. Figure 2.11 depicts the block diagram of the final setup of the Stokes pulse arm.

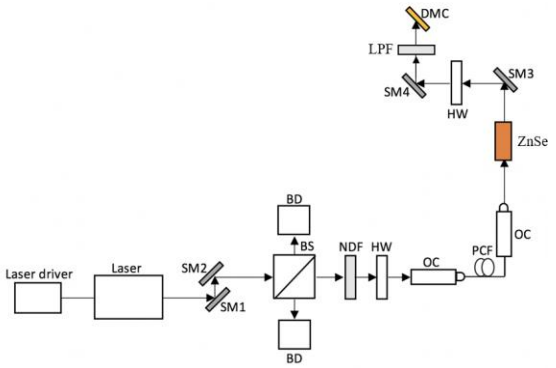

Figure 2.11 The final setup for SRS spectroscopy of the Stokes pulse arm. Laser - Coherent Fidelity-2 high power femtosecond fiber-based laser, SM1 – silver mirror, SM2 – silver mirror 2, SM3 – silver mirror3, SM4 – silver mirror 4, BS – beam splitter (30 % transmission and 70 % reflection), BD – beam dumper, HW- half-waveplate, NDF - round step neutral density filter, OC – optical collimator, PCF – photonic crystal filter, ZnSe – ZnSe crystal, LPF – long pass filter (1150 nm), and DMC – dichroic mirror combiner (1180 nm).

2.5 The pump pulse arm alignment for the pump pulse wavelength measurement

The first step in building and aligning the pump pulse arm was to measure the wavelength of the pump pulse beam. To achieve this the Stokes pulse arm was disconnected by placing the beam dumper in the transmission path of the beam after the beam splitter that transmitted 30 % and reflected 70 % of the laser beam. Then the silver mirror 3 was placed in front of the beam splitter to direct the beam to the SMF which was placed on the mount. Next, a round step neutral density filter was placed in between the silver mirror 3 and the SMF to control the pump pulse beam intensity and power that enters the SMF. The reason for that was that the SMF could be damaged if too much power would enter. Furthermore, to make sure that the pump pulse beam was aligned properly with the SMF the alignment laser was connected to the SMF. Next, the laser source and the alignment laser were turned on. Next, the IR card was used to trace if two beams meet at the same spot on the path between the SMF and the silver mirror 3. Some fine adjustments were made on silver mirror 3 and the SMF mount. Figure 2.12 depicts the block diagram of this step. Then, the alignment laser was replaced with an optical power meter. The SMF mound and the silver mirror 3 were adjusted till the maximum power readings have been seen on an optical power meter screen. Figure 2.13 depicts the block diagram of this procedure. Next, an optical power meter was replaced with an optical spectrum analyzer. Figure 2.14 depicts the block diagram of this process. The measured spectrum of the pump pulse beam had two peaks. Larger in amplitude peak was at $1078\ nm$ and smaller in amplitude peak was at $1050\ nm$. It was noted that the peak that was at $1050\ nm$ came from the alignment mode and the peak at $1078\ nm$ came from the high power mode. Hence, the peak at $1078\ nm$ was used as the pump pulse wavelength

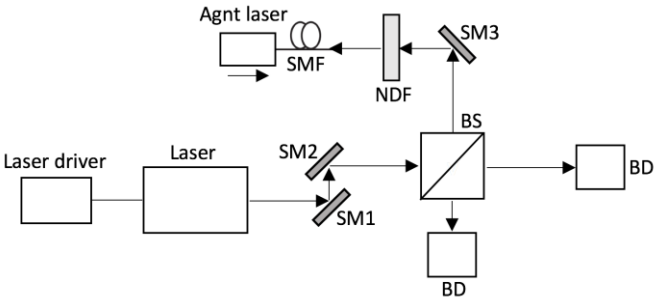

Figure 2.12 Block diagram for making sure that the pump pulse beam was properly aligned with the SMF by using an alignment laser. Laser - Coherent Fidelity-2 high power femtosecond fiber-based laser, SM1 – silver mirror 1, SM2 – silver mirror 2, SM3 – silver mirror 3, BS – beam splitter (30 % transmission and 70 % reflection), BD – beam dumper, NDF - round step neutral density filter, SMF – single mode fiber and Agnt laser – alignment laser (arrow bellow indicates the laser beam propagation direction).

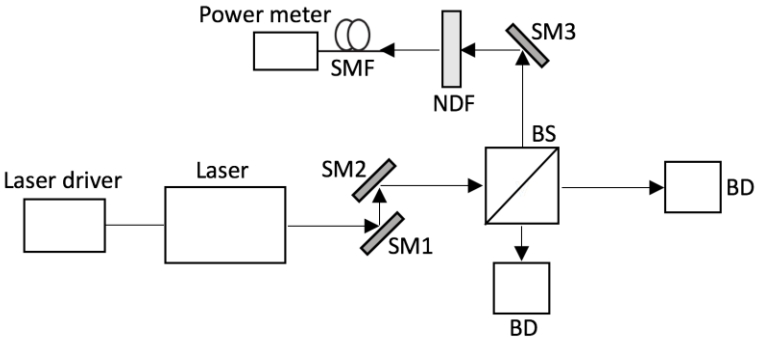

Figure 2.13 Block diagram for making sure that the pump pulse beam was properly aligned with the SMF by using an optical power meter. Laser - Coherent Fidelity-2 high power femtosecond fiber-based laser, SM1 – silver mirror 1, SM2 – silver mirror 2, SM3 – silver mirror 3, BS – beam splitter (30 % transmission and 70 % reflection), BD – beam dumper, NDF - round step neutral density filter, SMF – single mode fiber and Power meter – optical power meter.

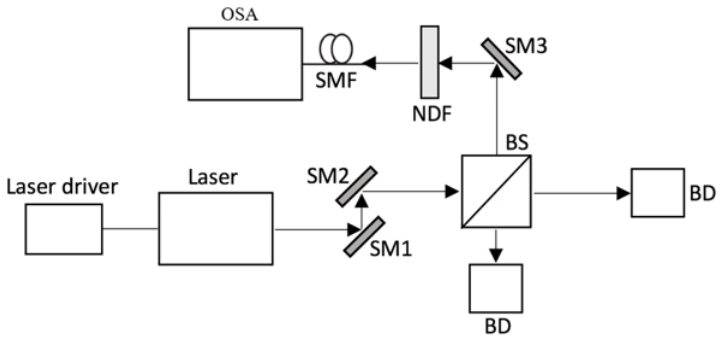

Figure 2.14 Block diagram of measuring the pump pulse beam wavelength by the optical spectrum analyzer. Laser - Coherent Fidelity-2 high power femtosecond fiber-based laser, SM1 – silver mirror 1, SM2 – silver mirror 2, SM3 – silver mirror 3, BS – beam splitter (30 % transmission and 70 % reflection), BD – beam dumper, NDF - round step neutral density filter, SMF – single mode fiber and OSA – optical spectrum analyzer.

2.6 The pump pulse arm alignment for the pump pulse broadening or chirping by SF6 crystal

The next step in building the pump pulse arm was to measure the pulse broadening or chirping by using a nonlinear crystal. The crystal was picked to be SF6 to chirp the pump pulse that had a central wavelength at $1078\ nm$. The reason for using this crystal was because it had the desired optical properties for the pump pulse to be broadened or chirped. The transmission spectrum of SF6 crystal is in the range from around $480\ nm$ to $2600\ nm$. Also, the refractive index of the SF6 crystal at $1078\ nm$ wavelength is about 1.77 and the chromatic dispersion is $192.14 \frac{ps}{nm \cdot km}$ [16,17]. Figure 2.15 illustrates the SF6 crystal and its dimensions.

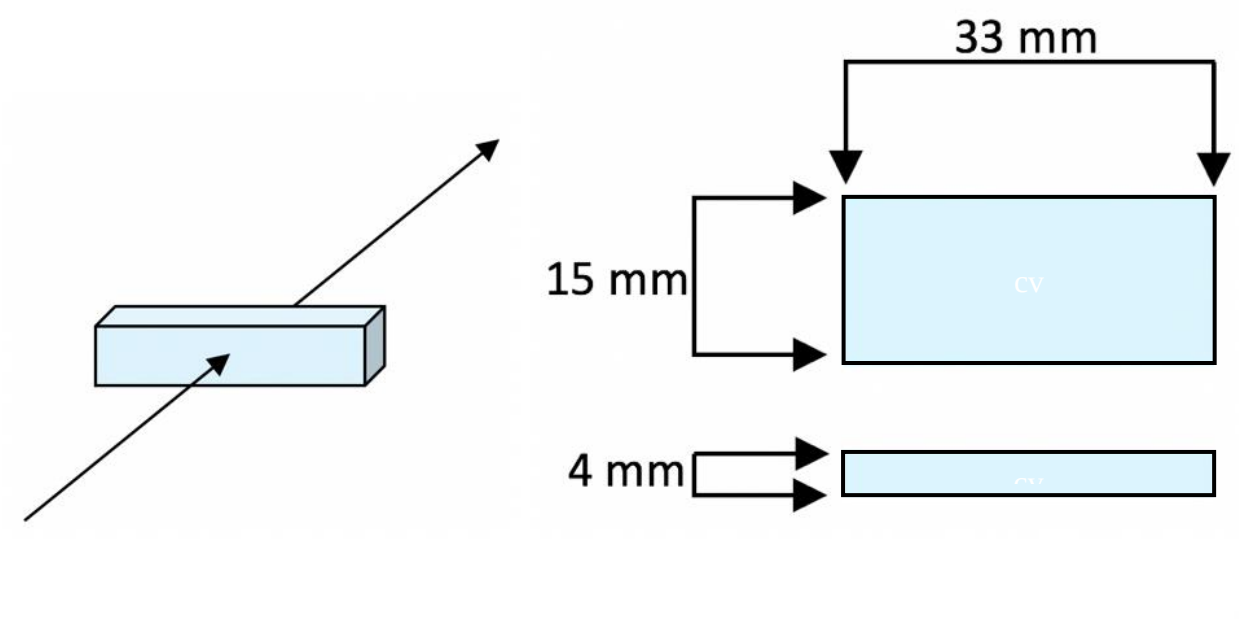

Figure 2.15 SF6 crystal and indication of entering and leaving positions of the beam, the height, the width, and the length are 4 mm, 33 mm and 15 mm, respectively [13].

After the crystal was picked, the experimental setup has been continued. Firstly, a half-wave plate was placed between the silver mirror 2 and the beam splitter that transmitted 30 % and reflected 70 % of the laser beam. The reflected portion of the laser beam served as the pump pulse beam. Furthermore, silver mirrors 3, 4, and 5 were placed after the beam splitter to redirect the pump beam to the FROG aperture which was placed in front of the silver mirror 5. Then, the FROG was connected to the laptop to get the data from the FROG. The FROG that was used to measure and observe the broadening of the pump pulse was Grenouille 8-50-USB which is also referred to as near-IR Grenouille that can measure the pulse profile in the wavelength range from 700 nm to 1100 nm. Moreover, it can measure the temporal pulse width in the range from 50 fs to 500 fs at 1050 nm. Furthermore, it can record the spectral range up to 125 nm at 1050 nm [18].

Moreover, SF6 crystal of 15 mm length and round step neutral density filter was placed in between silver mirrors 3 and 4. Then the silver mirror 3 was adjusted till the pump pulse beam was passing through the SF6 crystal and was hitting the center of the silver mirror 4. The purpose of the round step neutral density filter was to control the optical power of the pump pulse beam or the pump pulse beam intensity that enters the FROG because it is sensitive to optical power. Next, silver mirrors 4 and 5 were adjusted till the pump pulse beam was centered to the FROG aperture. The data was collected and recorded. Figure 2.16 depicts the block diagram of this setup.

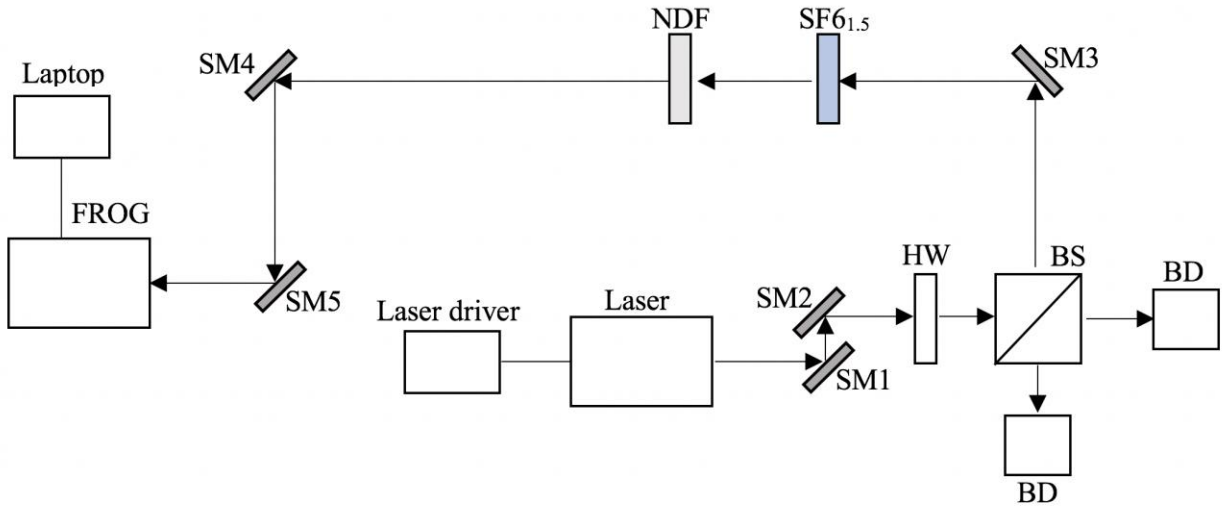

Figure 2.16 Setup for chirp measurement for 1.5 cm length SF6 crystal (beam propagates through crystal one time). Laser - Coherent Fidelity-2 high power femtosecond fiber-based laser, SM1 – silver mirror 1, SM2 – silver mirror 2, SM3 – silver mirror 3, SM4 – silver mirror 4, SM5 – silver mirror 5, BS – beam splitter (30 % transmission and 70 % reflection), BD – beam dumper, NDF - round step neutral density filter, SF6$_{1.5}$ - 1.5 cm length SF6 crystal, HW – half-waveplate and FROG – frequency-resolved optical gating.

Next, the second SF6 crystal that had the same dimensions was placed in between SF6 crystal and round step neutral density filter. The reason for this step was to collect and record the pump pulse broadening while the pump pulse beam was propagating through the total of 30 mm length of the SF6 crystal. Figure 2.17 depicts the block diagram of this step.

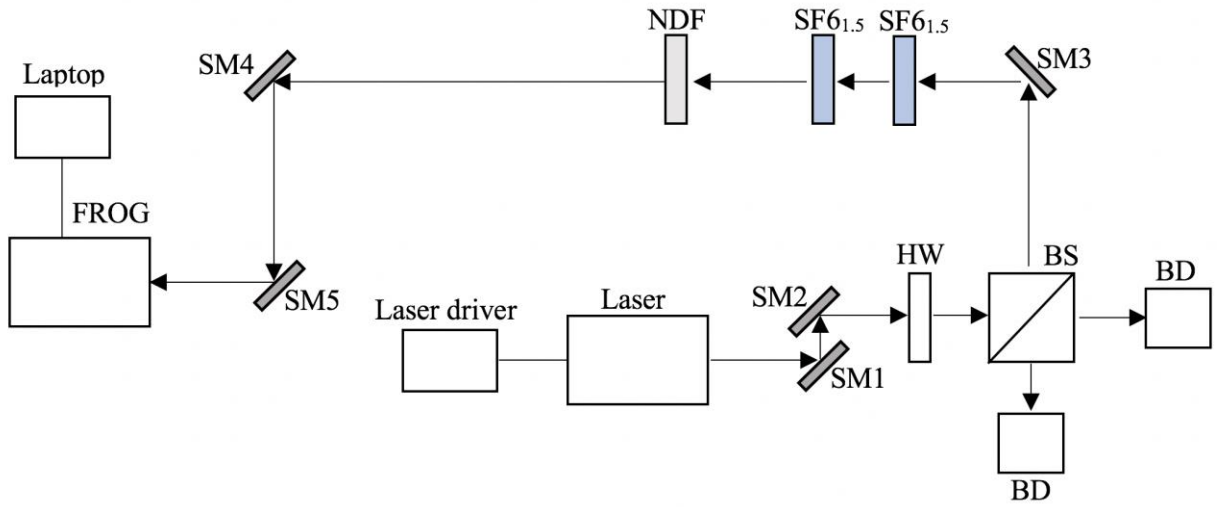

Figure 2.17 Setup for chirp measurement for two 1.5 cm length SF6 crystals (beam propagates through each crystal one time). Laser - Coherent Fidelity-2 high power femtosecond fiber-based laser, SM1 – silver mirror 1, SM2 – silver mirror 2, SM3 – silver mirror 3, SM4 – silver mirror 4, SM5 – silver mirror 5, BS – beam splitter (30 % transmission and 70 % reflection), BD – beam dumper, NDF - round step neutral density filter, SF6$_{1.5}$ - 1.5 cm length SF6 crystal, HW – half-waveplate and FROG – frequency-resolved optical gating.

Furthermore, to measure the chirp effect of the SF6 crystal the next setup was used. This time the pump pulse beam was passing through the crystal two times. To achieve this more mirrors were placed to redirect the path of the pump pulse beam. Next, two SF6 crystals were removed from the setup from Figure 2.17. Moreover, silver mirrors 4 and 5 were placed in a way that they would

make a 90° angle so that the pump pulse beam could hit silver mirrors 4 and 5 and come back in a parallel fashion. Then one of the SF6 crystals was placed in front of the round step neutral density filter so that the pump pulse beam would pass through it two times. Next, silver mirrors 6, 7, and 8 were placed to guide the pump pulse beam to the center of the aperture of the FROG. The data was collected and recorded. Figure 2.18 illustrates the block diagram of this setup.

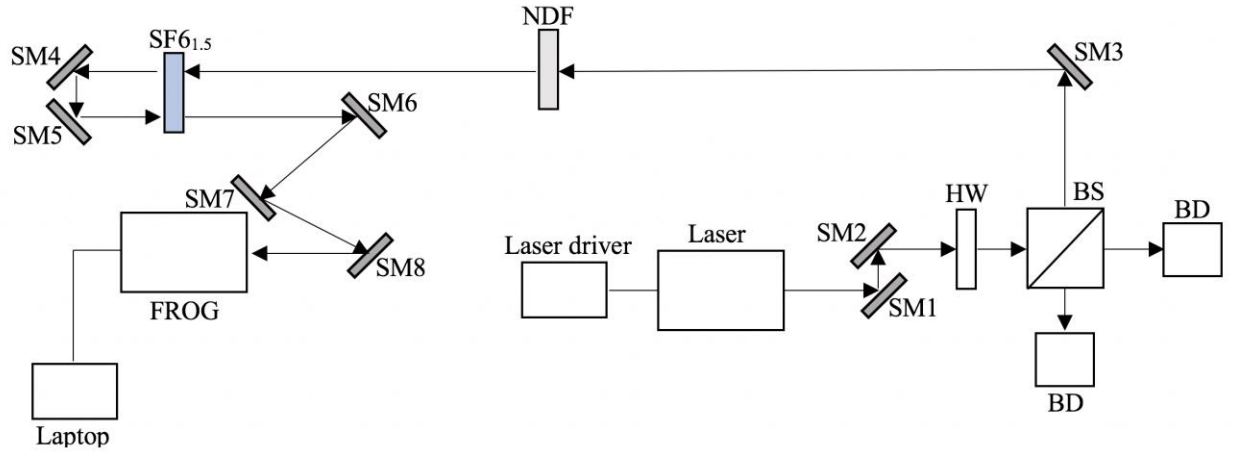

Figure 2.18 Setup for chirp measurement for 1.5 cm length SF6 crystal (beam propagates through each crystal two times. Laser - Coherent Fidelity-2 high power femtosecond fiber-based laser, SM1-8 – silver mirror 1-8, BS – beam splitter (30 % transmission and 70 % reflection), BD – beam dumper, NDF - round step neutral density filter, SF6$_{1.5}$ - 1.5 cm length SF6 crystal, HW – half-waveplate and FROG – frequency-resolved optical gating.

Moreover, the second SF6 crystal was placed in between silver mirrors 6 and 7 to increase the path of the pump pulse beam that would propagate through the SF6 crystal. Again, the data was collected and recorded. Figure 2.19 depicts the block diagram of this step.

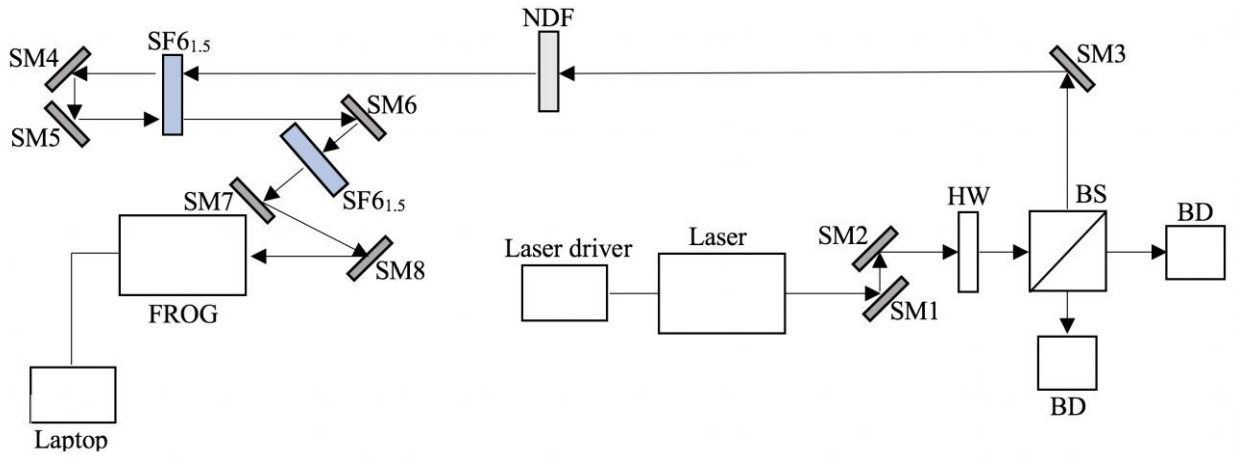

Figure 2.19 Setup for chirp measurement for two $1.5\,cm$ length SF6 crystals (beam propagates through one crystal two times and through another one time). Laser - Coherent Fidelity-2 high power femtosecond fiber-based laser, SM1-8 – silver mirror 1-8, BS – beam splitter (30 % transmission and 70 % reflection), BD – beam dumper, NDF - round step neutral density filter, SF6$_{1.5}$ - $1.5\,cm$ length SF6 crystal, HW – half-waveplate and FROG – frequency-resolved optical gating.

2.7 The pump pulse arm alignment for the pump pulse broadening or chirping by Pockels cell and two SF6 crystals

After measuring the pump pulse broadening by using SF6 crystals it was decided to measure how much broadening or chirping the Pockels cell (PC) was used. The PC that was used was model 350-105 from Conopics. This PC is an electro-optic modulator which is a transverse field type, meaning that the electric field produced by the applied signal voltage is perpendicular to the optical propagation direction. The nonlinear crystal inside the PC is KDP crystal of length of $105\,mm$. Moreover, this crystal wavelength limits are from $240\,nm$ to $1100\,nm$ [19]. To achieve the chirp measurement for the PC some changes were made in the setup for the pump pulse arm. Firstly, all components were removed after the silver mirror 3. Next, the half-waveplate

was moved from being placed after the silver mirror 2 to the location after the $30/70$ beam splitter. Next, the polarizing beam splitter (PBS) was placed after the half-waveplate. The purpose of the PBS was to reduce the power of the pump pulse beam, which was too powerful, and could damage the sample. Hence, by rotating the half-wave plate the polarization of the beam was controlled. Furthermore, as the PBS was transmitting the horizontally polarized light which was the same polarization as the laser source. On the other hand, the PBS was reflecting the vertically polarized light. Furthermore, two more beam dumpers were placed on both sides of the PBS to dump the reflected beams. Then the silver mirror 3 was placed in the way that the pump pulse beam would go from the silver mirror 3 and then through the center of the PC aperture. Next, a round step neutral density filter and the CCD camera were placed after the PC. The purpose of this round step neutral density filter was to reduce the optical power of the pump pulse beam that would enter the CCD camera. The CCD camera was connected to the laptop. The CCD camera was used to make sure that the pump pulse beam profile was still Gaussian after the PC. The name of the camera was LaserCam-HR from Coherent. This camera is a high-resolution laser beam profiling system with a spectral range from $300\ nm$ to $1100\ nm$. Also, it operates for a pulse and constant wave laser beams [20]. Fine adjustments were made on the silver mirror 3 to redirect the pump pulse beam that would propagate directly through the nonlinear crystal of the PC until it was seen the proper Gaussian beam profile on the laptop screen. Figure 2.20 depicts the block diagram of the setup for this step. At this point, the laser source was operating on the high power mode.

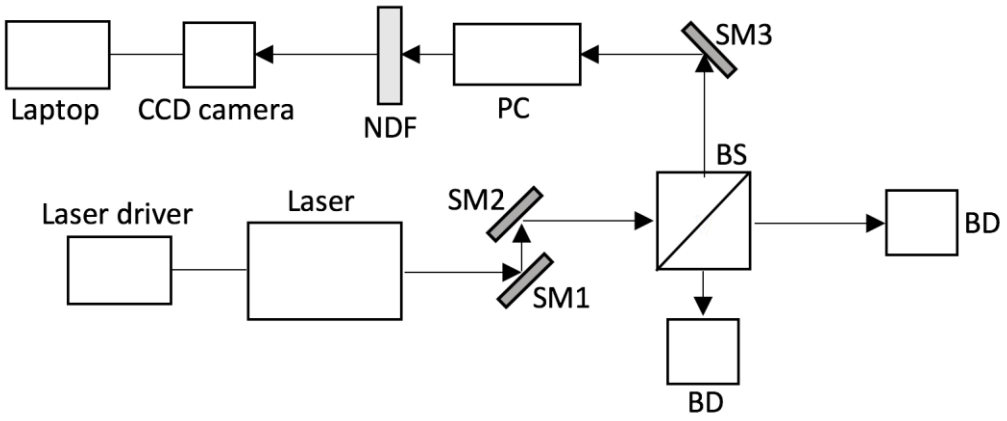

Figure 2.20 The block diagram for checking the pump pulse beam profile by using a CCD camera. Laser - Coherent Fidelity-2 high power femtosecond fiber-based laser, SM1 – silver mirror 1, SM2 – silver mirror 2, SM3 - silver mirror 3, BS – beam splitter (30 % transmission and 70 % reflection), BD – beam dumper, CCD camera – changer coupled device camera, PC- Pockels cell and NDF - round step neutral density filter.

After it was made sure that the pump pulse beam profile was Gaussian the CCD camera was removed from the setup. Then, silver mirrors 4 and 5 were placed in the pump pulse beam's path. Moreover, the FROG was placed in front of the silver mirror 4. Next, the FROG was connected to the laptop. The purpose of placing the FROG was to measure how much broadening or chirping the pump pulse beam experienced after the PC. The data from the FROG was recorded and collected. Figure 2.21 depicts the block diagram of this setup.

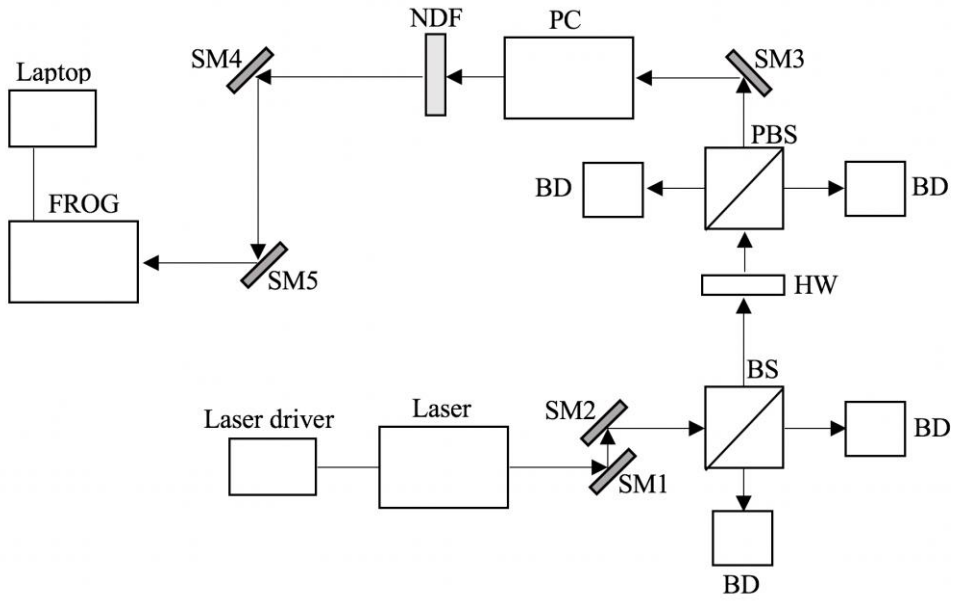

Figure 2.21 Setup for chirp measurement for the Pockels cell. Laser - Coherent Fidelity-2 high power femtosecond fiber-based laser, SM1 – silver mirror 1, SM2 – silver mirror 2, SM3 - silver mirror 3, SM4 – silver mirror 4, SM5 – silver mirror 5, BS – beam splitter (30 % transmission and 70 % reflection), PBS – polarized beam splitter, HW- half-waveplate, BD – beam dumper, PC- Pockels cell and NDF - round step neutral density filter and FROG - frequency-resolved optical gating.

After that, 15 mm length SF6 crystal was placed in between silver mirrors 4 and 5 so that the pump pulse beam would go through it. Again, the FROG was used to collect and record the data for the pump pulse beam broadening. Figure 2.22 depicts the block diagram of this setup. Next, the second 15 mm SF6 crystal was placed after the first one. The data was again collected and recorded by the FROG. Figure 2.23 depicts the block diagram of this procedure.

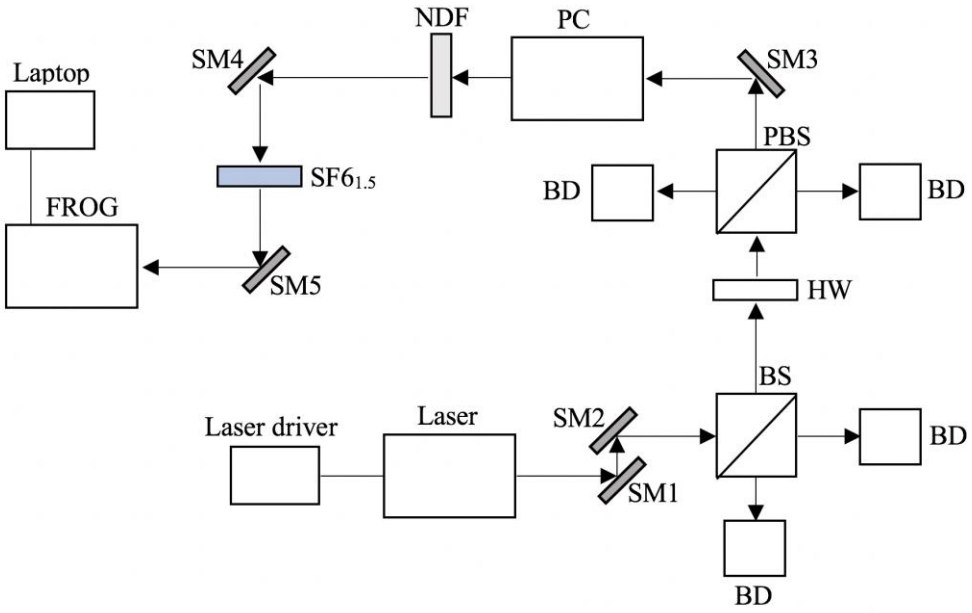

Figure 2.22 Setup for chirp measurement for the Pockels cell with one 1.5 cm length SF6 crystal. Laser - Coherent Fidelity-2 high power femtosecond fiber-based laser, SM1 – silver mirror 1, SM2 – silver mirror 2, SM3 - silver mirror 3, SM4 – silver mirror 4, SM5 – silver mirror 5, BS – beam splitter (30 % transmission and 70 % reflection), PBS – polarized beam splitter, HW- half-waveplate, BD – beam dumper, PC- Pockels cell and NDF - round step neutral density filter, SF6$_{1.5}$ – 1.5 cm length SF6 crystal and FROG - frequency-resolved optical gating.

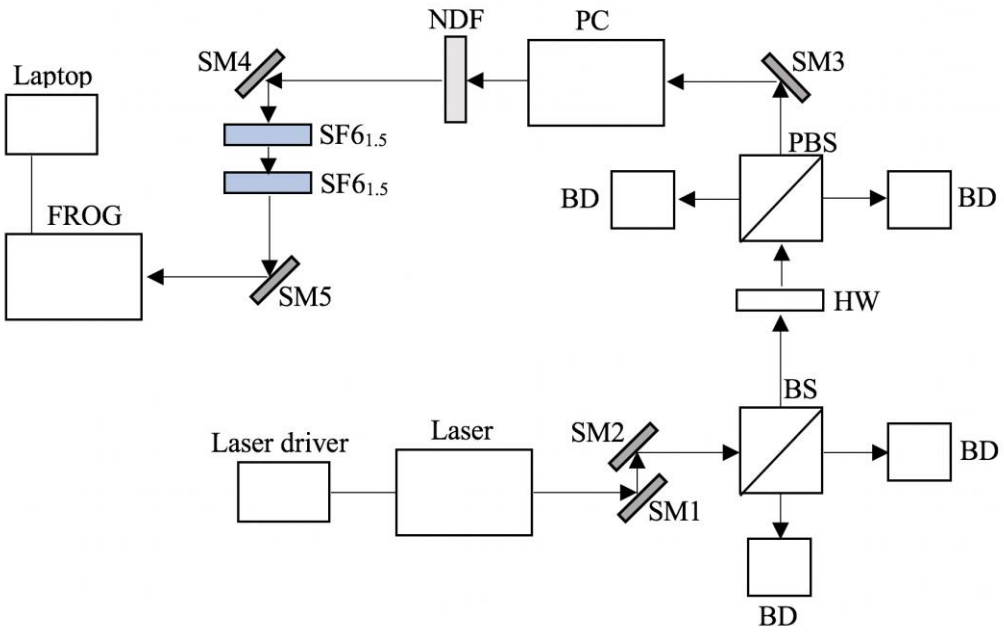

Figure 2.23 Setup for chirp measurement for the Pockels cell with two 1.5 cm length SF6 crystal. . Laser - Coherent Fidelity-2 high power femtosecond fiber-based laser, SM1 – silver mirror 1, SM2 – silver mirror 2, SM3 - silver mirror 3, SM4 – silver mirror 4, SM5 – silver mirror 5, BS – beam splitter (30 % transmission and 70 % reflection), PBS – polarized beam splitter, HW- half-waveplate, BD – beam dumper, PC- Pockels cell and NDF - round step neutral density filter, SF6$_{1.5}$ – 1.5 cm length SF6 crystal and FROG - frequency-resolved optical gating.

2.8 The pump pulse arm alignment until the DMC

The last part for the pump pulse arm was to build and align it until the DMC. Hence, all components and instruments after the PC were removed. Then, the SF6 crystal rod was placed after the PC. Moreover, roughly two thirds of the ends of the SF6 crystal rod was covered by the gold coating. The purpose of covering the ends with gold was to let the beam inside be reflected to increase the path the beam in the crystal if needed. The reason for the SF6 crystal was to broaden

the pump pulse beam to the desired temporal pulse width. Figure 2.24 depicts the SF6 crystal rod with the places where the pump pulse beam enters and leaves as well as rods dimensions.

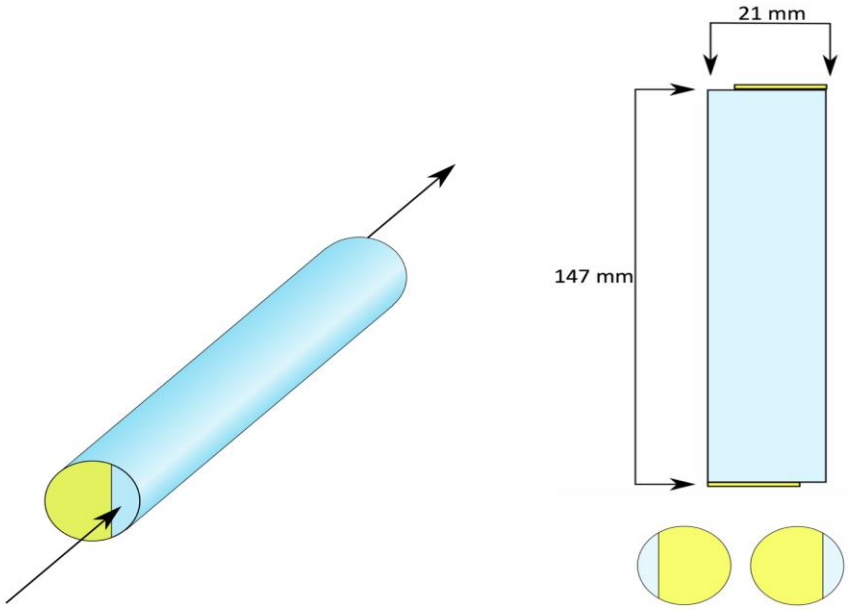

Figure 2.24 SF6 crystal rod and an indication of entering and leaving positions of the beam, the diameter and the length of the crystal are 21 mm and 147 mm, respectively [13].

Moreover, as the Stokes pulse beam was broadened to around one picosecond, the pump pulse beam had to be broadened to one picosecond as well. The reason for this is to achieve the best possible spectral resolution for the SRS or CARS spectroscopies. The length L_p of the SF6 crystal needed to achieve this amount of broadening was calculated to be as follows

$$\Delta\tau_g = D_p \cdot L_p \cdot \delta\lambda_p \tag{2.4}$$

$$1.0 = 192.14 \frac{ps}{nm \cdot km} \cdot L_p \cdot 30nm \tag{2.5}$$

$$L_p = 0.173m = 173mm \tag{2.6}$$

where the pulse width of the pump pulse beam $\delta\lambda_p$ was measured by using the optical spectrum analyzer to be $30\,nm$ and the chromatic dispersion coefficient D_p was observed to be $192.14\ \frac{ps}{nm \cdot km}$ from the database [17]. Hence, to broaden the pump pulse beam to around one picosecond SF6 crystal rod as well as two $15\,mm$ in length SF6 crystals were placed in the propagation path of the pump pulse beam. Next, silver mirrors 6 and 7 were placed to redirect the pump pulse beam to the electrically controlled delay line that had silver mirrors 8 and 9 mounted on it. The purpose of this delay line was to compensate for the time difference in arriving time between the Stokes pulse and the pump pulse. The arriving time differences came from the fact that the Stokes pulse and the pump pulse propagated through different materials. Also, silver mirrors 8 and 9 were placed in the way to redirect the pump pulse beam to the CCD camera. In between two round step neutral density filters, the LPF with a cutoff wavelength of $1050\ nm$ and the polarizer were placed. The purpose of the LPF was to filter out an alignment mode pulse peak that was measured to be at 1070 nm. Also, the reason for placing a polarized was to adjust the pump pulse beam to the desired optical axis. In addition, to reduce the optical power that would enter the CCD camera two round step neutral density filters were placed. Moreover, a CCD camera was used to make sure that the pump pulse beam profile was still Gaussian and was not changing in space while moving the delay line. Figure 2.25 depicts the block diagram of this setup. The delay line was an electrically controlled delay line (ECDL) that could make the path of the pump pulse beam longer or shorter if needed. The ECDL was constructed by using two silver mirrors that were placed in a way that would form a 90° angle between them and by using a motor stage. The motor stage that was used was Sigma Koki SGSP26-100 linear stepping motor stage. This stage travels in the z-direction by covering $100\ mm$ distance and can be controlled by a computer [21].

Furthermore, to make sure that the pump pulse beam was operating at desired 1078 nm wavelength and that the LPF of $1050\ nm$ cutoff wavelength was working the optical spectrum analyzer with the SMF were used. To achieve this, first, the mount with the SMF was placed and the alignment laser was connected to the SMF. Figure 2.26 depicts the block diagram of this step. Then, silver mirrors 8 and 9 were adjusted as well as the SMF position by using the mount. The IR card was used to trace if the alignment laser beam and the pump pulse beam meet at the same position on the card. The card was moved from the silver mirror 9 to the SMF mount. Next, the alignment laser was replaced with an optical power meter. The fine adjustments on the silver mirror 9 and the mount of the SMF were made till the maximum power readings have been seen on an optical power meter screen. Figure 2.27 illustrates the block diagram of this setup. Furthermore, an optical power meter was replaced with the optical spectrum analyzer to measure the optical spectrum of the pump pulse beam. Figure 2.28 depicts the block diagram of the setup of measuring the pump pulse beam wavelength.

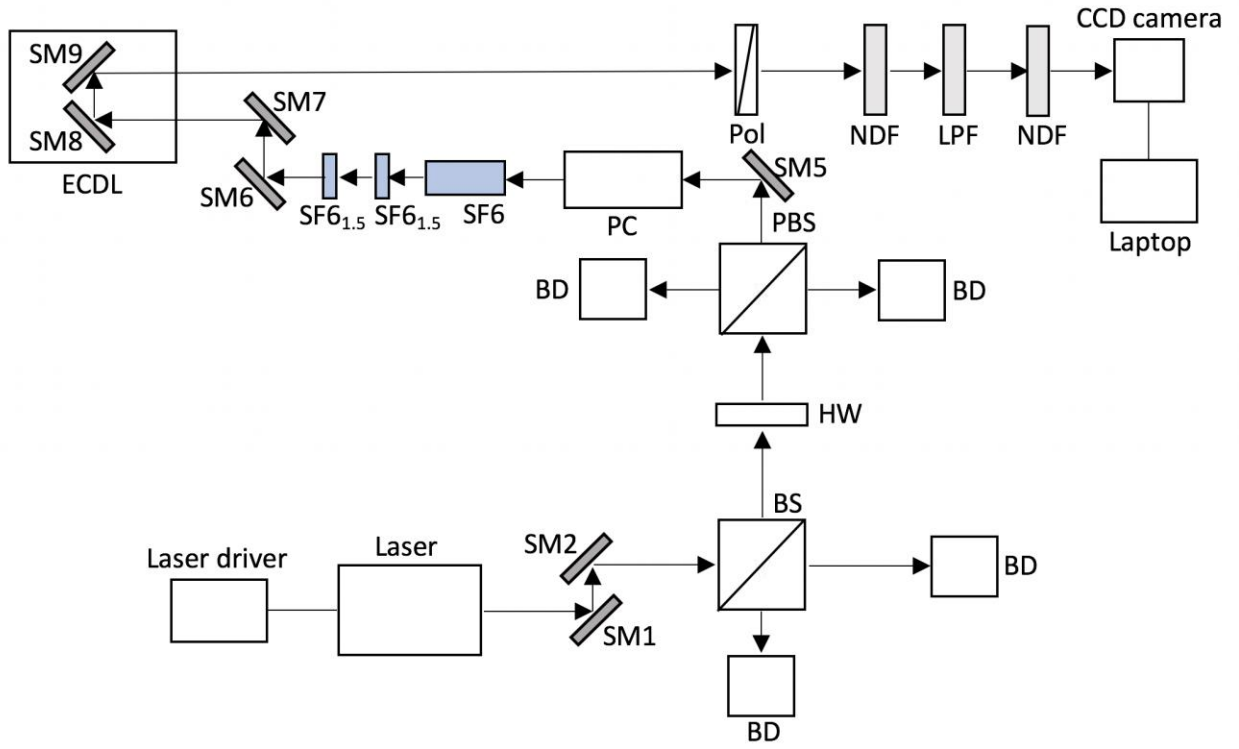

Figure 2.25 The block diagram for the pump pulse arm to check if the pulse shape is Gaussian by using charged coupled device camera (CCD camera). Laser - Coherent Fidelity-2 high power femtosecond fiber-based laser, SM1-9 – silver mirror 1-9, BS – beam splitter (30 % transmission and 70 % reflection), BD – beam dumper, HW – half-waveplate, PBS – polarizing beam splitter, PC – Pockels cell, SF6 – SF6 crystal rod, SF6$_{1.5}$ – 1.5 cm length SF6 crystal, ECDL – electronically controlled delay line, Pol – polarizer, CCD camera – changer coupled device camera, NDF - round step neutral density filter and LFP – long pass filter ($1050\ nm$).

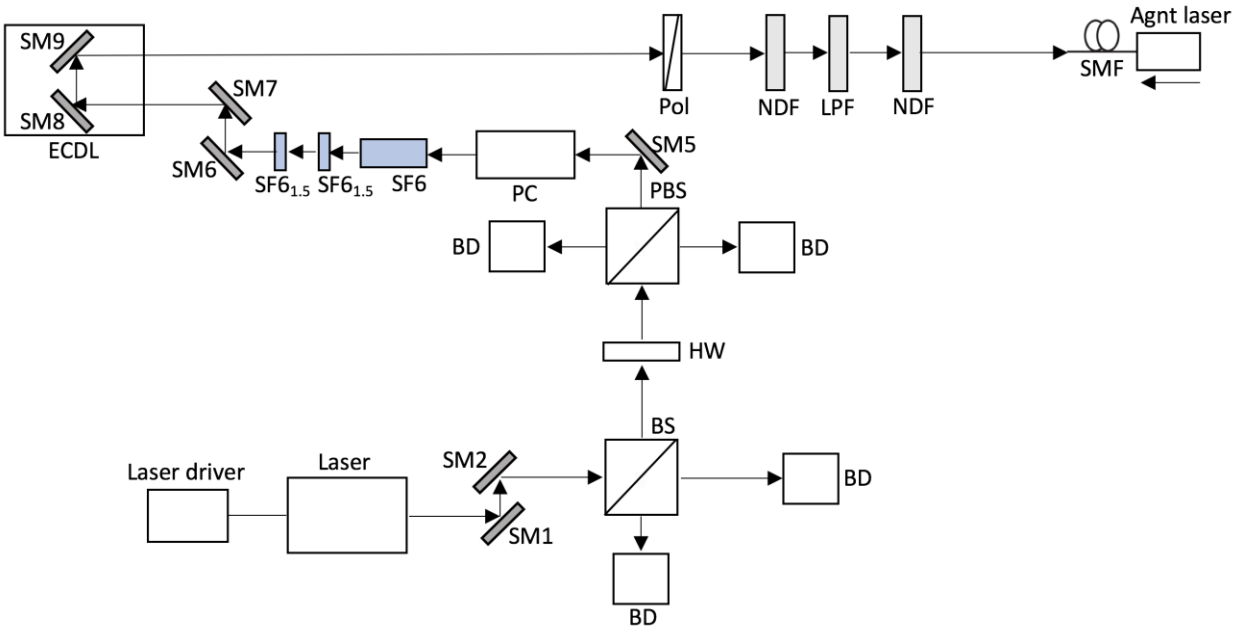

Figure 2.26 The block diagram for checking if the pump pulse beam hits the SMF at the desired location by using an alignment laser. Laser - Coherent Fidelity-2 high power femtosecond fiber-based laser, SM1-9 – silver mirror 1-9, BS – beam splitter (30 % transmission and 70 % reflection), BD – beam dumper, HW – half-waveplate, PBS – polarizing beam splitter, PC – Pockels cell, SF6 – SF6 crystal rod, SF6$_{1.5}$ – 1.5 cm length SF6 crystal, ECDL – electronically controlled delay line, Pol – polarizer, NDF - round step neutral density filter and LFP – long pass filter ($1050\ nm$), SMF – single mode fiber and Agnt laser – alignment laser (arrow bellow indicates the laser beam propagation direction).

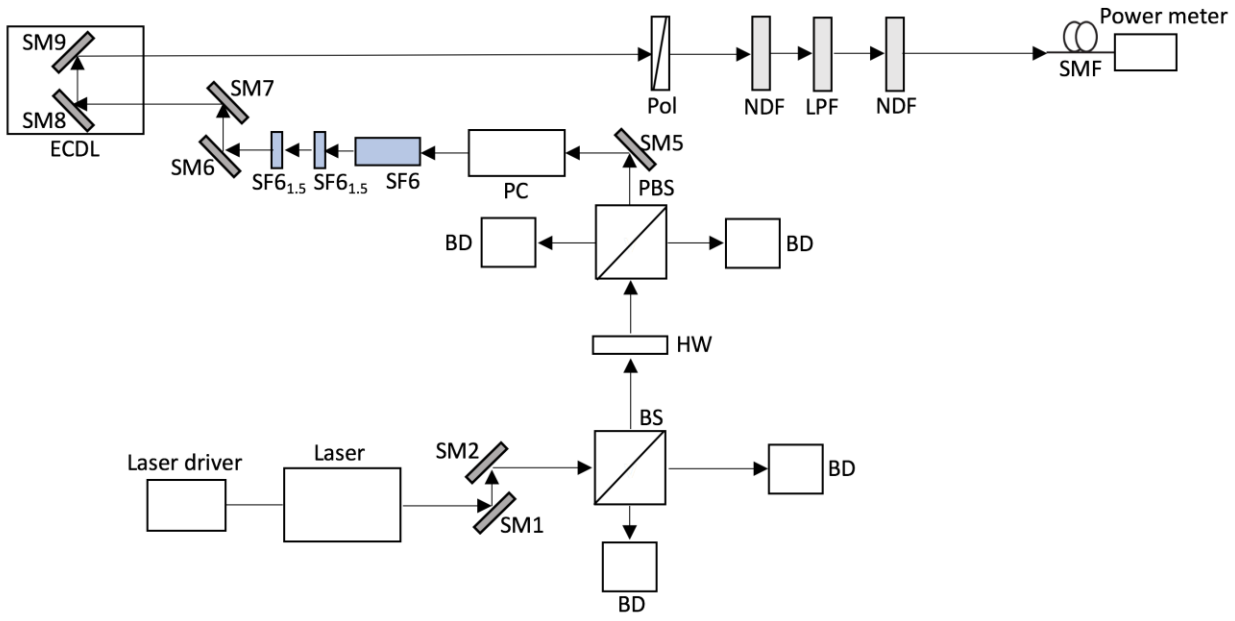

Figure 2.27 The block diagram for checking if the pump pulse beam hits the SMF at the desired location by using an optical power meter. Laser - Coherent Fidelity-2 high power femtosecond fiber-based laser, SM1-9 – silver mirror 1-9, BS – beam splitter (30 % transmission and 70 % reflection), BD – beam dumper, HW – half-waveplate, PBS – polarizing beam splitter, PC – Pockels cell, SF6 – SF6 crystal rod, SF6$_{1.5}$ – 1.5 cm length SF6 crystal, ECDL – electronically controlled delay line, Pol – polarizer, NDF - round step neutral density filter and LFP – long pass filter (1050 nm), SMF – single mode fiber and Power meter – optical power meter.

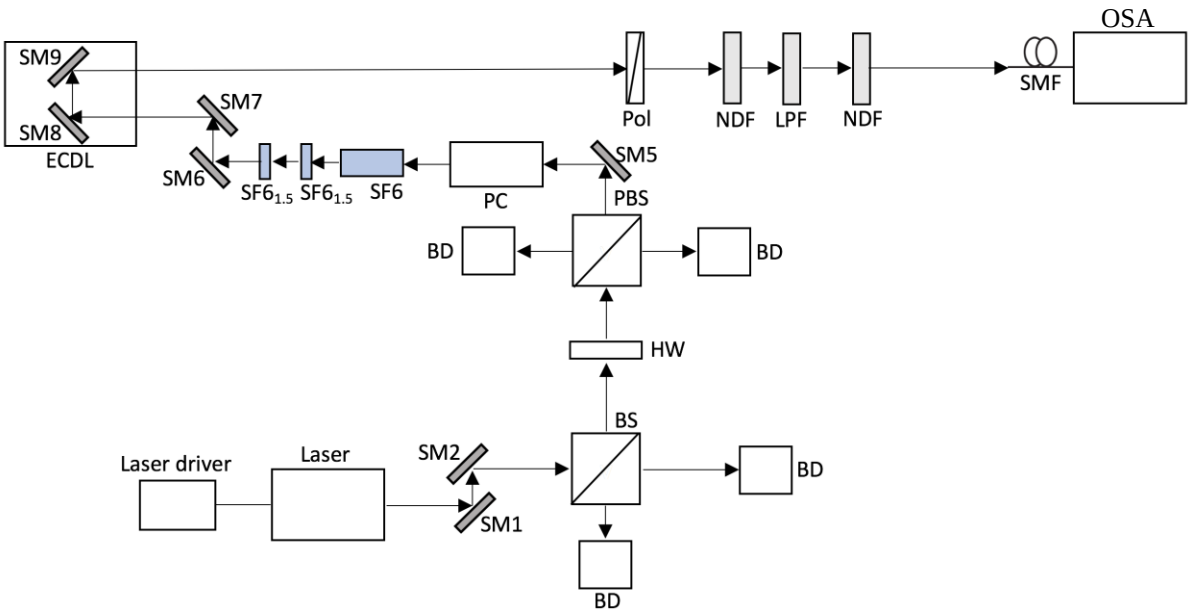

Figure 2.28 The block diagram for checking the wavelength of the pump pulse. Laser - Coherent Fidelity-2 high power femtosecond fiber-based laser, SM1-9 – silver mirror 1-9, BS – beam splitter (30 % transmission and 70 % reflection), BD – beam dumper, HW – half-waveplate, PBS – polarizing beam splitter, PC – Pockels cell, SF6 – SF6 crystal rod, SF6$_{1.5}$ – 1.5 cm length SF6 crystal, ECDL – electronically controlled delay line, Pol – polarizer, NDF - round step neutral density filter and LFP – long pass filter (1050 nm), SMF – single mode fiber and OSA – optical spectrum analyzer.

After that, the SMF, one of the round step neutral density filters, and the optical spectrum analyzer were removed. Moreover, the pump pulse beam was roughly directed to hit the same spot at the DMC as the Stokes pulse beam. Furthermore, fine adjustments were made on silver mirrors 8 and 9 to make sure that the pump pulse beam would hit the DMC at the same spot as the Stokes pulse beam. Figure 2.29 depicts the block of this final setup.

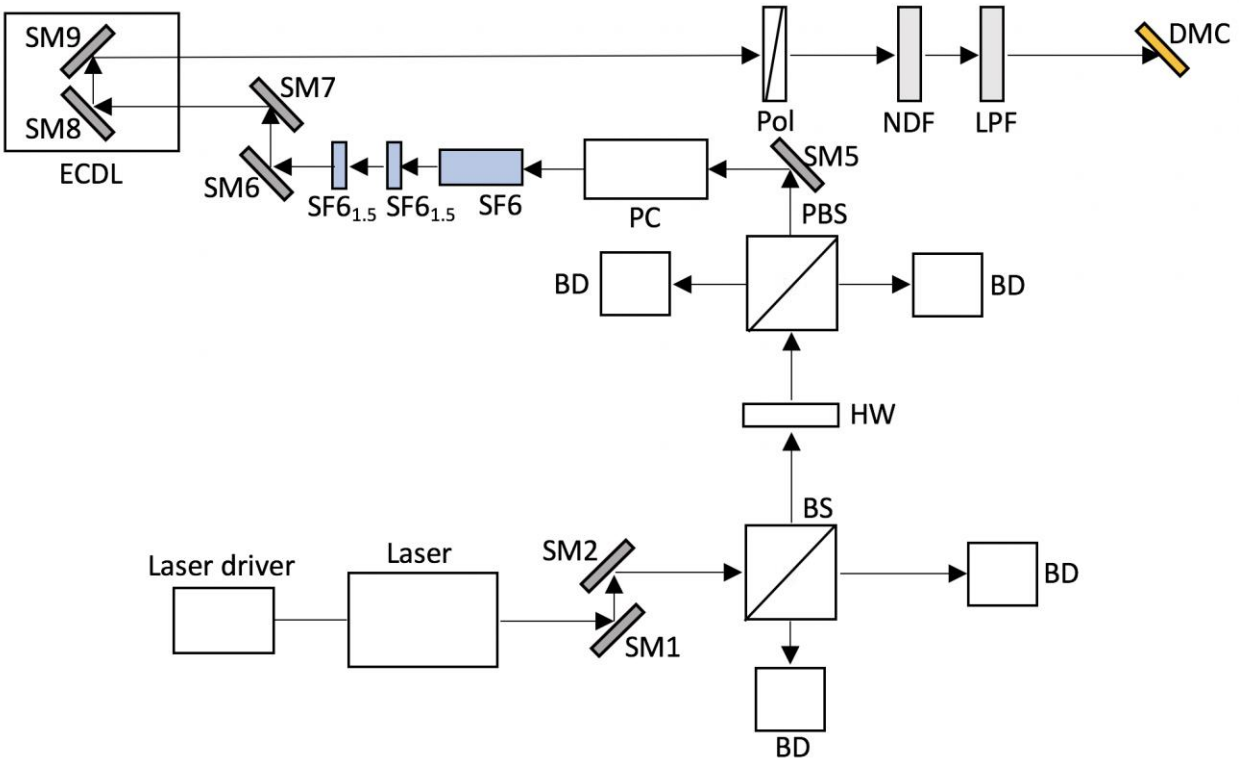

Figure 2.29 The block diagram for the pump pulse arm until the dichroic mirror combiner. Laser - Coherent Fidelity-2 high power femtosecond fiber-based laser, SM1-9 – silver mirror 1-9, BS – beam splitter (30 % transmission and 70 % reflection), BD – beam dumper, HW – half-waveplate, PBS – polarizing beam splitter, PC – Pockels cell, SF6 – SF6 crystal rod, SF6$_{1.5}$ – 1.5 cm length SF6 crystal, ECDL – electronically controlled delay line, Pol – polarizer, NDF - round step neutral density filter and LFP – long pass filter (1050 nm).and DMC – dichroic mirror combiner (1180 nm).

2.9 Setup for SRS spectroscopy after the DMC to make sure that the pump and the Stokes pulses are on top of each other

To make sure that the pump pulse and the Stokes pulse were on top of each other in space the pump pulse arm and the Stokes pulse arm setups were combined. Firstly, it was decided to level up the pump pulse. To do that the Stokes pulse had to be blocked. Thus, the beam dumber was placed in between the 30/70 beam splitter, and a round step neutral density filter was placed. Then, two irises and the CCD camera were placed after the DMC. After that, to level up the pump pulse beam, the same procedure was used as it was in making sure that the Stokes pulse beam was hitting the PCF core. The CCD camera was connected to the laptop to keep an eye on the pump pulse beam's profile if it was not clipped by the irises. Figure 2.30 depicts the block diagram of this process. After that, it had to be made sure that the Stokes pulse beam is on top of the pump pulse beam. Hence, to achieve this the BD was removed to unblock the Stokes pulse. Also, the CCD camera with the laptop were removed as it was not able to capture the Stokes pulse because it had a wavelength that exceeded the CCD camera's limitations. Then, the BD was placed in between silver mirror 9 and the polarizer to block the pump pulse beam. Moreover, the screen place was placed in front of the irises. The IR card as well as the IR camera was used to trace the Stokes pulse beam. Again, the same procedure was used in making sure that the Stokes pulse was hitting the PCF core. Figure 2.31 depicts the block diagram of this procedure. Next, the BD was removed from the pump pulse path, and again it was made sure that both pulses were on top of each other while both arms were not blocked. Figure 2.32 illustrates a block diagram of this setup.

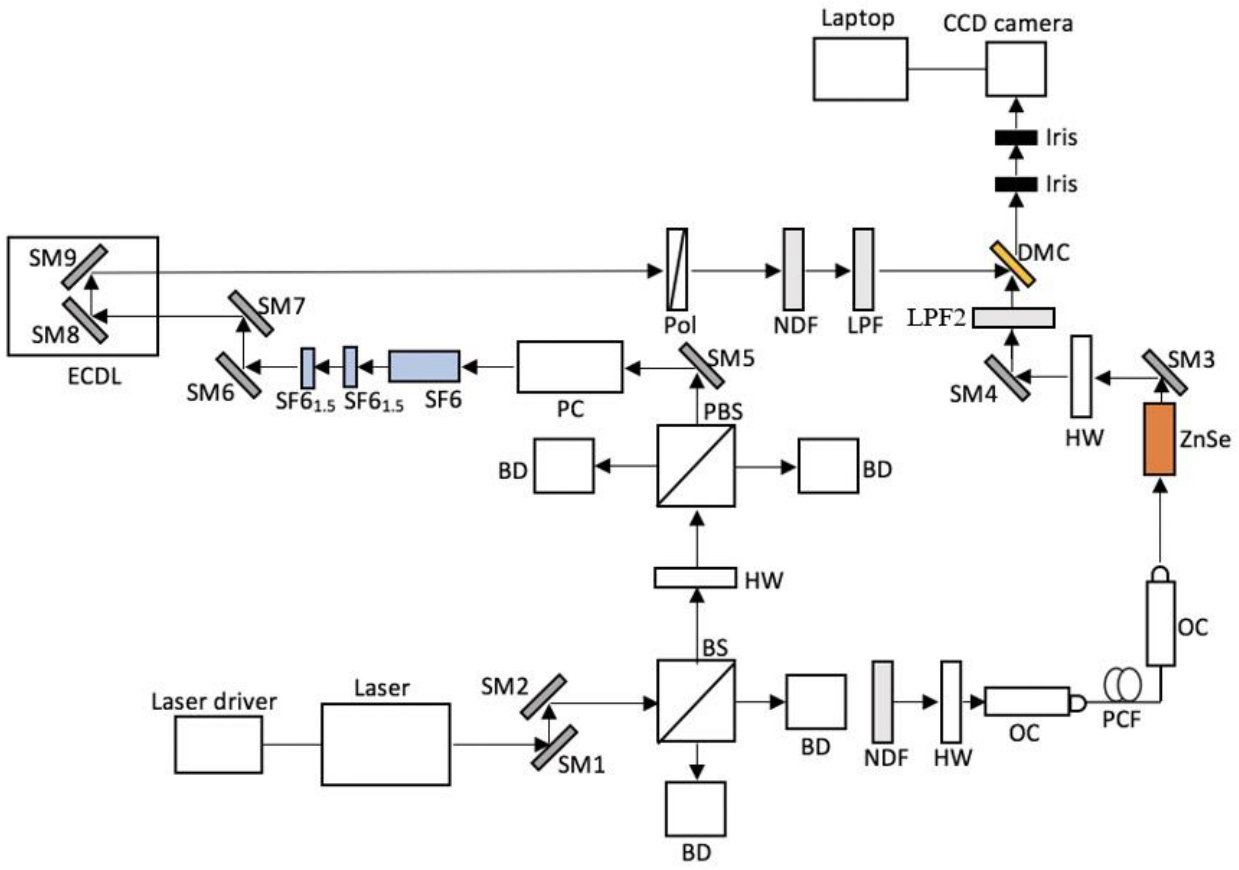

Figure 2.30 The block diagram of the setup to check the position in space of the pump pulse. Laser - Coherent Fidelity-2 high power femtosecond fiber-based laser, SM1-9 – silver mirror 1-9, BS – beam splitter (30 % transmission and 70 % reflection), BD – beam dumper, HW – half-waveplate, PBS – polarizing beam splitter, PC – Pockels cell, SF6 – SF6 crystal rod, SF6$_{1.5}$ – 1.5 cm length SF6 crystal, ECDL – electronically controlled delay line, Pol – polarizer, NDF - round step neutral density filter and LFP – long pass filter (1050 nm), OC – optical collimator, PCF – photonic crystal fiber, ZnSe – zinc selenide crystal, LPF2 – long pass filter (1150 nm) and DMC – dichroic mirror combiner (1180 nm).

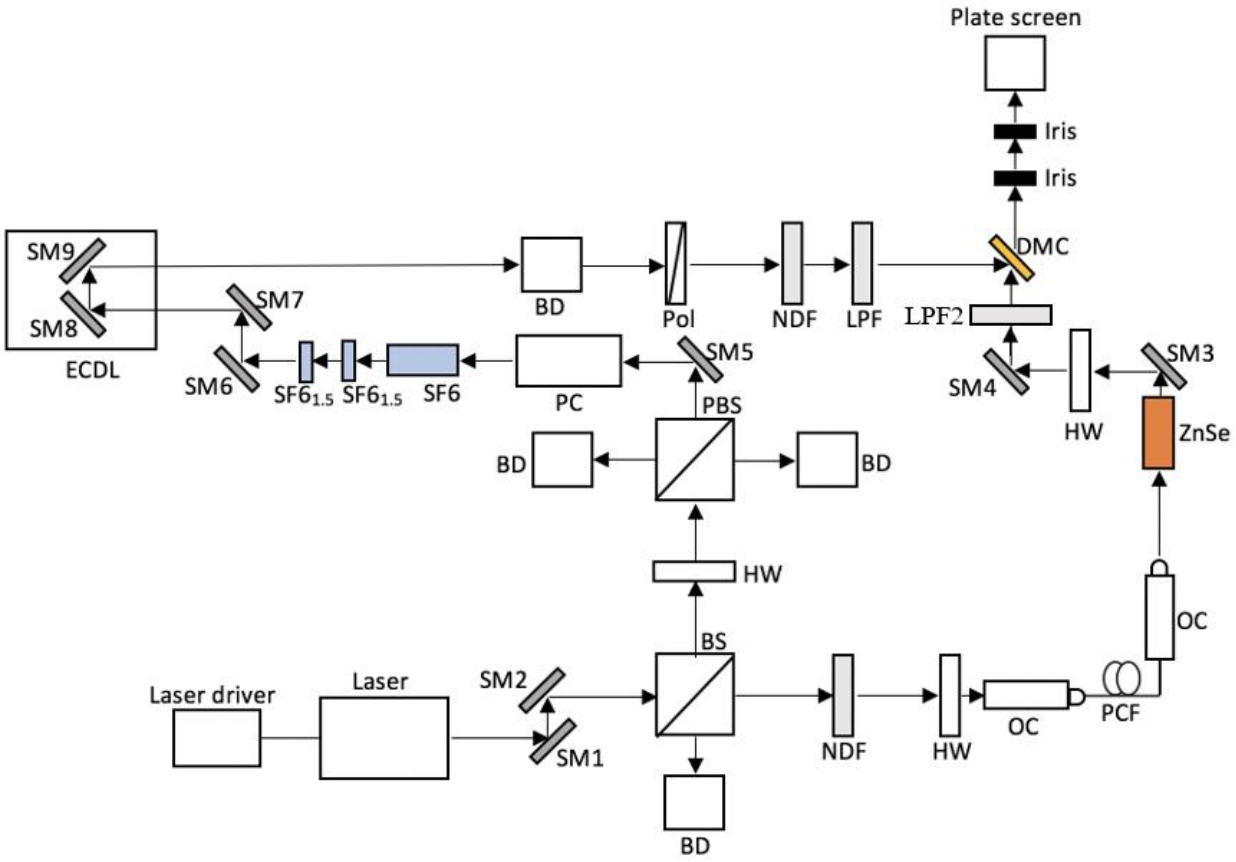

Figure 2.31 The block diagram of the setup to check the position in space of the Stokes pulse. Laser - Coherent Fidelity-2 high power femtosecond fiber-based laser, SM1-9 – silver mirror 1-9, BS – beam splitter (30 % transmission and 70 % reflection), BD – beam dumper, HW – half-waveplate, PBS – polarizing beam splitter, PC – Pockels cell, SF6 – SF6 crystal rod, SF6$_{1.5}$ – 1.5 cm length SF6 crystal, ECDL – electronically controlled delay line, Pol – polarizer, NDF - round step neutral density filter and LFP – long pass filter (1050 nm), OC – optical collimator, PCF – photonic crystal fiber, ZnSe – zinc selenide crystal, LPF2 – long pass filter (1150 nm) and DMC – dichroic mirror combiner (1180 nm).

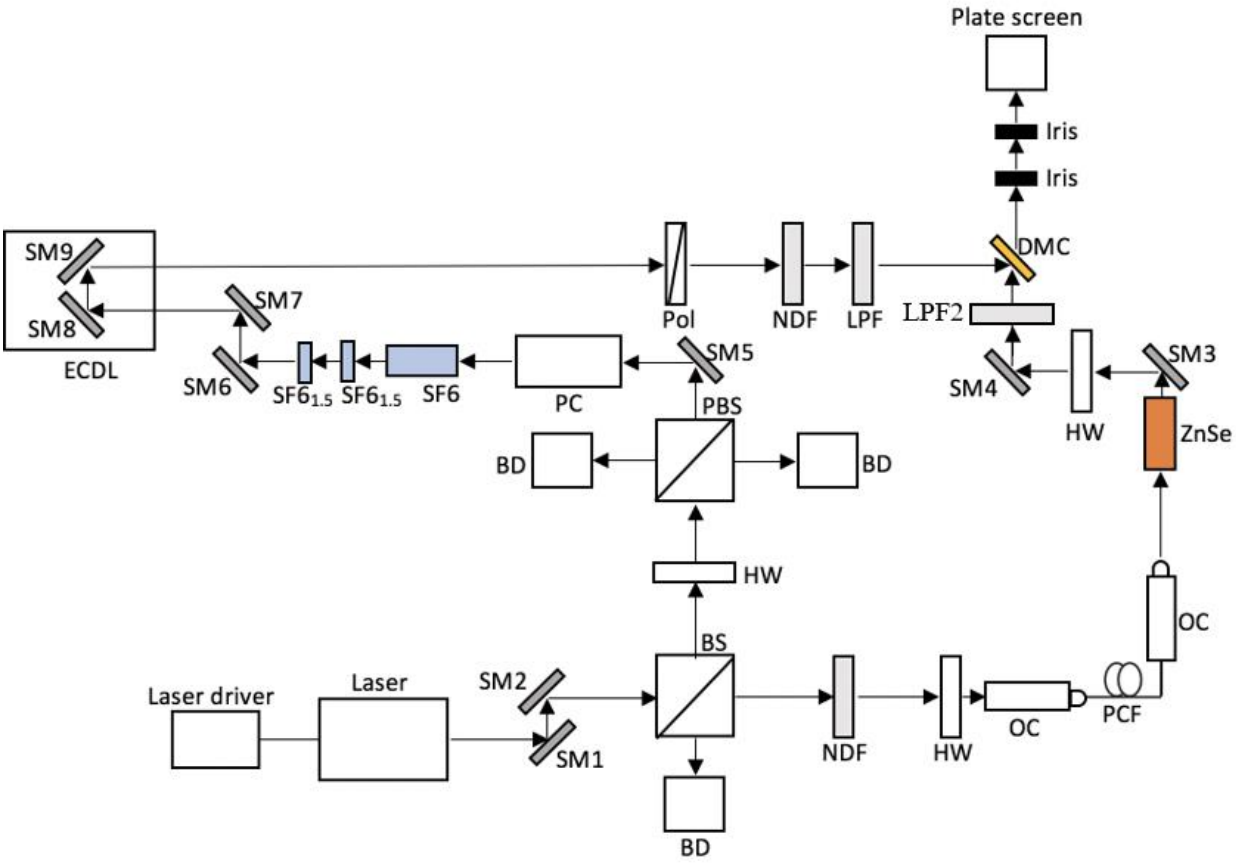

Figure 2.32 The block diagram of the setup to check that the pump pulse and the Stokes pulse are on top of each other. Laser - Coherent Fidelity-2 high power femtosecond fiber-based laser, SM1-9 – silver mirror 1-9, BS – beam splitter (30 % transmission and 70 % reflection), BD – beam dumper, HW – half-waveplate, PBS – polarizing beam splitter, PC – Pockels cell, SF6 – SF6 crystal rod, SF6$_{1.5}$ – 1.5 cm length SF6 crystal, ECDL – electronically controlled delay line, Pol – polarizer, NDF - round step neutral density filter and LFP – long pass filter (1050 nm), OC – optical collimator, PCF – photonic crystal fiber, ZnSe – zinc selenide crystal, LPF2 – long pass filter (1150 nm) and DMC – dichroic mirror combiner (1180 nm).

Finally, it is important to notice that the distances that the pump and the Stokes beam pulses traveled were measured, calculated, and arranged in such a way that both beams would arrive at the same time. The simple formula was used to determine the needed distances for both beams to arrive at the same time

$$t = \frac{d}{\left(\frac{c}{n}\right)} \tag{2.7}$$

where c is the speed of light, d is the distance, t is time, and n is the refractive index of the media. Hence, for the pump beam pulse, the arrival time at the DMC was calculated as follows

$$t = \frac{d_1}{\frac{c}{n_1}} + \frac{d_2}{\frac{c}{n_2}} + \frac{d_3}{\frac{c}{n_3}} = \frac{3.61}{\frac{3 * 10^8}{1}} + \frac{0.15}{\frac{3 * 10^8}{1.45}} + \frac{0.18}{\frac{3 * 10^8}{1.81}} = 1.384 \times 10^{-8} s \tag{2.8}$$

where d_1, d_2 and d_3 are the distances in meters that the pump beam traveled in free space, inside KDP crystal (Pockels Cell) and inside SF6 crystal, respectively. The refractive indices in free space, inside KDP crystal (Pockels Cell) and inside of SF6 crystal are n_1, n_2 and n_3, respectively. Similarly, for the Stokes beam pulse, the arrival time at the DMC was calculated as follows

$$t = \frac{d_1}{\frac{c}{n_1}} + \frac{d_2}{\frac{c}{n_2}} + \frac{d_3}{\frac{c}{n_3}} = \frac{1.22}{\frac{3 * 10^8}{1}} + \frac{2.00}{\frac{3 * 10^8}{1.45}} + \frac{0.075}{\frac{3 * 10^8}{2.45}} = 1.434 \times 10^{-8} s \tag{2.9}$$

where d_1, d_2 and d_3 are the distances in meters that the Stokes beam traveled in free space, inside the PCF, and inside of ZnSe crystal, respectively. The refractive indices in free space, inside the PCF, and inside of ZnSe crystal are n_1, n_2 and n_3, respectively. Thus, as the arrival times were very close it was made sure that the distances are roughly correct.

2.10 Setup for SRS spectroscopy after the DMC to make that the pump and the Stokes pulses arrive roughly at the same time

It is very important in the SRS spectroscopy to make sure that the pump and the Stokes pulses arrive and hit the sample at the same time. Hence, the ECDL played an important role as it could extend or reduce the path for the pump pulse beam arrival to the DMC. Furthermore, to make sure that both pulses arrive at the same time an oscilloscope was used. The name of the oscilloscope was Digital Communications Analyzer 83480A from Hewlett Packard. The bandwidth can be set to be from $1\ GHz$ to $15\ GHz$ [22]. An oscilloscope was connected to the laser source that acted as the trigger for an oscilloscope. Then the SMF and its mount were placed in front of the DMC. After that, the SMF was connected to the photodetector (PD) to convert the optical signal to the RF signal. The photodetector that was used to convert the optical signal to the RF signal and detect it was Agilent 11982A Amplified Lightwave Converter $1200 - 1600\ nm$. This device has bandwidths from DC to $15\ GHz$ [23]. Moreover, the PD was connected to an oscilloscope. Figure 2.33 depicts the setup. Furthermore, the laser source was turned on by using the high power mode. The electronically controlled delay line was connected to the ECDL controller and then to the laptop to move silver mirrors 8 and 9 on the motorized stage back and forth till the pump and the Stokes pulses overlapped on an oscilloscope screen. At this point, it was made sure that both pulses were roughly on top of each other which meant that they arrive at the same time.

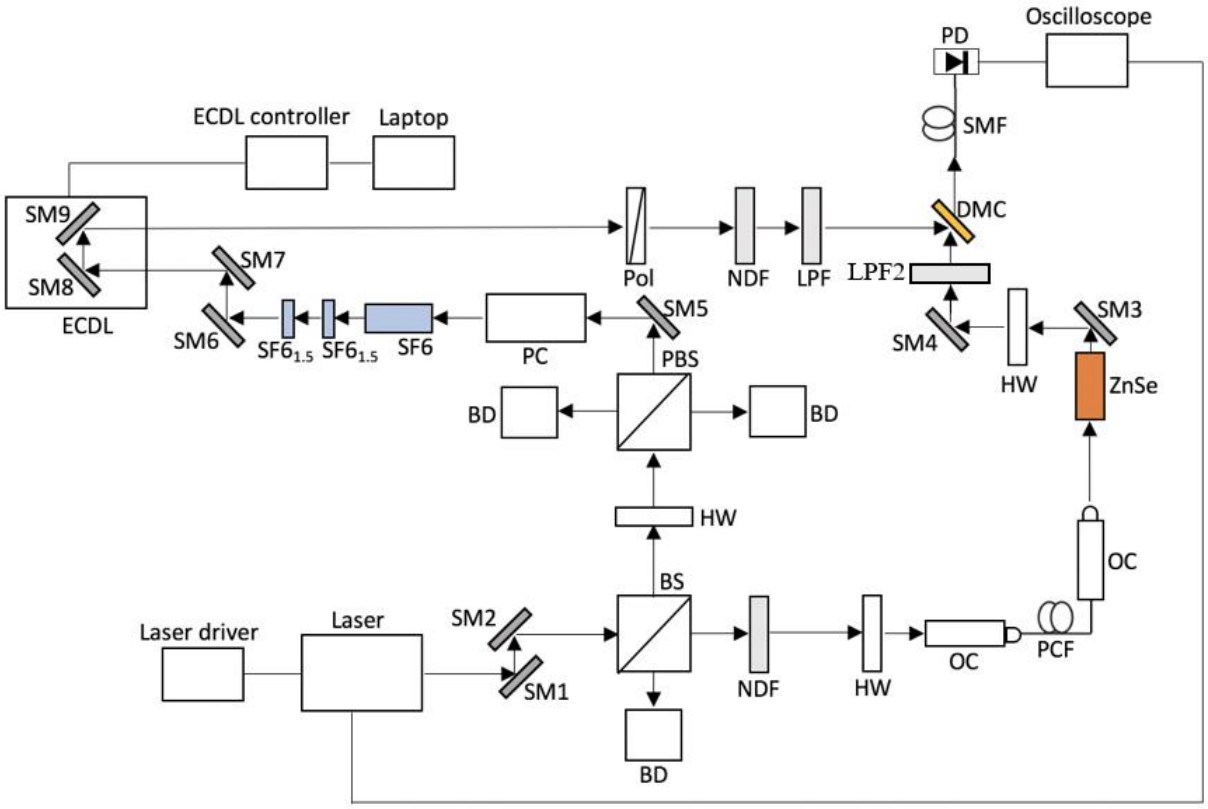

Figure 2.33 The block diagram for estimating that the Stokes and the pump pulses arrive just after the DMC roughly at the same time. Laser - Coherent Fidelity-2 high power femtosecond fiber-based laser, SM1-9 – silver mirror 1-9, BS – beam splitter (30 % transmission and 70 % reflection), BD – beam dumper, HW – half-waveplate, PBS – polarizing beam splitter, PC – Pockels cell, SF6 – SF6 crystal rod, SF6$_{1.5}$ – 1.5 cm length SF6 crystal, ECDL – electronically controlled delay line, Pol – polarizer, NDF - round step neutral density filter and LFP – long pass filter (1050 nm), OC – optical collimator, PCF – photonic crystal fiber, ZnSe – zinc selenide crystal, LPF2 – long pass filter (1150 nm), DMC – dichroic mirror combiner (1180 nm), SMF – single mode fiber and PD – photodetector.

2.11 Setup for SRS spectroscopy after the DMC

The third part of building and aligning the SRS spectroscopy was to build the optical system after the DMC. The remaining SRS spectroscopy was built on Nikon Inverted Microscope Eclipse TE300 which was modified and placed in front of the DMC. Figure 2.34 and Figure 2.35 depict the right-hand side and left-hand side views of the microscope, respectively. Note that the microscope's top part was replaced and modified to meet the experiment's requirements. Moreover, Figure 2.36 illustrates the rear view of the microscope with the place where the combined Stokes and pump pulses entered. The place where combined pulses were entered has the mirror that redirects the entering beam to go straight up.

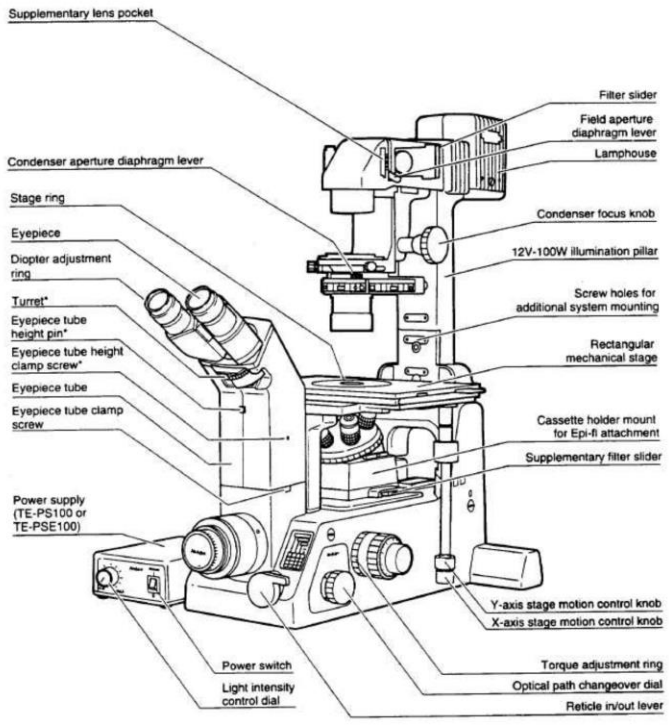

Figure 2.34 The right-hand side view of the microscope [24].

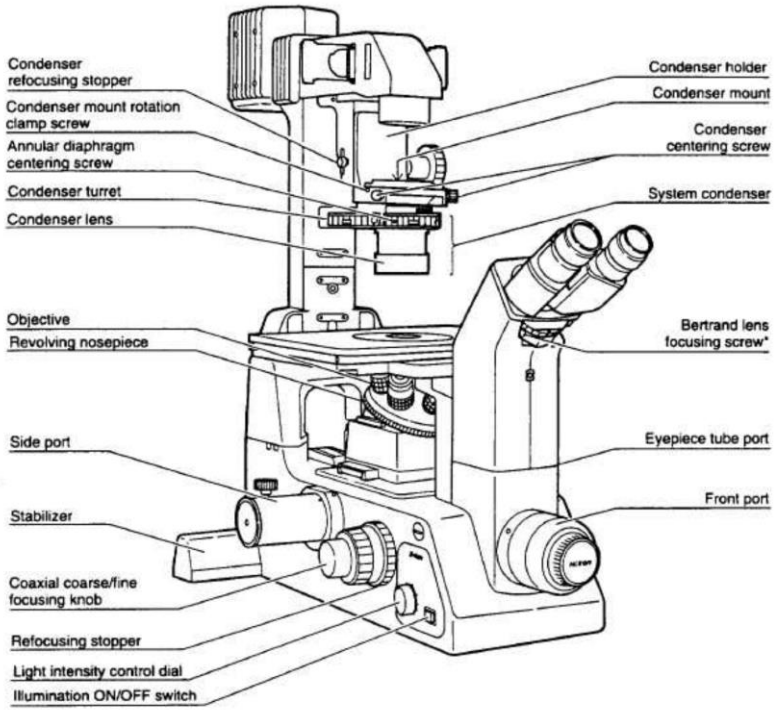

Figure 2.35 The left-hand side view of the microscope [24].

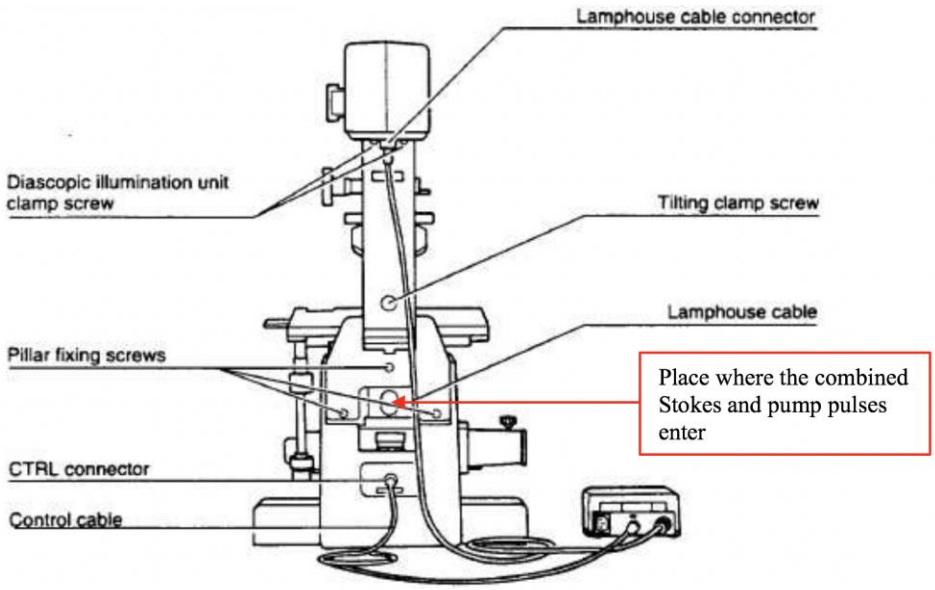

Figure 2.36 Rear view of the microscope [24].

Next, as the microscope system with components had an elevated height with respect to the combined Stokes and the pump beams silver mirrors 10 and 11 were placed to lift the combined beam pulses to the desired height. After that, it was made sure that the combined beam pulses go straight up. To achieve that two steps were taken. Firstly, it was made sure that the pump pulse beam went straight. Hence, the Stokes pulse was blocked using the beam dumber. Then, the place of the optical objective was left without the optical objective. Then two irises were placed in the way that the optical objective place and two irises would be directly above each other. After that CCD camera was placed after the second iris and both variable iris diaphragm adjustable apertures for both irises were closed until it was just slightly smaller than the pump pulse beam. By the time the pump pulse beam was properly centered, only a halo of light has been seen around the aperture of the iris. Also, the profile of the pump pulse beam has been observed by the CCD camera and it was Gaussian without any cuts or diffractions. Figure 2.37 depicts the block diagram of this setup. After that, it was made sure that the Stokes pulse beam went straight up. To achieve the Stokes pulse beam was unblocked and the pump pulse beam was blocked by using the beam dumper. Next, the CCD camera was replaced with the plate screen and an IR camera with the IR card was used to trace the beam. Figure 2.38 shows the block diagram of this step.

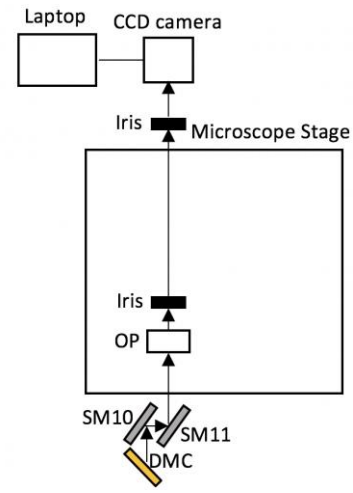

Figure 2.37 Make sure that the Stokes pulse beam goes through the center of the objective place and propagates straight up. DMC – dichroic mirror combiner, SM10 – silver mirror 10, SM11 – silver mirror 11, and OP – optical objective place.

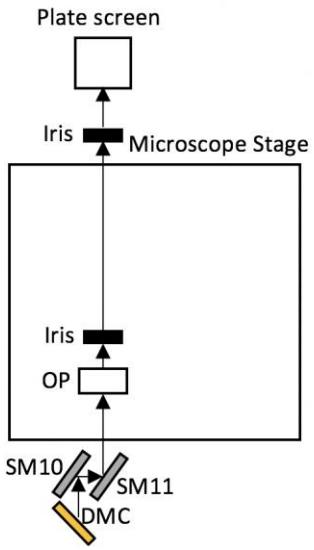

Figure 2.38 Make sure that the pump pulse beam goes through the center of the objective place and propagates straight up. DMC – dichroic mirror combiner, SM10 – silver mirror 10, SM11 – silver mirror 11, and OP – optical objective place.

Furthermore, two irises and the plate screen were removed. After that, two optical objectives and the sample stage between them were placed. The sample stage was Nano-H100-X which is a compact 2-axis positioning stage that provides a range of motion of $100\ \mu m\ x\ 100\ \mu m$. This stage comes with a driver that controls the motion of the x-axis and y axis [25]. The purpose of the first optical objective was to focus the Stokes and the pump beams on the sample to create the SRS signal. The second optical objective was collecting the SRS signal. Moreover, the optical objective 1 that was used was Newport M-40x. It has a numerical aperture of 0.65 and a working distance of $0.6\ mm$ [26]. The optical objective 2 was picked to be Olympus PLCN 40X. This objective has a numerical aperture of 0.65 and a working distance of $0.6\ mm$ [27]. Both objectives are air/dry immersive objectives.

Next, the sample chamber was made by using two microscope cover glasses, epoxy glue, and two injection needles. The microscope cover glasses that were used were from Fisher Scientific named Fisherbrand Cover Glasses: Rectangles 12-545-J. These cover glasses are $22\ mm$ in width, $60\ mm$ in length, and $0.13 - 1.17\ mm$ in thickness and are made from Borosilicate glass [28]. The needles were BD 309571 Disposable 3mL Luer-Lok Syringes with 23g x 1"L Needles. The needle gauge is 23 meaning that the outer diameter of the needle is $0.64\ mm$ [29,30]. Firstly, epoxy glue was put on the edges of the microscope cover glass and two injection needles were placed on one side of the microscope cove glass. The purpose of one needle was to fill up the chamber space with sample and another one was for the air pockets to get out. Next, the second microscope cover glass was placed on top of the first one. After that, some pressure was applied to make sure that no gaps were present on the sides between the two cover glasses. Figure 2.39 depicts the top and side views of the sample chamber.

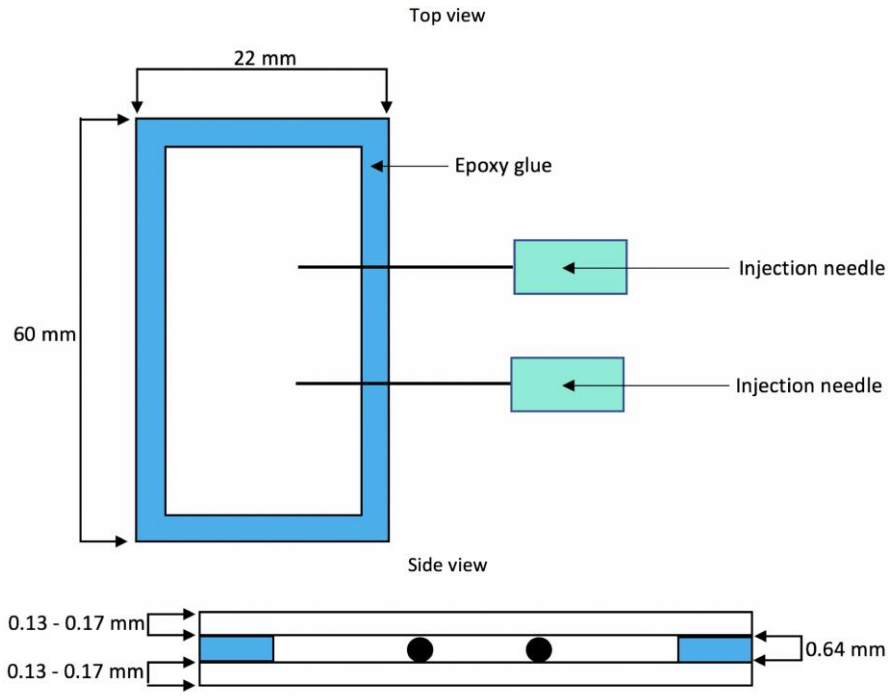

Figure 2.39 The top and the side views of the sample chamber.

After that, the sample chamber was filled up with the sample and placed on the sample stage. Moreover, the sample stage was connected to the sample stage driver. The driver was controlled by applying the voltage. The voltage was generated by using two function generators as it can produce DC voltage. They were connected to the driver. Two function generators were used as one was used for x-direction movement and another one was used for y-direction movement. Function generators that were used were Agilent 33220A 20 MHz Function/Arbitrary Waveform Generator. These function generators can produce square waves with fast rise and fall times up to $20\,MHz$ with the frequency range from $1\,\mu Hz$ to $20\,MHz$. The duty cycle for $20\,MHz$ square waveform is from 40% to 60%. The amplitude can be entered in V_{pp}, V_{rms}, or dBm values [31]. By applying the voltage on x and y ports on the sample stage driver the sample stage could be moved in x and y directions separately. To help to focus the SRS signal the optical objective 1 could be moved up and down in z-direction by the knobs on the microscope stage named coaxial

coarse/line focusing knob (see Figure 2.35). Next, after the second optical objective, the silver mirror 13 was placed to redirect the beam to the silver mirror 14 which was placed on the mount that could flip with a 90° angle. On the reflected beam path after the silver mirror 14, the CCD camera was placed to be able to capture the optical image of the sample. The CCD camera that was used was from Thorlabs DCC164C-HQ. It has a resolution up to $1280H\ x\ 1024V$ [32]. After that, two irises were placed on the transmitted path after the silver mirror 14. The purpose of these two irises was to make sure that the SRS signal goes straight without any angles or tilts. At the end the plate screen was placed. The laser was turned on to the alignment mode for this step. To see the laser IR card and IR camera were used. The knobs of the silver mirror 13 and the knobs of the second objective were tuned till the SRS signal went through both almost closed irises. Moreover, in between the silver mirror 11 and the first optical objective, the white light on the stage and the silver mirror 12 on the mount that could flip with a 90° angle were placed. The purpose of the white light was to produce light for optical imaging. The white light source was OSL2 Fiber Illuminator. It has maximum bulb intensity of $1.4\ W$ [33]. Figure 2.40 depicts the setup of this step. The reason for placing the silver mirror 12 was to redirect both the pump and Stokes beams to the optical spectrum analyzer to obtain the wavelength of each beam if needed. After that, both irises were removed and after the silver mirror 14, the LPF with a cutoff wavelength of $1150\ nm$ was placed. The purpose of this filter was to filter out the pump pulse. Then, the photodetector was placed after the LPF. The photo detector was TIA-500 InGaAs Detector that has the spectrum range from $900\ nm$ to $1700\ nm$ [34]. The reason for placing the photodetector was to convert the optical SRS signal to the RF signal and detect it. Also, the SMF with its mount was placed in front of the silver mirror 12. One end of the fiber was connected to the alignment laser then an IR card was placed in between the silver mirror 12 and the SMF and the two beams one of which is from

the alignment laser and another one which is from the laser source was traced to make sure that they overlap on each other on the whole path by adjusting the silver mirror 12 knobs and the SMF mount knobs. Figure 2.40 illustrates this step. After that, an alignment laser was replaced with an optical power meter and again the knobs of the silver mirror 12 and the SMF mount were tuned till the maximum reading has been seen on the optical power meter. Figure 2.41 depicts this step. Finally, the optical power meter was replaced with Ando AQ-6315B Optical Spectrum Analyzer. It provides high sensitivity from $350\,nm$ to $1750\,nm$ with low polarization dependency [35]. Figure 2.42 depicts the block diagram of the final setup.

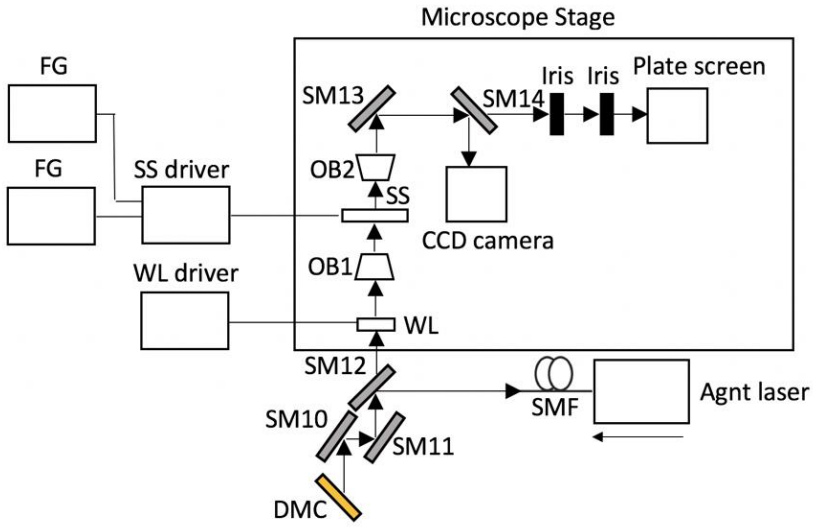

Figure 2.40 The block diagram after dichroic mirror combiner for SRS spectroscopy. DMC – dichroic mirror combiner, SM10,11,13 – silver mirror 10,11,13, SM14 – silver mirror 14 (flipping mirror), SM12 – silver mirror 12 (flipping mirror), OB1-2 – optical objective 1-2, SS – sample stage, CCD camera – changer coupled device camera, FG – function generator, SMF – single mode fiber, WL – white light and Agnt laser- alignment laser (arrow bellow indicates the laser beam propagation direction).

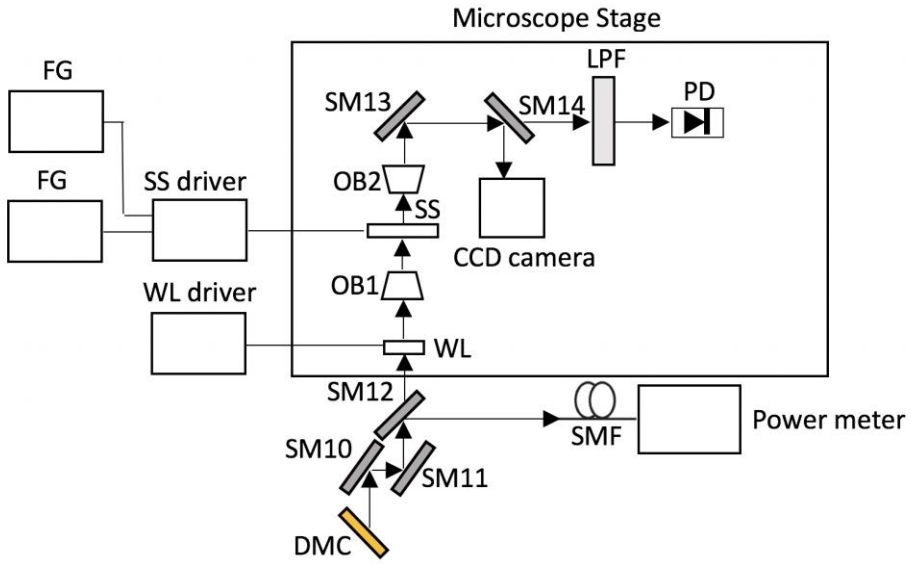

Figure 2.41 The block diagram after dichroic mirror combiner for SRS spectroscopy. DMC – dichroic mirror combiner, SM10,11,13 – silver mirror 10,11,13, SM14 – silver mirror 14 (flipping mirror), SM12 – silver mirror 12 (flipping mirror), OB1-2 – optical objective 1-2, SS – sample stage, CCD camera – changer coupled device camera, FG – function generator, LPF – long pass filter ($1150\ nm$), SMF – single mode fiber, WL – white light, Power meter – optical power meter and PD – photodetector.

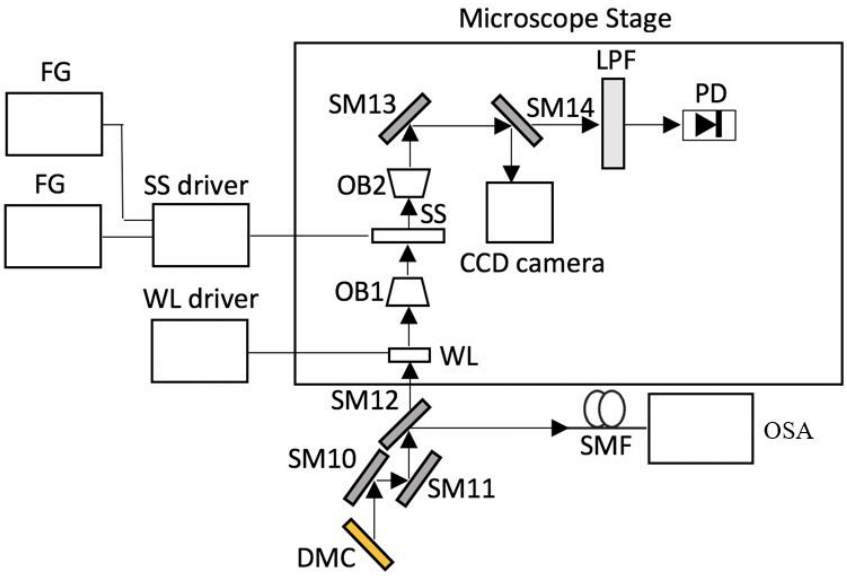

Figure 2.42 The block diagram after dichroic mirror combiner for SRS spectroscopy. DMC – dichroic mirror combiner, SM10,11,13 – silver mirror 10,11,13, SM14 – silver mirror 14 (flipping mirror), SM12 – silver mirror 12 (flipping mirror), OB1-2 – optical objective 1-2, SS – sample stage, CCD camera – changer coupled device camera, FG – function generator, LPF – long pass filter ($1150\ nm$), SMF – single mode fiber, WL – white light, PD – photodetector and OSA – optical spectrum analyzer.

2.12 The final setup for SRS spectroscopy

The final setup for the SRS spectroscopy can be seen in Figure 2.43. The PD was first connected to the oscilloscope to check the modulation depth of the pump. The oscilloscope that was used in this step was LeCroy 9324 QUAD 1GHz Oscilloscope. It has bandwidth for $-3\ dB$ range from DC to 1 GHz [36]. Then after checking the modulation depth of the pump the PD was connected to the lock-in amplifier. The purpose of the lock-in amplifier was to recover a very weak SRS signal. The lock-in amplifier that was used was MODEL SR810 DSP Lock-in Amplifier. The

frequency range for this lock-in amplifier is from $1\ mHz$ to $102.4\ kHz$. This device displays the magnitude of the signal. Moreover, it can be set to show in-phase component X, quadrature component Y, the magnitude R, and the phase component between the signal and lock-in reference θ. The reference can be set to be internal or external [37]. After that, the lock-in amplifier was connected to the function generator to generate the function which served as the turn on/off signal for the PC driver and also as an external trigger for the lock-in amplifier. The lock-in amplifier was set to $300\ ms$ integration time with a sensitivity of $100\ mV$. Also, the filter was set to be $6\ dB$ and setting the external references signal frequency at 80 kHz. Moreover, the function generator that was used to generate the square wave function for the PC driver and to generate the external trigger for the lock-in amplifier was Agilent 33220A $20\ MHz$ Function/Arbitrary Waveform Generator. The optimum choice was to generate a square waveform as the PC had to be turned on and off. Furthermore, to drive the PC it was connected to the PC driver and then the PC driver was connected to the function generator, Moreover, the ECDL was connected to the ECDL controller to move the delay line back and forth. Next, a variable optical attenuator-retarder (VOA) was placed in the Stokes pulse arm between the round step neutral density filter and the half-waveplate. The VOA that was used was from Thorlabs LCC1221-B. It has a retardance range from about $30\ nm$ to $\lambda/2$. It also has a clear aperture of the diameter of $20\ mm$ [38]. Then it was connected to the function generator (Agilent 33220A 20 MHz Function/Arbitrary Waveform Generator). The frequency was set to be $2\ kHz$ with VRMS from 0.6 to 1.2 V. The purpose of the VOA was essentially to control the entering power to the PCF to help to shift the optical solitons in the PCF as they served as the Stokes pulses. All devices were run with MATLAB, hence they were connected to the laptop.

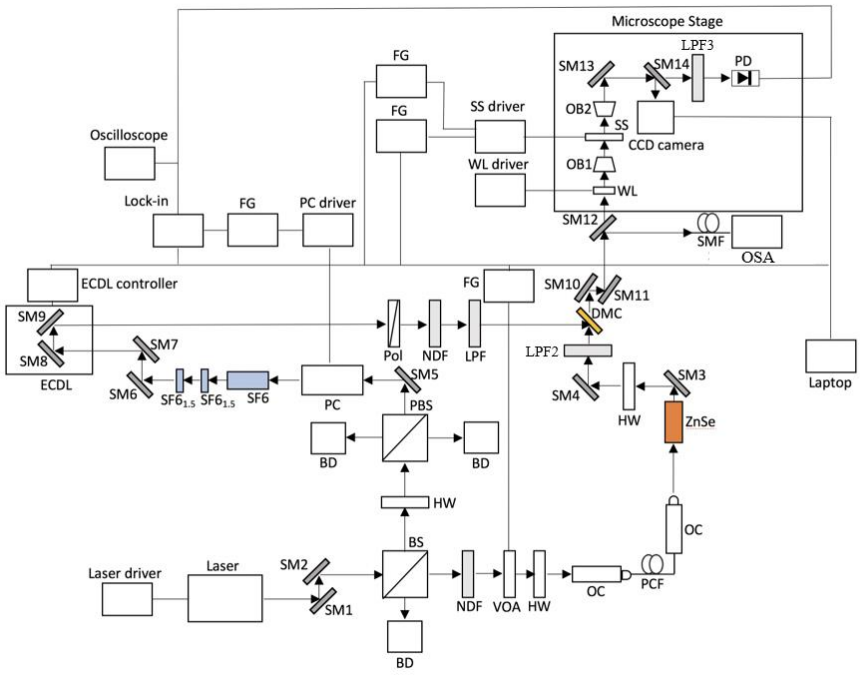

Figure 2.43 The block diagram of the final SRS spectroscopy setup. Laser - Coherent Fidelity-2 high power femtosecond fiber-based laser, SM1-13 – silver mirror 1-13, SM12,14 – silver mirror 12,14 (flipping mirror), BS – beam splitter (30 % transmission and 70 % reflection), BD – beam dumper, HW – half-waveplate, PBS – polarizing beam splitter, PC – Pockels cell, SF6 – SF6 crystal rod, $SF6_{1.5}$ – 1.5 cm length SF6 crystal, ECDL – electronically controlled delay line, Pol – polarizer, NDF - round step neutral density filter, LPF – long pass filter (1050 nm), LPF2 – long pass filter (1150 nm), LPF3 – long pass filter (1150 nm), VOA – variable optical attenuator (retarder), OC – optical collimator, PCF – photonic crystal fiber, ZnSe – ZnSe crystal, DMC – dichroic mirror combiner (1180 nm), OB – optical objective, SS – sample stage, PD – photodetector, SMF – single mode fiber, Lock-in – lock-in amplifier, SMF – single mode fiber, FG – function generator, WL – white light, CCD camera – charge couple device camera and OSA – optical spectrum analyzer.

Mathematica code was written in order to compute the wavelength of the Stokes pulse beam needed to get the Raman shift for the various samples. This code told what Stokes pulse wavelength is needed in order to get particular Raman shift wavelength and particular Raman shift wavenumber of the particular sample. Hence, by changing the Stokes pulse wavelength value in the code, the anti-Stokes pulse wavelength and wavenumber can be determined. Figure 2.44 depicts Mathematica code.

```
In[41]:=
nm = 10^-9;
ToNm = 10^9;
c = 3 × 10^8;
λS = 1180 nm;
λp = 1078 nm;
fAS = (2 c/λp - c/λS) // N;
RamanShift = 10^7 (1/(λp / nm) - 1/(λS / nm)) // N (*cm^-1*)
λAS = c/fAS;
λASnm = λAS * ToNm // N (*nm*)
Out[47]= 801.862
Out[49]= 992.231
```

Figure 2.44 Mathematica code for Raman shift for the varies samples computation (example in the code is for cyclohexane Raman shift). nm - the conversion factor to nanometers, $ToNm$ – the conversion factor to convert wavelength to nanometers, c – light speed, λ_S – wavelength of the Stokes pulse, λ_P – wavelength of the pump pulse, f_{AS} – frequency of the anti-Stokes pulse, λ_{AS} – wavelength of the anti-Stokes pulse and λ_{ASnm} – wavelength of the anti-Stokes pulse in nanometers.

Finally, in order to perform the spectroscopy scan of the sample, which was selected to be cyclohexane, the VOA was programmed in such a way that would give about 40 nm in wavelength shift of the Stokes beam pulse. Also, the delay line was programmed to move back and forth at the same time. The reason to move the delay line was that as the wavelength of Stokes beam pulse changes it faces different refractive indexes in the ZnSe crystal. This means that the Stokes beam pulse slows down. Hence, the delay line of the pump pulse has to increase to compensate for this effect. Thus, if the Stokes pulses wavelength increases than the length of the delay line of the pump pulse has to increase. On the other hand, if the Stokes pulse wavelength decreases than the length of the delay line of the pump pulse has to decrease. Furthermore, as it was known that Raman shift for cyclohexene is 801 cm^{-1} [39] the Stokes pulse wavelength scan was set to be from about 1160 nm to 1200 nm. As all necessary devices including the lock-in amplifier were connected to the laptop and as all of them were run with MATLAB it processed data and produced plots for the optical spectrum of the scanned sample.

2.13 CARS spectroscopy and microscopy procedure overview

CARS and SRS spectroscopies are very similar in nature. Hence, the Stokes pulse arm was not changed until the DMC. However, the pump pulse arm was changed a little bit. The Pockels cell driver was turned off and the polarizer was removed. Thus, the Pockels cell for the CARS spectroscopy worked only as of the nonlinear KDP crystal. The setup after the DMC had to be changed as well. Instead of the PD, the spectrometer was placed. The spectrometer that was used was Maya 2000 pro. It covers the spectrum range from 165 nm to 1100 nm and integration time can be set from 6 ms to 5 s [40]. Also, the LFP3 was replaced with SPF 1000 nm in order to block the Stokes and pump pulses. Figure 45 depicts the final setup of CARS spectroscopy. The same setup was used for CARS microscopy as well.

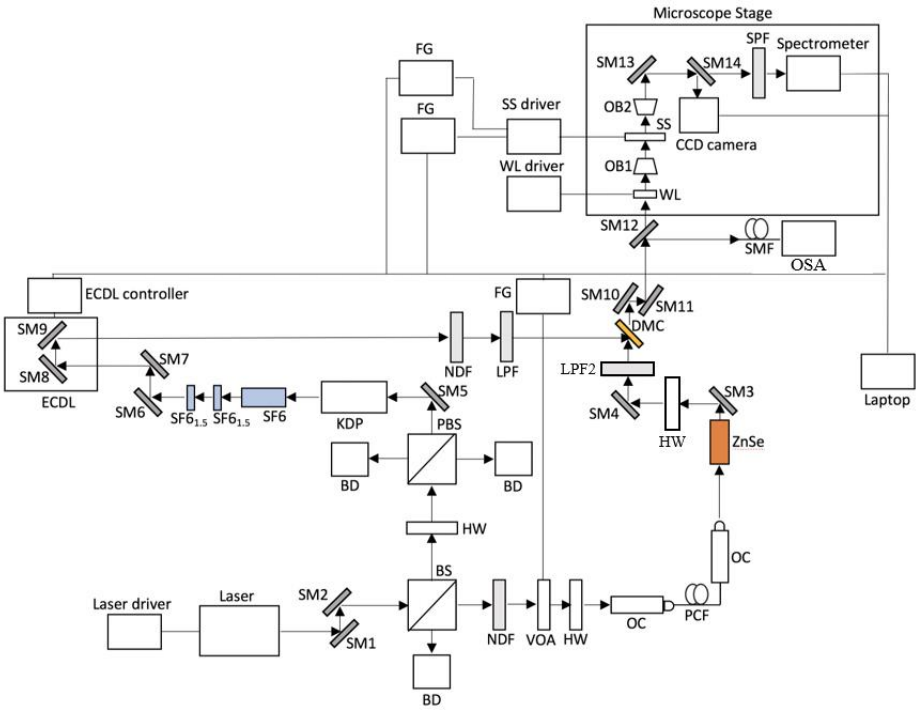

Figure 2.45 The block diagram of the final CARS spectroscopy and microscopy setup. Laser - Coherent Fidelity-2 high power femtosecond fiber-based laser, SM1-13 – silver mirror 1-13, SM12,14 – silver mirror 12,14 (flipping mirror), BS – beam splitter (30 % transmission and 70 % reflection), BD – beam dumper, HW – half-waveplate, PBS – polarizing beam splitter, PC – Pockels cell, SF6 – SF6 crystal rod, $SF6_{1.5}$ – 1.5 cm length SF6 crystal, ECDL – electronically controlled delay line, Pol – polarizer, NDF - round step neutral density filter, LPF – long pass filter (1050 nm), LPF2 – long pass filter (1150 nm), SPF – short pass filter (1000 nm), VOA – variable optical attenuator (retarder), OC – optical collimator, PCF – photonic crystal fiber, ZnSe – ZnSe crystal, DMC – dichroic mirror combiner (1180 nm), OB – optical objective, SS – sample stage, SMF – single mode fiber, Lock-in – lock-in amplifier, SMF – single mode fiber, FG – function generator, WL – white light, CCD camera – charge couple device camera and OSA – optical spectrum analyzer.

CARS spectroscopy was performed similarly to SRS spectroscopy, besides the fact of small differences in working principles. The delay line for the pump beam pulse was moved and the Stokes beam pulse wavelength was shifted using the same concept as in the SRS spectroscopy. Stokes beam pulse scan was from about $1160\,nm$ to $1200\,nm$ to perform cyclohexane spectroscopy. However, CARS microscopy was performed a little bit differently. The Stokes beam pulse wavelength was tuned to the desired Raman shift of the sample used for imaging as well as the delay line for the pump beam pulse was tuned. The Tuning of the system was completed by the time the highest peak was observed on Maya 2000 pro spectrometer. As polystyrene beads and ethanol were used for CARS microscopy it was important to set the optimum Stokes beam pulse wavelength. As Raman shift of polystyrene beads is $997\ cm^{-1}$ [41] and as Raman shift of ethanol is $867\ cm^{-1}$ [42], the Stokes beam pulse wavelength was set to be $1208\,nm$ and $1189\,nm$, respectively. The pump beam pulse wavelength was $1078\,nm$ as it is fixed. Then the sample stage with the sample was moved from top to bottom and from left to right in the x-y plane using MATLAB to perform the scan and plot scanned images. Figure 2.46 represents the scanning movement.

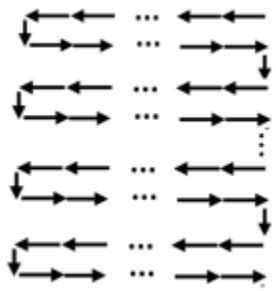

Figure 2.46 The sample stage movement representation of the CARS microscopy.

References

[1] J. Su, R. Xie, C. K. Johnson and R. Hui., "Single fiber laser based wavelength tunable excitation for CRS spectroscopy.", *Journal of the Optical Society of America B,* **2013**, 30(6): 1671-1682.

[2] Optical Table, 4x8 Ft., 8 in. Thick, ¼-20 Threads, RPR Series, Newport Corporation, Irvine, CA, USA, **2020**.

[3] Fidelity-2 High Power Femtosecond Fiber Laser, Coherent, Inc., Santa Clara, CA, USA, (accessed Apr. 30, **2020**).

[4] SC-3.7-875 Nonlinear fiber for supercontinuum generation, NKT Photonics GmbH, Cologne, Germany, (accessed Apr. 30, **2020**).

[5] Newport Corporation., "Tutorial: Fiber Optics Basics.", Newport.com., https://www.newport.com/t/fiber-optic-basics (accessed Apr. 30, **2020**).

[6] FIS OV-VFL Visible Laser Fault Locator, Fiber Instrument Sales, Oriskany, NY, USA, (accessed March 15, **2020**).

[7] Optical Sources/Power Meter/Attenuator, Tektronix, Inc., Beaverton, OR, **2000**.

[8] A. Al-Azzawi., *Photonics Principles and Practices*. Boca Raton, FL: CRC Press Taylor & Francis Group, **2006**, p. 672-674.

[9] Laser Viewing Card VRC2, Thorlabs, Inc., Newton, NJ, USA, **1999-2015**.

[10] Model IRV1 Infrared Viewing Device, Newport Corporation, Irvine, CA, USA, **2011**.

[11] Information Sheet Zinc Selenide (ZnSe), Continental Trade Sp. z z.o., Warsaw, (accessed Apr. 30, **2020**).

[12] RefractiveIndex.INFO, Refractive index database, **2008-2020**. [Online]. Available: https://refractiveindex.info/?shelf=main&book=ZnSe&page=Marple

[13] E. C. Rentchler, "Advancing Techniques in Coherent Raman and Single Molecule Studies," Ph.D. dissertation, Dept. Chem., University of Kansas., Lawrence, KS, USA, **2016**.

[14] Optical Spectrum Analyzers, 600 nm to 1700 nm HP 71450A, 71451A, Hewlett-Packard, Palo Alto, CA, USA, (accessed May 30, **2020**).

[15] IR Grenouilles, Swamp Optics, LLC, Atlanta, GA, USA, **2015**.

[16] J. Cimek, et al., "Experimental investigation of the nonlinear refractive index of various soft glasses dedicated for development of nonlinear photonic crystal fibers.", *Optical Materials Express*, **2017**, 7(10), 3471.

[17] RefractiveIndex.INFO, Refractive index database, **2008-2020**. [Online]. Available: https://refractiveindex.info/?shelf=main&book=SF6&page=Vukovic

[18] Near-IR Grenouilles, Swamp Optics, LLC, Atlanta, GA, USA, **2015**.

[19] Products Detail Electro-Optic Modulators, Conoptics, Inc., Danbury, CT, USA, **2019**.

[20] LaserCam-HR High-Resolution Laser Beam Profiling System, Coherent, Inc., Santa Clara, CA, USA, **2008**.

[21] SGSP26-100, Sigma Koki Co., LTD., Tokyo, (accessed June 4, **2020**).

[22] HP 83480A Series Digital Communications Analyzer, Hewlett-Packard Company, Englewood, CO, USA, **1999**.

[23] Agilent 11982A Amplified Lightwave Converter, Agilent Technologies, Inc., Santa Clara, CA, USA, **2004**.

[24] Inverted Microscope Eclipse TE300, Nikon Corporation, Tokyo, (accessed May. 30, **2020**).

[25] Nano-H Series, Mad City Labs, Inc., Madison, WI, USA, (accessed May. 30, **2020**).

[26] Microscope Objective Lens, 40x, 0.65 NA, 4.5 mm Focal Length, Newport Corporation, Irvine, CA, USA, (accessed August 24, **2021**)

[27] Olympus PLNC 40x/0.65 Plan Achromat Objective, Olympus Corporation, Tokyo, (accessed August 24, **2021**).

[28] Fisherbrand Cover Glasses: Rectangles, Fisher Scientific, Pittsburgh, PA, USA, (accessed May. 30, **2020**).

[29] BD 309571 Disposable 3mL Luer-Lok Syringes with 23g x 1"L Needles**,** General Laboratory Supply, Pasadena, TX, **2020**.

[30] Syringe Needle Gauge Chart, Milipore Sigma, Burlington, MA, **2020**.

[31] Agilent 33220A 20MHz function/ Arbitrary Waveform Generator Data Sheet, Agilent Technologies, Inc., USA, **2011**.

[32] DigitalClarity Technology MT9M131, Micron Technology, Inc., Boise, ID, USA, (accessed August 30, **2021**).

[33] Broadband Halogen Fiber Optic Illuminators, Thorlabs Company, Newton, NJ, USA, (accessed August 30, **2021**).

[34] TIA-500 High Speed Fiber Optic O/E Converter, Terahertz Technologies, Inc., Oriskany, NY, USA, (accessed May 30, **2020**).

[35] Optical Spectrum Analyzer AQ-6315A/-6315B, Yokogawa Electric, Tokyo, Japan, (accessed August 24, **2021**).

[36] 9320 and 9324, 1GHz Bandwidth Portable Digital Oscilloscopes, LeCroy Corporation, Chestnut Ridge, NY, USA, (accessed May. 30, **2020**).

[37] Digital Lock-In Amplifiers SR810 and SR830 – DSP lock-in amplifiers, Stanford Research Systems, Sunnyvale, CA, USA, (accessed May 7, **2020**).

[38] Half-Wave Liquid Crystal Variable Retarders / Wave Plates, Thorlabs Company, Newton, NJ, USA, (accessed August 24, **2021**).

[39] McCreery research group, Standard Spectra, **2014**. [Online]. Available: https://www.chem.ualberta.ca/~mccreery/ramanmaterials.html

[40] Maya2000 and Maya2000Pro Data Sheet, Ocean Optics (Halma Group company), Dunedin, FL, USA, (accessed August 24, **2021**).

[41] A. Bankapur, E. Zachariah, S. Chidangil, M. Valiathan and D. Mathur., "Raman Tweezers Spectroscopy of Live, Single Red and White Blood Cells.", *PLoS ONE*, **2010**, 5(4):e10427.

[42] L. Song, et al., "Online detection of distilled spirit quality based on laser Raman spectroscopy.", *Journal of the Institute of Brewing*, **2017**, 123: 121-129.

Chapter 3 - Results

3.0 The Stokes pulse beam broadening or chirping and wavelength

Firstly, it is important to note that the FROG Grenouille 15-100-USB that was used to measure the Stokes pulse chirp had limitations. It can measure temporal pulse width from $100\ fs$ to $1000\ fs$ for the wavelength range from $1230\ nm$ to $1620\ nm$. Hence, some assumptions for the Stokes pulse broadening or chirping was made. The wavelength that was used to measure the impact on chirp due to the PCF and ZnSe crystal was $1390\ nm$. The measured pulse broadening or chirping after the PCF and after $69\ mm$ of ZnSe crystal with PCF were as follows

$$PCF = 180.4\ fs \tag{3.1}$$

$$ZnSe_{69mm} + PCF = 722.4\ fs \tag{3.2}$$

where expression 3.1 represents the measured Stokes pulse temporal width after the PCF and expression 3.2 depicts the measured Stokes pulse temporal width after the PCF and ZnSe crystal. Hence, the pulse chirping that was done by the ZnSe crystal was computed to be as

$$ZnSe_{69mm} = 722.4 - 180.4 = 542\ fs \tag{3.3}$$

Next, the theoretical calculations were performed to make sure that the measured Stokes pulse broadening results were reliable by using the following formula

$$\Delta\tau_g = D_s \cdot L_s \cdot \delta\lambda_s \tag{3.4}$$

where $\Delta\tau_g$ is relative time delay between two wavelength components or in this case pulse width of the Stokes pulse, D_s is group delay dispersion parameter for the Stokes pulse at a wavelength of $1390\ nm$, L_s is the length of the ZnSe crystal and $\delta\lambda_s$ is the FWHM of the Stokes pulse. The

D_s parameter was observed to be $395.80\ \frac{ps}{nm \cdot km}$ from the database [1], L_s was measured $69\ mm$ and $\delta\lambda_s$ was measured to be $20\ nm$. Hence,

$$\Delta\tau_g = 395.80\ \frac{fs}{nm \cdot m} \cdot 0.069\ m \cdot 20\ nm = 546.2\ fs \tag{3.5}$$

Thus, as the measured and theoretical values for the Stokes pulse broadening were very close, hence the measured data was reliable. The difference might come from the fact that the ZnSe crystal that was used might have different doping from the database for the ZnSe crystal. Moreover, as it was impossible to measure the lower wavelength Stokes pulse broadening due to limitations of the FROG the assumption was made that the chirping is linear. Hence, by changing the wavelength of the Stokes pulse the chirping can be calculated. Then the pulse broadening for the Stokes pulse wavelength at $1150\ nm$ was estimated to be as follows

$$\Delta\tau_g = D_s \cdot L_s \cdot \delta\lambda_s + PCF \tag{3.6}$$

$$\Delta\tau_g = 763.15\frac{fs}{nm \cdot m} \cdot 0.069\ m \cdot 20\ nm + PCF = 1053.15 + 180.4 = 1233.55\ fs \tag{3.7}$$

where the chromatic dispersion parameter was obtained from the database [1], the ZnSe crystal length was measured, the FWHM for the Stokes pulse was measured and the chirp that was done by the PCF was estimated to be similar to the chirp of the PCF at $1390\ nm$. Hence, the expression 3.6 can be used to estimate the chirping for the Stokes pulse arm.

3.1 The pump pulse beam broadening or chirping and wavelength

The FROG Grenouille 8-50-USB was used to measure the chirp of the pump pulse which was at $1078\ nm$. The reason for using this FROG was that it was capable to measure temporal pulse width from $50\ fs$ to $500\ fs$ for the wavelength range from $700\ nm$ to $1100\ nm$. Firstly,

the pulse broadening or chirping for the pump pulse was measured by placing one $SF6_{1.5}$ crystal and by letting the beam propagate through it once. Next, the second $SF6_{1.5}$ crystal was added so that the beam would propagate through both crystals once. Moreover, the different configuration was used to measure how much chirping did the pump pulse experienced when the beam propagated through $SF6_{1.5}$ crystal twice. Furthermore, the second $SF6_{1.5}$ crystal was added so that the pump pulse beam would propagate through the first crystal twice and through the second crystal once. The following are the measured results

$$\text{one } SF6_{1.5} \text{ crystal beam propagates once } = 92.1\ fs \tag{3.7}$$

$$\text{two } SF6_{1.5} \text{crystals beam propagates once } = 228.2\ fs \tag{3.8}$$

$$\text{one } SF6_{1.5} \text{ crystal beam propagates twice } = 231.0\ fs \tag{3.9}$$

$$\text{two } SF6_{1.5} \text{ crystals beam propagates twice though first and once through second } = 349.3\ fs \tag{3.10}$$

After that, three additional pump pulse broadenings were measured after Pockels cell, Pockel cell plus one $SF6_{1.5}$ crystal and Pockel cell plus two $SF6_{1.5}$ crystal. Thus, the measured results are

$$Pockels\ cell = 187.5\ fs \tag{3.11}$$

$$Pockels\ cell + \ one\ SF6_{1.5}\ crystal = 258.4\ fs \tag{3.12}$$

$$Pockels\ cell + \ two\ SF6_{1.5}\ crystals = 344.8\ fs \tag{3.13}$$

Furthermore, theoretical calculations were performed to confirm that the measured pump pulse chirp was correct. Thus, the following formula was used

$$\Delta\tau_g = D_p \cdot L_p \cdot \delta\lambda_p \tag{3.14}$$

where $\Delta\tau_g$ is relative time delay between two wavelength components or in this case pulse width of the pump pulse, D_p is group delay dispersion parameter for the pump pulse at a wavelength of $1100\ nm$, L_p is the length of the SF6 crystal, and $\delta\lambda_p$ is the FWHM of the pump pulse. The D_p parameter was observed to be $192.14\ \frac{ps}{nm \cdot km}$ from database [2], L_p was measured to be $15\ mm$ for the SF6 crystal, L_p was measured to be $147\ mm$ for the SF6 crystal rod, and $\delta\lambda_p$ was measured to be $30\ nm$. Hence, for the SF6 crystal pump pulse broadening was calculated to be

$$\Delta\tau_g = 192.14\ \frac{fs}{nm \cdot m} \cdot 0.015\ m \cdot 30\ nm = 86.46\ fs \tag{3.15}$$

that is very close to the measured value. Also, for the SF6 crystal rod the pump pulse broadening was calculated to be

$$\Delta\tau_g = 192.14\ \frac{fs}{nm \cdot m} \cdot 0.147\ m \cdot 30\ nm = 847.38\ fs \tag{3.16}$$

The measure for the pump pulse broadening after the Pockels cell was not possible as the FROG can measure the pulse temporal width from $50\ fs$ to $500\ fs$. Hence, as the chirp was considered to be linear the chirp estimations and the measured chirp were combined for the pump pulse. Thus, the pump pulse chirp was calculated to be as follows

$$\begin{aligned} &Pockels\ cell + \text{two } SF6_{1.5} \text{crystals beam propagates once} + \text{SF6 crystal rod} \\ &= 187.5\ fs + 228.2\ fs + 847.38\ fs = 1263.08\ fs \end{aligned} \tag{3.17}$$

3.2 Calculations for the spectral and spatial resolutions for CRS

The estimation of the spectral resolution for CRS when both the pump and the Stokes pulses are linearly chirped was calculated using the following approach. Firstly, the effective linewidth of the mixing product of the pump and the Stokes pulses can be calculated as follows

$$\Delta_{eff} = \sqrt{\left(\frac{\Delta_p^2}{1+C_p^2} + \frac{\Delta_s^2}{1+C_s^2}\right)(1+C_{eff}^2)} \tag{3.18}$$

where the $\Delta_p = 30\,nm$ and $\Delta_s = 20\,nm$ are the FWHM spectral widths of the pump and the Stokes pulses, respectively, C_p and C_s are the chirp parameters of the pump and Stokes pulses, respectively, and C_{eff} is the effective chirp parameter. Next, the chirp parameters of the pump and Stokes pulses can be calculated as follows

$$C_p = \sqrt{\left(\frac{T_{pc}^2}{T_{p0}^2}\right) - 1} \tag{3.19}$$

and

$$C_s = \sqrt{\left(\frac{T_{sc}^2}{T_{s0}^2}\right) - 1} \tag{3.20}$$

where $T_{p0} = 50\,fs$ and $T_{s0} = 50\,fs$ are the FWHM temporal widths of the transform limited Gaussian pulses for the pump and the Stokes pulses, respectively, and T_{pc} and T_{sc} are FWHM widths for the chirped pump and Stokes pulses, respectively. Moreover, the effective chirp parameter can be calculated as follows

$$C_{eff} = \frac{C_p\Delta_p^2(1 + C_s^2) - C_s\Delta_s^2\left(1 + C_p^2\right)}{\Delta_p^2(1 + C_s^2) + \Delta_s^2\left(1 + C_p^2\right)} \tag{3.21}$$

Furthermore, the magnitude of the mixed product can be calculated as follows

$$E_{m0} = A_{p0}A_{s0}\sqrt{\frac{\pi\Delta_p\Delta_s}{\ln 2}}\left(\frac{1}{(1 + C_p^2)(1 + C_p^2)}\right) \tag{3.22}$$

where A_{p0} and A_{s0} are the amplitudes of the pump and the Stokes pulses, respectively. Thus, by knowing the parameters the estimation of the spectral resolution of the mixed product is as follows

$$C_p = \sqrt{\left(\frac{1263^2}{50^2}\right) - 1} = 25.2402 \tag{3.23}$$

and

$$C_s = \sqrt{\left(\frac{1233^2}{50^2}\right) - 1} = 24.6397 \tag{3.24}$$

then

$$C_{eff} = \frac{25.2402 \cdot 30^2(1 + 24.6397^2) - 24.6397 \cdot 20^2(1 + 25.2402^2)}{30^2(1 + 24.6397^2) + 20^2(1 + 25.2402^2)} = 9.3770 \tag{3.25}$$

Hence,

$$\Delta_{eff_{nm}} = \sqrt{\left(\frac{30^2}{1 + 25.2402^2} + \frac{20^2}{1 + 24.6397^2}\right)(1 + 9.3770^2)} = 13.56\ nm \tag{3.26}$$

The spectral resolution of the mixed product was estimated based on the paper [3]. Thus, for example, if the Stokes pulse central wavelength is $1180\,nm$ and the spectral resolution is $13.56\,nm$ it can be converted to wavenumber approximately as follows

$$\Delta_{eff_{cm^{-1}}} = \left(\frac{1}{\lambda_c} - \frac{1}{\lambda_c + \Delta_{eff_{nm}}}\right) * 10^7 \tag{3.27}$$

where λ_c is the central wavelength, hence

$$\Delta_{eff_{cm^{-1}}} = \left(\frac{1}{1180} - \frac{1}{1180 + 13.562}\right) * 10^7 = 96.29\ cm^{-1} \tag{3.28}$$

Moreover, the spatial lateral resolution for the Gaussian beam can be estimated by calculating the beam size at the focus. The smallest beam size of the pump and Stokes beams determines the spatial lateral resolution. Thus, the expression for the spatial lateral resolution is as follows

$$r_{lat} = \frac{0.61 * \lambda}{NA} \tag{3.29}$$

where λ is the wavelength of the light beam and NA is the numerical aperture of the objective [4]. Hence, the spatial lateral resolution for CARS microscopy in water and in ethanol was determined by the pump beam as it has a smaller wavelength. Equation 3.30 depicts calculation.

$$r_{lat} = \frac{0.61 * 1078 * 10^{-9}}{0.65} = 1.012 * 10^{-6}\ m = 1.012\ \mu m \tag{3.30}$$

3.3 CARS and SRS spectroscopies

Maximum scanning range for CARS and SRS spectroscopies can be achieved to be from $730\ cm^{-1}$ to $1870\ cm^{-1}$, respectively. This scanning range can be only achieved if the power to the PCF is adjusted by a round step neutral density filter. Stokes beam pulse wavelength needed to get this range is from $1170\ nm$ to $1350\ nm$, respectively. The scanning range without adjusting the round step neutral density filter and just controlling the VOA is about $40\ nm$. Hence, the scanning range was dictated by the VOA. Figure 3.0 depicts CARS and SRS spectroscopies for cyclohexane. The resulted plots were compared with the Raman spectrum from a research paper (Figure 3.1) [5]. It was noticed that the center wavelength of Raman shift is comparable, hence CARS and SRS spectroscopies are almost optimally performed. The reason for spectral resolution not being optimal is due to the fact that the pump and Stokes beam pulses have different spectral widths at FWHM even though their temporal stretches were the same. Also, due to the fact that CARS is noisier than SRS two spectroscopies are a little bit different.

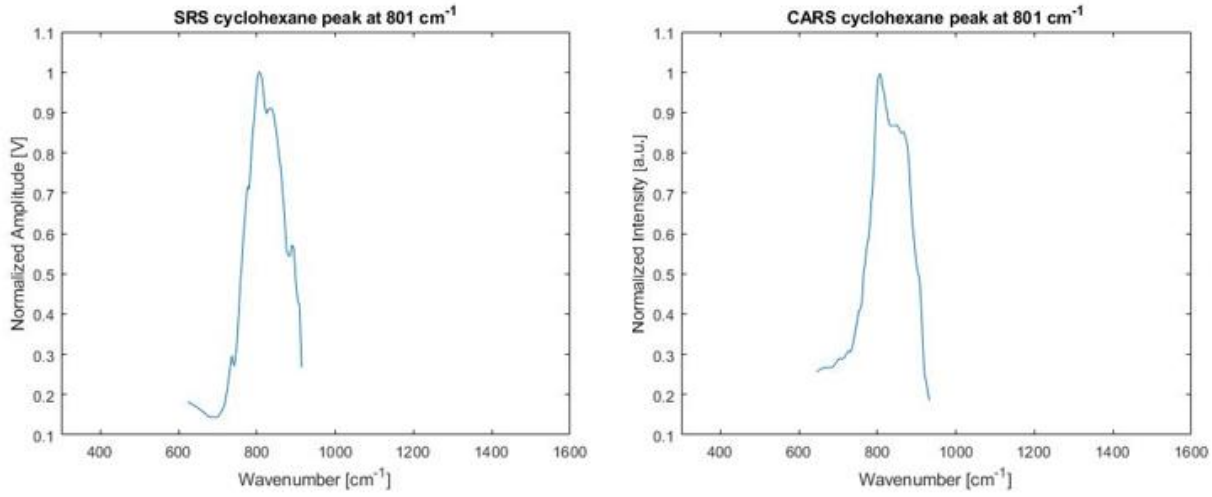

Figure 3.0 CARS and SRS spectra of cyclohexane.

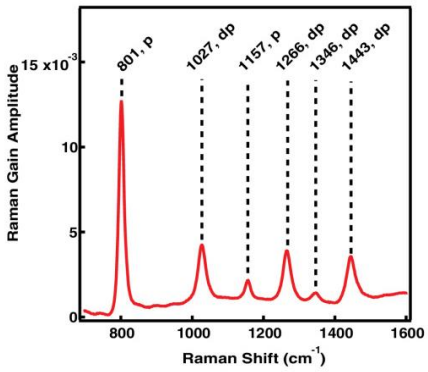

Figure 3.1 Raman spectroscopy of the cyclohexane [5].

3.4 CARS microscopy and images

CARS microscopy image and an optical image of polystyrene beads of 10 μm in diameter in ethanol solution can be observed in Figure 3.2. CARS image was done by getting the Raman signal of the ethanol which is yellow. It can be observed that the centers and sides of the beads are not uniformly blue. The reason that the center is lighter blue is due to fact that the polystyrene beads absorb the ethanol and the very small Raman signal is obtained. Also, the reason for the sides of polystyrene beads going from yellow to green to light blue and then to blue is due to the coating, which is not made from polystyrene. The image size is $35x35\mu m$ or $50x50$ pixels. It took 16 minutes with the step size of 0.7 μm to do that scan.

CARS microscopy image and an optical image of polystyrene beads of 10 μm in diameter in water can be observed in Figure 3.2. In this case, Raman signal is being collected from the polystyrene beads that gives yellow color in the CARS image. The reason why the sides of the beads are not yellow is due to the coating. The image size is $45x45$ μm or $50x50$ pixels. It took 16 minutes with the step size of 0.9 μm to do the scan.

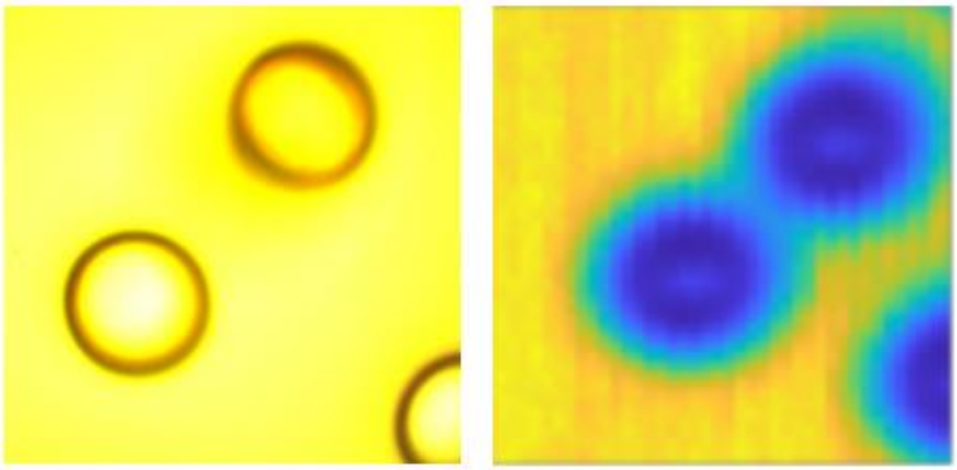

Figure 3.2 CARS image of polystyrene beads with a diameter of 10 μm in ethanol solution on the right and optical image of polystyrene beads with a diameter of 10 μm in ethanol solution on the left $35x35$ μm (both images were filtered using ImageJ with Gaussian blur 3D filter)

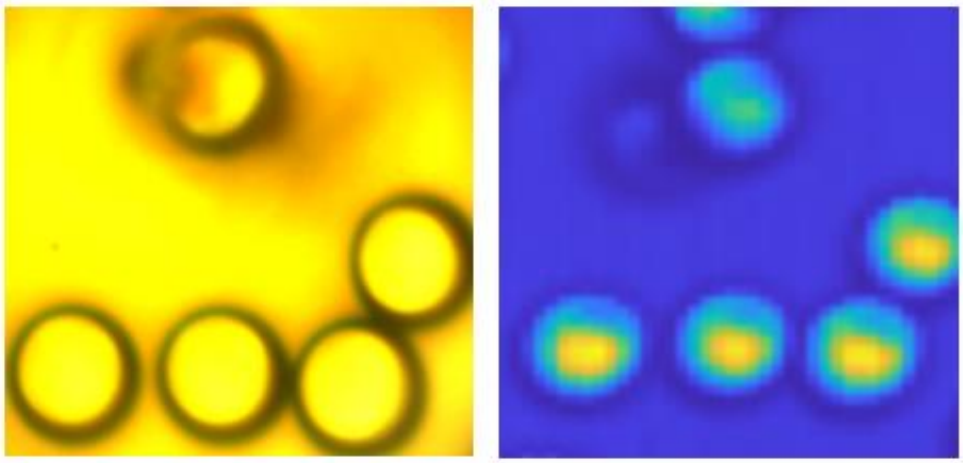

Figure 3.3 CARS image of polystyrene beads with a diameter of 10 μm in water solution on the right and optical image of polystyrene beads with a diameter of 10 μm in water solution on the left $45x45$ μm (both images were filtered using ImageJ with Gaussian blur 3D filter).

References

[1] RefractiveIndex.INFO, Refractive index database, **2008-2020**. [Online]. Available: https://refractiveindex.info/?shelf=main&book=ZnSe&page=Marple

[2] RefractiveIndex.INFO, Refractive index database, **2008-2020**. [Online]. Available: https://refractiveindex.info/?shelf=glass&book=SCHOTT-SF&page=SF6

[3] J. Su, R. Xie, C. K. Johnson and Rongqing Hui., "Single-fiber-laser-based wavelength tunable excitation for coherent Raman spectroscopy.", *Journal of the Optical Society of America B,* **2013**, 30(6):1671-1682.

[4] J. Tragardh, et al., "A simple but precise method for quantitative measurement of the quality of the laser focus in a scanning optical microscope.", *Journal of Microscopy*, **2015**, 259(1): 66-73.

[5] McCreery research group, Standard Spectra, **2014**. [Online]. Available: https://www.chem.ualberta.ca/~mccreery/ramanmaterials.html

[5] M. O. McAnally, Y. Guo, G. Balakrishnan, G. C. Schatz and R.P. VAN Duyne., "Understanding the vibrational mode-specific polarization effects in femtosecond Raman-induced Kerr-effect spectroscopy.", *Optics Letters*, **2016**, 41, 5357-5360.

Conclusion and Future Work

All in all, the experiment brought satisfactory results in CARS and SRS spectroscopies and CARS microscopy. On the other hand, some adjustments and improvements can be made. First of all, to get better spectral resolution spectral width of FWHM of both the pump and Stokes beam pulses have to be equal. It is nothing that can be done with the pump beam pulse, but the Stokes beam pulse can be modified. One of the solutions of modifying the Stokes beam pulse could be to change the PCF to another one that would not have such a nonlinear effect on the pulse that it would shrink the FWHM of Stokes's beam pulse. Another way to increase spectral resolution of CARS and SRS would be to increase chirping meaning stretching both the pump and Stokes beam pulses in time even more. To achieve that other nonlinear crystals have to be fabricated that would meet desired requirements. This fabrication might be time-consuming and expensive.

In addition, CARS microscopy imaging could be done for more than one Raman shift at the same time. It is doable, as the Stokes beam pulse wavelength can be shifted to scan several peaks at a time which could lead to images that have more than one Raman shift. For instance, the sample could be several particles. The only challenge in doing so is to find the different particles that would give Raman shift for the range from $730\ cm^{-1}$ to $1870\ cm^{-1}$which is the same as from $900\ nm$ to $1000\ nm$.

Finally, SRS microscopy can be done as well with this system. It is very similar procedure as for CARS microscopy, but due to time constraints, this was not done in this thesis. It could have even better image quality than CARS because it is less affected by residual and background noise. Additionally, the photodiode that collects and converts the SRS signal probably has to be changed as the signal is not always stable on the lock-in amplifier display.